Technische Universität München
Lehrstuhl für Bioverfahrenstechnik
Prof. Dr.-Ing. Dirk Weuster-Botz

Max-Planck-Institut für Kohlenforschung
(rechtsfähige Stiftung)
Abteilung Heterogene Katalyse
Prof. Dr. Ferdi Schüth

Diploma thesis

High-Throughput Reactor Automatization and Multi-objective Optimization of deNOx Catalysts

submitted by

cand. Dipl.-Ing. Oliver Christian Gobin
2348255

Munich University of Technology, April 2007

Supervisors: Dipl.-Ing. Hannes Link
Prof. Dr.-Ing. Dirk Weuster-Botz
Prof. Dr. Ferdi Schüth

München, April 27, 2007

I, Oliver C. Gobin (student of Chemical Engineering at the Munich University of Technology, student ID no. 2348255), solemnly declare that I have written this thesis independently, and that I did not make use of any aids other than those acknowledged in this thesis. Neither this thesis, nor any similar work, have previously been submitted to any examination board.

Oliver C. Gobin

The ideal engineer is a composite ... He is not a scientist, he is not a mathematician, he is not a sociologist or a writer; but he may use the knowledge and techniques of any or all of these disciplines in solving engineering problems.

–N. W. Dougherty (1955)

Contents

Acknowledgments

First of all, I would like to thank Professor Ferdi Schüth for giving me the chance to work in his group at the Max-Planck-Institut für Kohlenforschung (coal research) on the highly interdisciplinary and exciting field of combinatorial chemistry. I am deeply grateful for the great supervision and guidance during the work and for the freedom I was given.

I am sincerely grateful to Professor Dirk Weuster-Botz and to Hannes Link who supervised my diploma thesis at the Munich University of Technology.

I wish to thank the whole group of Ferdi Schüth for the exceptional and stimulating working atmosphere. Especially I would like to thank Alberto Martinez-Joaristi for introducing me to the chemical and engineering techniques necessary for this project and for various discussions during the work. I would also thank Nikita Ardentov, Stefan Olejnik and the department of fine mechanics (MPI) for the help during the assembly of the reactor set-up. For the discussions about genetic algorithms and various soft computing techniques I would like to thank Dr. Joanna Procelewska. Of cause I also thank the further members of the 'ausländer Büro', Dr. Jean-Sébastien Girardon and Massimiliano Comotti and also my lab neighbor Michael Paul.

Special thanks go to Professor Freddy Kleitz who gave me the idea to join Ferdi Schüth's group.

For performing XRD investigations on several samples I thank Dr. Claudia Weidenthaler and Anastasia Schneider for the proof-reading of the manuscript.

Finaly, I wish to thank my family for their invaluable personal and financial support.

Symbols and abbreviations

Latin symbols

d	(m)	diameter
f, g		functions
H	(m)	height of the packed bed
l	(m)	length
n		control variable, index
N	(-)	total number of elements of a set
m	(kg)	mass
M	(-)	convergence metric
p	(-)	probability
p	(Pa)	pressure
P		population
r	(m)	radius
R	(m^2 kg s^{-2} mol^{-1} K^{-1})	molar universal gas constant
t	(s)	time variable or coordinate
t		iteration step or generation
T	(K)	temperature
v	(m s^{-1})	velocity of the fluid
v_{pore}	(ml g^{-1})	pore volume per gram
V_{solution}	(ml)	volume of precursor solution
$\dot{V}$	(m^3 s^{-1})	flow rate
x		variable
X	(-)	conversion
Y	(-)	yield

Greek symbols

α		initial population
Δ		difference of two physical states
ϵ	(-)	porosity
λ	(-)	pressure drop coefficient
λ	(-)	air to fuel ratio
λ		offspring population
μ		parent population
π	(-)	number Pi
ρ	(kg m^{-3})	density

Indices

0	reference or initial value
AC	activated carbon
c	crossover
bed	packed bed
i, m	control variable, index
m	mutation
max	maximum
min	minimum
p	particle

Dimensionless numbers

Re	(-)	Reynolds number, $\mathrm{Re} = \rho v L / \mu$

Abbreviations

BET		Brunauer-Emmett-Teller plot
deNOx		nitrogen oxide emission control and abatement techniques
EFI		electronic fuel injection
FTIR		Fourier transform infrared spectrometer
GUI		graphical user interface
GSHV	(h^{-1})	gas space hourly velocity
HC		hydrocarbons
HTE		high-throughput experimentation
HTML		hypertext markup language
HTTP		hypertext transport protocol
HTTP-GET		a method to retrieve information from a HTTP server
IUPAC		international union of pure and applied chemistry
IBEA		indicator based evolutionary algorithm
IP		Internet protocol
IR		infrared
MySQL		open source database
MCM-22		Mobil Composition of Matter number 22 (a zeolite)
MOR		Mordenite (a zeolite)
NOx		Nitrogen oxides: $NO + NO_2$
NSGAn		non-dominated sorting genetic algorithm version n
NSR		NOx storage and reduction system
OLE		object linking and embedding
OPC		OLE for process control
PHP		hypertext preprocessor (a server-side HTML embedded scripting language)
PID		proportional-integral-derivative controller (PID controller)
RS232		standard for serial binary data interconnection
SBX		simulated binary crossover
SEM		scanning electron microscopy
SCR		selective catalytic reduction
SNCR		selective non-catalytic reduction
SOx		sulfur oxides
SPEAn		strength Pareto evolutionary algorithm version n
SQL		structured query language
TC		test case
TCP		transport communication protocol
TRUST		terminal repeller unconstrained subenergy tunneling
TWC		three way catalyst
URI		uniform resource identifier
VMX		vanadium/metal based catalysts
XRD		X-ray diffraction
ZSM-5		A zeolite, developed by Mobil Oil

1 Introduction and motivation

In the last few years, in the light of the energy problem and global warming, additional effort has been made to prevent the release of substances which amplify these enviromental problems. Therefore the diesel and lean-burn gasoline engines are becoming more and more the alternative to regular gasoline engines due to the higher efficiency with respect to the fuel consumption. Also stronger emission regulations of harmful substances for vehicles over the past few years require new catalysts, which are highly active for the selective reduction of nitrogen oxides in oxygen rich conditions. One group of possible catalysts are noble metal free metal oxides. A huge number of combinations is possible to think of and some of them were already investigated on various types of support over the last years.

In this work we will focus on the optimization of metal oxides consisting of combinations of 10 elements, selected from the transition metals (Cu, Ni, Co, Fe, Mn), the lanthanides (La, Ce, Sm) and the alkali metal (K, Sr) group. Alumina was chosen as support, due to its ability to form a high surface area and its high hydrothermal stability. A combinatorial, evolutionary directed, high-thoughput multi-objective optimization approach is applied to this system. Wolf et al. (2000) were the first to use a single objective evolutionary optimization algorithm for the search of optimal combinations of elements of solid catalysts. However, in real world problems and especially in catalysis, several often conflicting objectives are generally to be taken into account. Thus it is necessary to develop methods, which are able to find optimal solutions in multidimensional spaces. Due to its importance in industry, the selective catalytic reduction of nitrogen oxides was chosen as test case for this approach. The catalyst will be optimized with respect to the conversion to nitrogen and the temperature at which the yield is maximal (the so called peak temperature). Two different multi-objective algorithms, namely SPEA2 (Zitzler et al., 2002) and IBEA (Zitzler and Kunzli, 2004) will be applied to this problem. The results of the two algorithms will be compared and discussed. Also some implementation and encoding issues, common to combinatorial chemistry problems, will be emphasized.

2 State of the art in deNOx technology

2.1 Introduction

In this chapter, the current situation in catalytic removal of nitrogen oxides (NOx) from exhaust gases will be described with a focus on the selective catalytic reduction of NOx by propene. Nitrogen oxides are one type of environmental pollutants which are predominantly generated during the combustion of fossil fuels. In order to meet society's requirements of energy, large amounts of fossil fuels are required corresponding to a high quantity of pollutants discharged into the atmosphere.

These pollutants influence the environment and human health especially in congested urban areas but also worldwide. Nitrogen oxides are the source of severe environmental problems, such as acid rain, smog and ozone formation, which is a pollutant itself due to global warming impacts and its strong oxidizing properties. Figure 2.1 shows a general scheme of emission sources, transformations and transport in the environment, natural removal options and environmental effects (EPA).

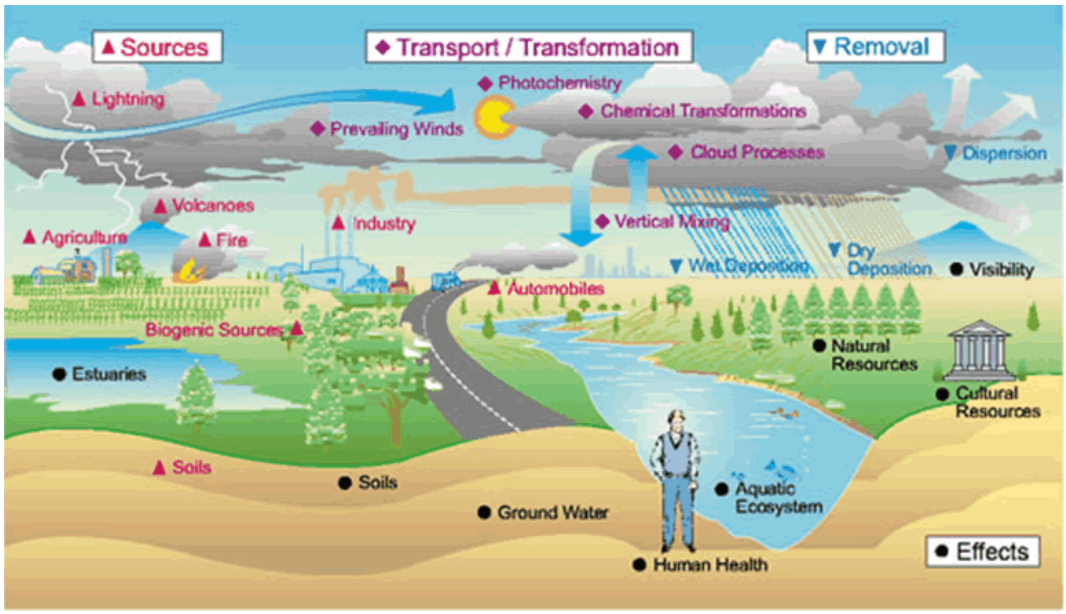

Figure 2.1: Sources, transformations and transport, natural removal and effects of emissions (Dathe, 2005).

For instance, the increased use of cars in the 1960s and 1970s resulted in serious decrease of the air quality caused by exhaust gas emissions from automobile engines.

The oxidation of gasoline in engines to carbon dioxide (CO_2) and water was incomplete and led to the production of unburned hydrocarbons (HC) and lower levels of partially combusted organic products, together with large amounts of carbon monoxide (CO). The solid particles are generally referred to particulate matter (PM) and consist of carbon particles and organic compounds of less than 3 μm as approximated by the U.S. environmental protection agency (EPA). Nitrogen oxides are generated at high temperature during the combustion process mostly as a result of the equilibrium between NO and $N_2 + O_2$ (so called thermal NOx), but also by oxidation of nitrogen compounds present in the fuel. The primary man made sources of nitrogen oxides are therefore motor vehicles, electric utilities, and other industrial, commercial, and residential sources that burn fuels. NOx can also be formed naturally as shown in figure 2.1. In figure 2.2 the reactions of atmospheric NOx resulting in secondary pollutants are illustrated.

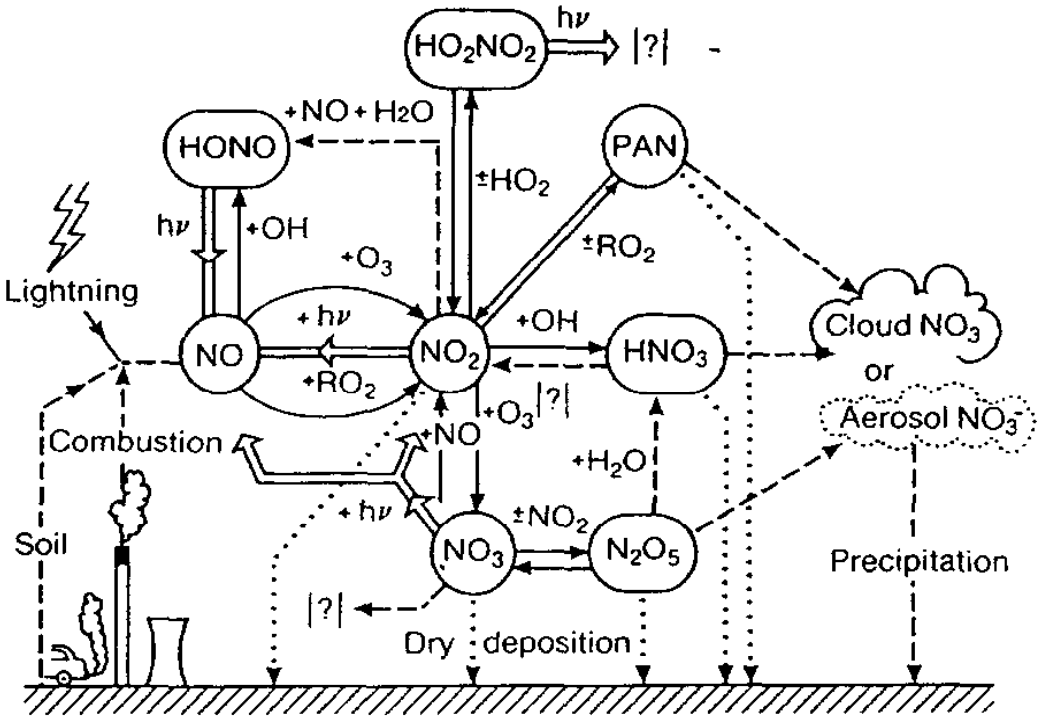

Figure 2.2: Chemical transformations of atmospheric NOx through photochemical processes (=), thermal gas-phase processes (–), dry deposition (· · ·), and heterogeneous reactions (- -) (Bosch and Janssen, 1988).

More than 50% (EPA) of the nitrogen oxides are formed by fossil fuel combustion in motor vehicles. The typical mixture of emissions from diesel exhaust gas consists of 0 - 800 ppm HC, 0 - 500 ppm NOx, CO_2 and H_2O (Dathe, 2005). A good emission control technique should be able to reduce these emissions to a minimum.

2.2 Emission control techniques

The emission control techniques (deNOx) can be divided in two main groups: combustion control and post-combustion abatement techniques. The combustion control methods are also named as clean methods, whereas the abatement of emissions after the combustion is generally referred as clean-up technique or flue gas treatment (Armor, 1992, Bosch and Janssen, 1988, Busca et al., 1998).

Combustion control tries to minimize NOx formation by designing better burning devices that minimize the oxygen concentration, the flame temperature and the residence time in the combustion zone. Also the use of fuels with low levels of nitrogen content is an option. Examples of combustion control devices are low NOx burners, flue gas recirculation, fuel reburning, staged combustion and water or steam injection. The combustion control technologies are the most cost-effective and energy efficient techniques. The main disadvantage is the low NOx conversion (less than 70%) compared to some post-combustion methods (90-99%) (Bosch and Janssen, 1988, Hums, 1998, Parvulescu et al., 1998).

Post-combustion techniques are secondary measures for the treatment of the flue gas already containing NOx. In general five methods are available: absorption, adsorption, condensation, incineration and chemical reaction. Specific problems require often a combination of several methods. An example of a non catalytic method is the selective non-catalytic reduction (SNCR), developed by Exxon. It is an homogeneous gas phase reduction process in which NOx is selectively reduced by NH_3 to N_2. This process requires low capital investment, however its temperature operation window (1123 - 1323 K) is very narrow and difficult to meet in larger facilities. In comparison to the non-catalytic solutions, catalytic methods offer lower operating temperatures and are the common method to control gas emissions from vehicles (Armor, 1995). The possible catalytic solutions can be divided into four categories: the direct NO decomposition, the three way catalyst (TWC), the NOx storage techniques and the selective catalytic reduction using ammonia (SCR) or hydrocarbons (HC-SCR) as reductant.

2.2.1 Direct decomposition of NO

The direct catalytic decomposition of NO to N_2 and O_2 is an attractive option because it does not involve the use of an additional reductant. NO is thermodynamically unstable ($NO \rightarrow 0.5\,N_2 + 0.5\,O_2$, $\Delta G^0 = -86$ kJ/mol) up to 1273 K, however due to its high activation energy of 364 kJ/mol (Glick et al., 1957) a catalyst is necessary. In their pioneering work Iwamoto et al. (1986) reported 1986 that Cu-ZSM-5 was an active catalyst for the decomposition of NO to N_2 at 773 K. This lead to great enthusiasm amongst scientists. As a result many catalysts were tested (Fritz and Pitchon, 1997), and it was shown that complete NO conversion to N_2 could be obtained. However, up to now no catalyst was found to be suitable for practical application due to the impossibility to suppress the inhibiting effect of oxygen and water under reaction conditions (Armor, 1995). It has become clear that the direct decomposition is not suitable for a real technological application in the presence of a complex exhaust mixture.

2.2.2 Three way catalyst technology

The earliest catalytic emission control systems, where fuel and air were mixed using so called carburetors and not by injection, were not able to precisely control the air fuel ratio and performed rather poorly. However, it was observed, that Pt/Rh catalysts could, under appropriate conditions, simultaneously oxidize CO and HC to CO_2 and H_2O and reduce NOx to N_2 and O_2 with a high efficiency (Twigg, 2007). This lead to the development of an emission control system, which is nowadays one of the principal methods of controlling the combustion emissions from Otto engines. This system is well known as the three way catalyst technology (TWC), as it is able to remove all three pollutants from the exhaust gas simultaneously. In 1979 (Shelef and Graham, 1994) all the elements necessary to precisely control the air to fuel ratio were available: The electronic fuel injection (EFI) allowed a precise fuel injection to provide a stoichiometric air fuel mixture. A mixture of λ = air/fuel = 1.0 is at stoichiometry, rich mixtures are less than 1.0, and lean mixture are greater than 1.0. The lambda or oxygen sensor was able to provide an electrical signal to the EFI indicating if the engine is operating in fuel rich or lean conditions by measuring the residual oxygen (for lean mixtures) or hydrocarbons (for rich mixture) in the exhaust gas. Finally a microprocessor was able to calculate the exact amount of fuel and air to be injected to maintain the exhaust gas close to the stoichiometric point.

Figure 2.3 shows the influence of the air/fuel ratio on the operation characteristics of a three way catalyst. If the air to fuel ratio is not in a narrow window near the stoichiometric point large amounts of NOx are emitted in the case of an air rich mixture and large amounts of CO and unburned hydrocarbons in the case of a fuel rich mixture.

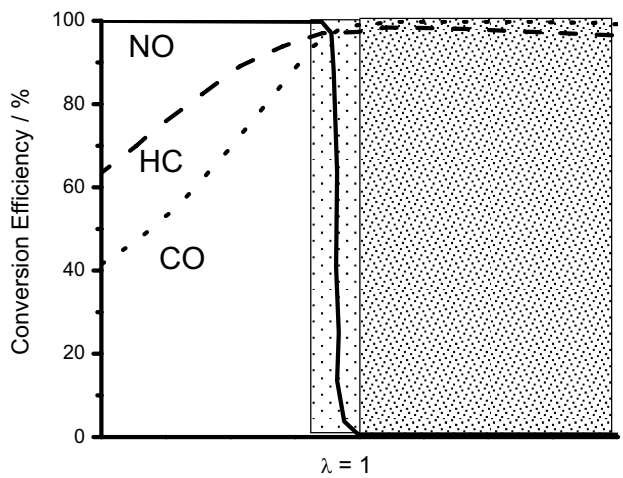

Figure 2.3: Three way catalyst performance at fuel rich ($\lambda < 1$), lean ($\lambda > 1$, diesel engine) or stoichiometric ($\lambda = 1$, Otto engine) conditions (Kreuzer et al., 1996).

The three way catalysts, which are in use nowadays, are manufactured in a honey comb monolithic form and are composed of 0.1-0.15% precious metals with a ratio of

Pt to Rh of 5 to 1 and varying concentrations of bulk high surface area CeO_2 mixed with a Al_2O_3 wash-coat stabilized with 1-2% of La_2O_3 and BaO (Farrauto and Heck, 1999). Pt is involved in the oxidation, Rh in NO reduction while the main role of CeO_2 is in the storage of O_2 needed in the case of fuel rich conditions. The catalysts are very efficient (< 95% NOx conversion) (Farrauto and Heck, 1999) under appropriate conditions. Among the problems of the TWC are their poisoning by sulfur compounds and the formation of unburned hydrocarbons during cold start of the engine. The main problem nowadays is that the environmental regulations demand better fuel efficiency. This is achieved with engines that operate under lean burn conditions. Under these conditions the NOx formation is favored and in the presence of excess O_2 these catalysts are not able to reduce the nitrogen oxides. The same problem exists for applications in diesel engines and power plants.

2.2.3 NOx storage materials

A promising approach to remove nitrogen oxides from exhaust gases is the NOx storage and reduction system (NSR) introduced by Toyota and widely tested in the automobile industry. It operates under lean burn conditions and results in 5-6% fuel economy savings. The NOx generated is stored as nitrate in an alkaline earth metal oxide such as BaO incorporated in the TWC. Periodically the engine goes to fuel rich conditions for a short time in which the NOx is reduced (Farrauto and Heck, 1999) as illustrated in figure 2.4.

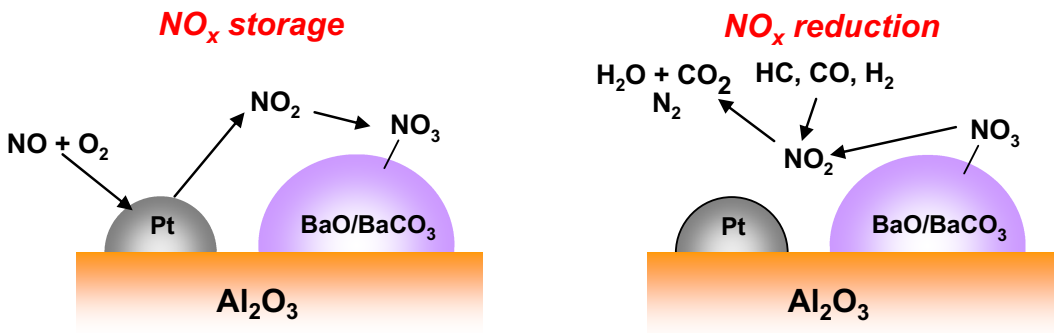

Figure 2.4: NOx storage and reduction mechanism on the NSR catalysts (Dathe, 2005).

The major drawback for an industrial application is the deactivation of the catalyst by sulfur oxides (SOx) present in the exhaust gas. They form sulfates, which are thermodynamically more stable than the corresponding nitrates and cause a permanent deactivation of the storage function. Dathe (2005) studied the concept of using sulfur traps to protect the NSR catalysts and to avoid the irreversible deactivation of the system.

2.2.4 Selective catalytic reduction

The most widely applied method among the emission control technologies is the selective catalytic reduction with ammonia (NH_3-SCR) (Armor, 1995, Busca et al., 1998, Hums, 1998, Parvulescu et al., 1998). This method is considered as the best available control technique for industrial deNOx. NH_3 is injected into the flue gas and reduces with the help of a catalyst NOx to N_2 and H_2O. NH_3 is used as reductant because it is very selective and reacts mostly with NOx and not with O_2. The selective or desired reactions are shown equation (2.1) and (2.2):

$$4NO + 4NH_3 + O_2 \longrightarrow 4N_2 + 6H_2O \tag{2.1}$$

$$2NO_2 + 4NH_3 + O_2 \longrightarrow 3N_2 + 6H_2O \tag{2.2}$$

The non-selective reactions mainly involve the oxidation of NH_3 and SO_2 to the corresponding oxides or to N_2 and H_2O.

Depending on the catalyst the process operates at low (423 - 573 K), medium (533 - 700 K) or high temperatures (618 - 863 K). V_2O_5/TiO_2 (VMX^{TM}) catalysts supported on a monolith are most broadly used and operate in the medium temperature region (Heck, 1999). They are highly active and sulfur tolerant. Platinum based LT catalysts are active in the low temperature region, but not sulfur tolerant. The major advantage of the selective catalytic reduction with ammonia is the high degree of NOx conversion that can be achieved (> 95 % conversion) (Hums, 1998, Parvulescu et al., 1998) under oxygen rich conditions. However, this method has several known disadvantages: it is quite expensive compared to the combustion control methods because of the sophisticated injection and distribution pipes and nozzles and ammonia or an ammonia source has to be transported additionally to the fuel. Beside the engineering difficulties the oxidation of sulfur present in the fuel forms SO_2 and SO_3 that subsequently form ammonium sulfate and bisulfate by reaction of SO_3 with NH_3 and H_2O. These salts cause plugging and corrosion. All these problems make the operation of the NH_3-SCR complicated. Chemical and mechanistic aspects of the selective catalytic reduction of NOx by ammonia over oxide catalysts were reviewed by Busca et al. (1998) and Parvulescu et al. (1998) in 1998.

An alternative approach to reduce the nitrogen oxides is the selective catalytic reduction of NOx by hydrocarbons (HC-SCR). HC-SCR was first discovered in the 1970's but was abandoned at this time due to the low selectivity to nitrogen compared to NH_3-SCR. Nowadays HC-SCR is attracting a lot of interest and is believed to be a very promising way to eliminate nitrogen oxides (Fritz and Pitchon, 1997, Iwamoto, 1996, Parvulescu et al., 1998, Traa et al., 1999) under lean burn conditions. Low levels of unburned hydrocarbons are present in the exhaust gases and their reductive power can be utilized. Also a second possibility for this approach could be the injection of these hydrocarbons from an external source as in the case of NH_3. Due to the focus of this work on the optimization of catalysts for the HC-SCR, in the following section this approach will be discussed in more detail.

2.3 Selective reduction of NOx by hydrocarbons

The selective catalytic reduction by hydrocarbons (HC-SCR) is an interesting option to control the emissions in automobile lean burn exhaust gases. The following set of selected overall reactions describes best the competition of oxygen and nitrogen oxide during the HC-SCR with propene:

$$2\,C_3H_6 + 9\,O_2 \longrightarrow 6\,H_2O + 6\,CO_2 \tag{2.3}$$
$$2\,NO + O_2 \longleftrightarrow 2\,NO_2 \tag{2.4}$$
$$2\,C_3H_6 + 18\,NO \longrightarrow 9\,N_2 + 6\,CO_2 + 6\,H_2O \tag{2.5}$$
$$4\,C_3H_6 + 18\,NO_2 \longrightarrow 9\,N_2 + 12\,CO_2 + 12\,H_2O \tag{2.6}$$
$$C_3H_6 + 12\,NO \longrightarrow 6\,N_2O + 3\,CO_2 + 3\,H_2O \tag{2.7}$$

The selective reactions leading to the generation of nitrogen are (2.5) and (2.6). These two reactions are very difficult under lean burn conditions, because propene, which is required for the reduction of the nitrogen oxides, can also react with oxygen as shown in equation (2.3). The full combustion of propene by oxygen is under lean burn conditions mush faster than the combustion even without a catalyst. A catalyst is required to selectively lower the activation energies of reaction (2.5) and (2.6) but not of reaction (2.3) and (2.7). Reaction (2.4), the oxidation of NO to NO_2, can improve the SCR activity, as NO_2 can be a key intermediate in the NO reduction depending on the catalyst and reaction condition (Ansell et al., 1993). In the next part of this section, a short overview of the different solid catalyst systems tested in the last years for HC-SCR activity will be given. Three different reaction mechanisms which lead to nitrogen formation will also be discussed briefly.

Catalysts for HC-SCR

Iwamoto et al. (1986) discovered that Cu-zeolites were suitable for the selective reduction of NO. The NO reduction was performed by alkanes and alkenes over Cu-ZSM-5 under lean burn conditions. Since then a large number of catalysts were investigated and the results were published in the literature (Castagnola et al., 2004, Garcia-Cortes et al., 2000, Liu et al., 2006, Nejar et al., 2005, Neylon et al., 2004, Sadykov et al., 2005). The catalysts can be roughly divided in the following categories: metal oxides, metals supported on zeolites and supported noble metals. Among the oxide based catalysts, the following catalysts were reported to be active in the HC-SCR: simple oxides: Al_2O_3, SiO_2-Al_2O_3, TiO_2, ZrO_2, CeO_2, La_2O_3, oxides of transition metals (Cu, Co, Ni, Mn, Fe, Ag) supported on oxides from the first group, as for instance silica or alumina, and spinel or perovskites metal oxides (Liu and Woo, 2006).

The early findings of active Cu-zeolites attracted the special interest in transition metals supported zeolites. Zeolite based catalysts have a high activity and a relative wide operation temperature window. Co and Fe and other metals on ZSM-5 show good activity and selectivity to N_2. ZSM-5 seems to be more active than MOR or MCM-22 due to the high concentration of strong acid sites if propane is used as reductant (Liu

and Woo, 2006). Also it was shown that the pore structure of the zeolite is important (Liu and Woo, 2006). However, the main problem of these metal-zeolite based catalysts is the poor hydrothermal stability.

Transition metal oxides supported on alumina or other supports have especially attracted attention due to their high hydrothermal stability. However, many factors related to the synthesis, as for instance the type of support, the metal loading, the calcination temperature and the preparation method are influencing the activity of these metal oxides. Also combinations of binary, ternary or higher order metal oxides which may form active spinel or perovskite phases are influencing the final activity. Studying the influence of the support, it was found, that alumina is the most suitable, while silica supported catalysts are not active at all (Kintaichi et al., 1990). The peak activity temperature range is generally from 573 to 773 K. Liu and Woo (2006) reviewed the influences of these different parameters.

Common for both metal oxide and zeolite-based catalyst is the poor low temperature activity, which is especially desired during the cold start period. In contrast, supported noble metal catalysts (Pt/Al_2O_3, Rh/Al_2O_3) are highly active at low temperatures (< 523 K). Drawbacks are the very narrow temperature window and the moderate selectivity to N_2, due to substantial formation of N_2O, which is a pollutant by it self.

As a conclusion, no single catalyst satisfying all the practical demands for HC-SCR is up to now available. Mechanical mixtures of several systems were investigated by some researchers and lead to interesting features such as low temperature activity, wider temperature window and higher selectivity. However, up to now the tolerance to sulfur and water is not sufficient for a practical application (Liu and Woo, 2006).

3 High-throughput reactor automatization

3.1 Introduction

High-throughput techniques, such as for instance the synthesis and screening of organic molecules for their activity or their potential as drugs, are well established techniques in the pharmaceutical industry. In the field of heterogeneous catalysis and material research, the interest in high-throughput techniques for the discovery of new functional materials has received considerable interest in the last years (Baerns and Holena, 2002, Hahndorf et al., 2002, Kiener et al., 2003, Murphy et al., 2003, Schuth and Demuth, 2006, Schuth et al., 2002, Weinberg and McFarland, 1999). High throughput techniques are parallelized screening techniques ranging from a massive degree of parallelization and rather low information depth of the analysis in the case of the so called stage I screening, and a high information depth but a lower degree of parallelization in the case of stage II screening. In this work, for the optimization of deNOx catalysts, an accurate analysis with a high information depth is needed and therefore a stage II screening concept will be used.

In this chapter first the assembly and automatization of a 49 parallel stainless steel gas-phase reactor set-up bought for this project will be described and afterwards the set-up will be tested and checked by performing several measurements.

3.2 Concept of the set-up

A flow diagram of the stage II screening set-up installed during this work is shown in figure 3.1. The set-up consists of the 49 channel parallel reactor, the analysis device and several gas feeds. The flow system is build up using fittings, valves and capillary tubings of stainless steel from Swagelok. First the gas feeds are mixed together to obtain a feed with the right gas composition (A). The feds with a high flow rate are first fed in and afterwards the ones with a low flow rate, to obtain a good and reproducible mixing. The gas mixture is than fed into the parallel channel reactor (B), where the flow is equally distributed into each of the 49 channels of the reactor. Subsequently each channel of the reactor is connected to the analysis device. The interconnecting capillary is denoted as analysis line or analysis capillary (C). The other 48 gas streams not connected to the analysis device are mixed together and feed into the exhaust line (D). The selection of the channel to analyze is done by the multiport valve. The analysis is performed by a FTIR Nicolet Avatar 370 from Thermon Electron using a small gas cell for a fast analysis. The complete system is pressurised using metering valves from Swagelok and two low

pressure manometers from WIKA for the exhaust and analysis line. The FTIR gas cell is heated to 403 K.

In figure 3.2 a closer look at the reactor and the multiport valve is given. The reactor was bought from the hte company (hte) and is a state-of-the-art system for stage II solid catalyst testing under real-world conditions. The heating of the reactor is achieved by 48 heating elements, which are placed around each reactor channel as can be seen in figure 3.2C. They provide a homogeneous temperature distribution and an accurate and responsive temperature control. Graphite gaskets are used to seal the reactor also at high temperatures.

The multiport valve is a construction from the fein mechanic department at the Max-Planck-Institut für Kohlenforschung (coal research). The exact description can be found in the PhD thesis from Hoffmann (2002) and Kiener (2004).

3.3 Automatization

For an autonomous and continuous operation of the set-up, the reactor heating, the multiport valve and the analysis device have to be automated and synchronised with each other. To change the gas composition during the reaction, the mass flow controllers have also to be automated. However, in this work the gas composition was constant for all experiments, therefore it was not necessary to automate the gas streams. They were just set once to a specific value before each experiment.

The heating elements of the reactor are controlled by a Mini8 controller from Eurotherm. The controller is capable of accepting commands from a RS232 serial line using the Modbus serial protocol or from an Ethernet connection over TCP/IP using the Modbus TCP protocol. In both cases it is also possible to use an OPC server, which is capable of speaking the Modbus protocol. Using an OPC server, it is possible to open an OPC datasocket connection for instance from Labview to write and to read records to the Mini8 controller. In figure 3.3 a schema showing the different possibilities to communicate with the Mini8 controller is given.

Rotation of the multiport valve is achieved by using a high torque motor model SECM268 from EC motion controlled by a SMCI 46 controller from Nanotec. The SMCI 46 controller is capable of accepting data from a RS232 serial line.

The FTIR Nicolet Avatar 370 system is controlled through a parallel line by OMNIC, a commercial software from Thermo Electron.

All these three independent devices have to be automated and synchronized to work together. For this purpose a Labview program was written, tested and continuously revised throughout this work. The next sections will describe the features of the Labview program and of the automatization process at the final state of their development.

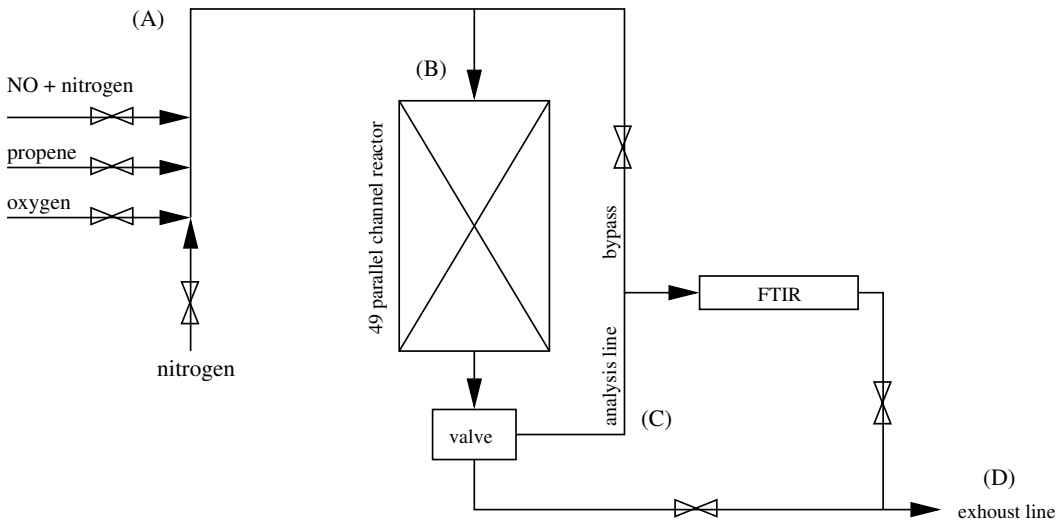

Figure 3.1: Flow diagram of the 49 channel reactor set-up.

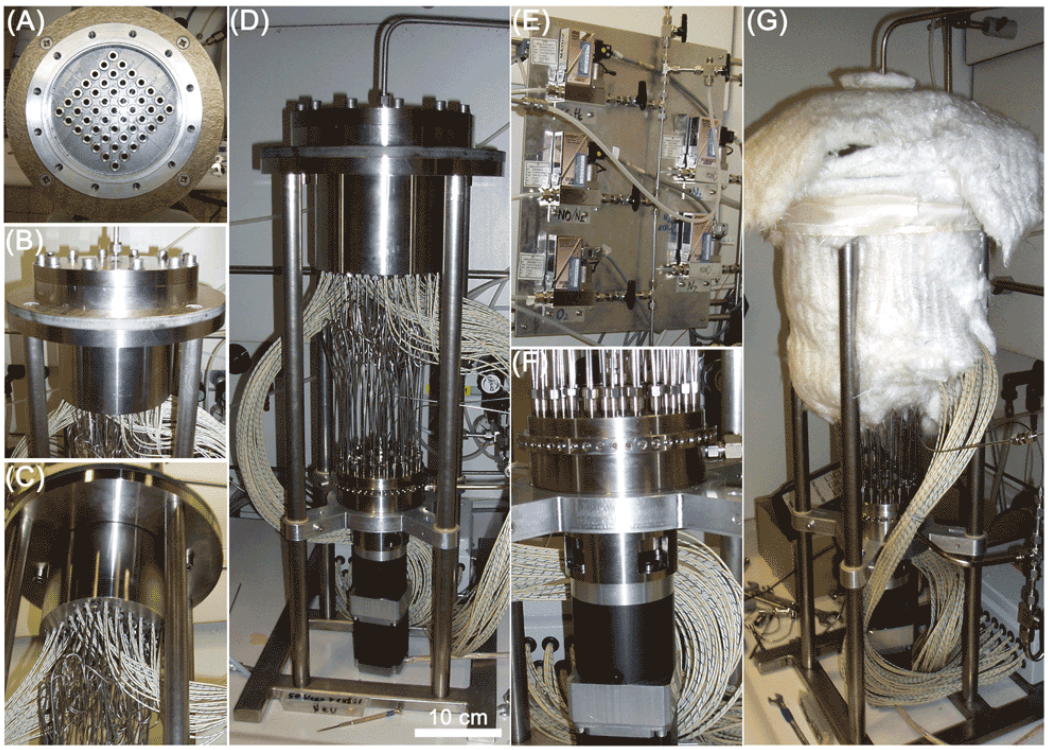

Figure 3.2: Images of the 49 parallel channel reactor setup: (A) top view on the open reactor, (B) closed reactor (C) bottom view on the thermo elements and reactor capillaries, (D) side view on the complete setup, (E) gas streams and mass flow controllers, (F) multiport valve and stepping motor and (G) side view on the complete setup with insulation.

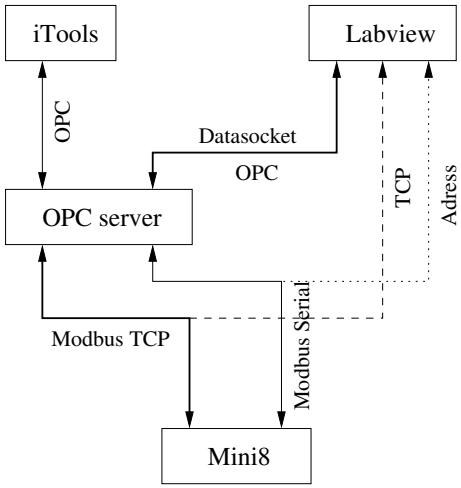

Figure 3.3: Mini8 protocols and communication possibilities.

3.3.1 Communication process

The Labview program is responsible for managing several automatization tasks: it controls the temperature of the reactor, the position of the valve and analyzes the data obtained from the FTIR software. Additionally, the Labview program is also capable to store the analysed data directly into a SQL database. The data storage and management process will be described more in detail in section 3.4.

To synchronize the different devices, a simple solution based on the use of a shared memory and a communication protocol was implemented. The communication process is intended to synchronise the Labview program with the FTIR software. In figure 3.4 a simple petri net illustrates this concept.

The communication is done through text files which have to be accessible at the same time by the Labview program and the FTIR software. For instance this can be achieved by using text files, which are located on the same hard drive or on a common network share. Thus it is possible to install and to operate the FTIR software on a different computer than the Labview program. The main loop of the communication process in figure 3.4 can be described as follows:

When the state is 4, the Labview program changes the valve position by one step by sending a sequence of bits to the control of the motor through the serial line. Before setting the state to 5 the Labview program waits a certain time, which should be equal or greater than the dead time of the set-up. After the dead time, the state is set to 5 and the FTIR software starts to record a predefined amount of spectra of the gas stream in the IR cell. Afterwards it sets the state to 4, to give the Labview program the instruction to change the valve position. The analysis of the obtained spectra is than done by the FTIR software automatically using OMNIC macros. The macros analyze the spectra and write the results of the analysis into a text file. This file is being processed by the Labview program, which recognizes new entries and starts to convert the intensities to concentrations and to calculate the mean and the standard deviation of the data. During

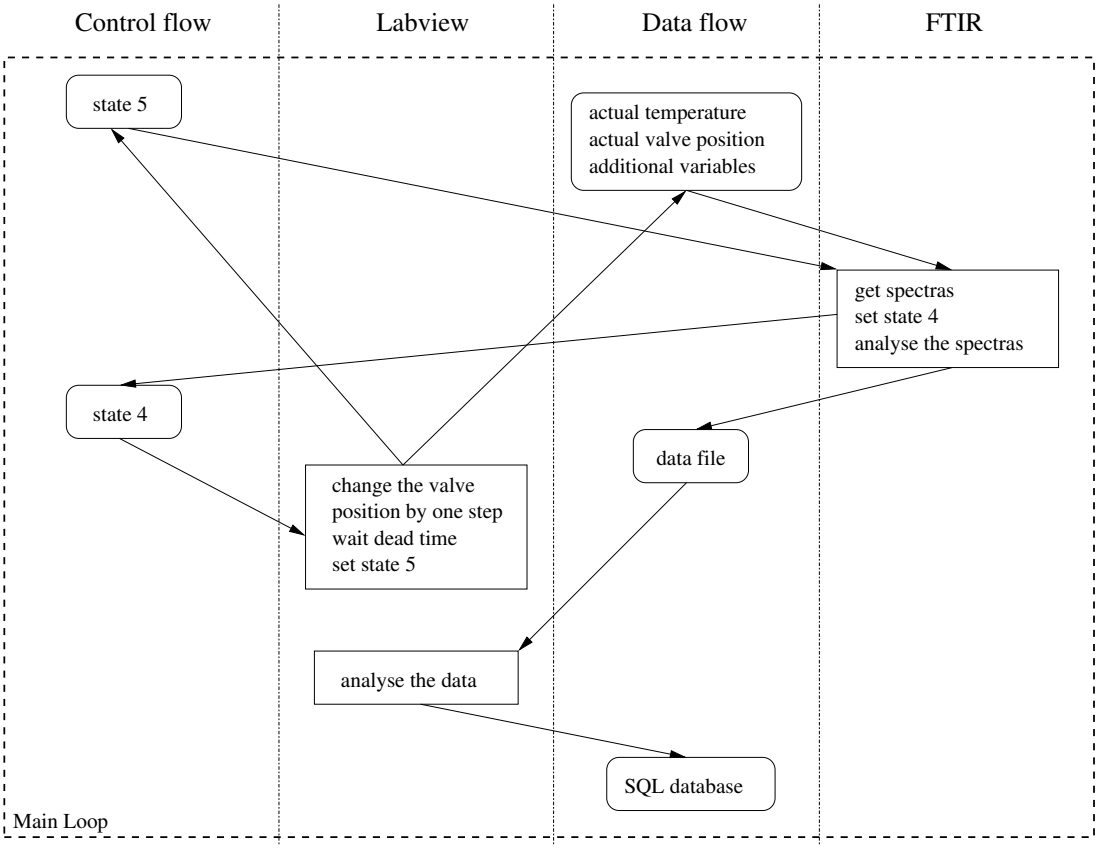

Figure 3.4: Control and data flowchart of the Labview - FTIR - SQL Database communication process represented as a petri net.

this process, the actual temperature, the valve position and some additional information, as for instance the time, are written into text files, which are processed by the FTIR software during state 5.

The FTIR software is setting the state to 4 directly after the measurement of the spectra but before performing the actual analysis. This was done, because generally the dead time of the set-up is longer than the time needed to analyse the spectra, hence the time of the analysis is gained, which results in a time reduction of approximately one minute per analysis.

3.3.2 Temperature control

The temperature control of the reactor is kept very simple in the version of the Labview program developed for this work. The Labview program gives the reactor control a setpoint on the basis of a linear ramp. The user just has to enter the start, and the end temperature and the ramp in Kelvin per hour The controller used to reach this setpoint is a PID controller. The proportional, integral and differential portion of the controller have to be trained previously using the iTools software. The training was

done at an intermediate temperature of 573 K and no overshooting could be observed afterwards for all temperatures. In the case of a too big gap between the reactor and the setpoint temperature, the Labview program stops the ramp and waits until the actual temperature reaches the setpoint temperature within a range of 5 Kelvin. A detailed study of the temperature characteristics of the reactor will be given in section 3.5.1.

The Labview program communicates with the temperature controller (Mini8) using an OPC datasocket connection through an Ethernet line. The records can be read or written simply by opening a connection specified by a so called URI. An example for a valid URI to read or write the setpoint record of the controller is:

```
opc://localhost/Eurotherm.ModbusServer.1/Network.192-168-0-50-502-ID001-Mini8.Loop.1.Main.WorkingSP
```

Where `localhost` is the location of the OPC server and `192.168.0.50` the IP address of the reactor control.

3.3.3 Multiport valve control

The multiport valve is connected to a motor which can be controlled through a serial line from a computer. The controller of the motor (SMCI 46) is programmable and has a small memory to store the previously defined programs. The program used in this work moves the multiport valve by one step. The Labview program just has to send a start command through the serial line to initiate the rotation of the motor. The start command for the program currently selected in memory is a 0x04 character. One should note, that it is not possible to get the actual position from the controller of the motor, thus the Labview program has to memorize the actual position.

3.3.4 FTIR automatization

The control and the automatization of the FTIR analyser is essentially done by the macro system included in the OMNIC software. Using this system, it is relatively easy to control the FTIR hardware, to manipulate and analyze the spectra and to report the results. For each component, the spectrum is evaluated at two points. Representative source code listings for the synchronization and automatization can be found in the appendix C.

In a normal experiment, the resolution of the FTIR system was set to 1.0 cm^{-1}, the aperture to 100 and the gain to 8. Generally 8 scans were taken for each spectrum and a total of four spectra was recorded for each analysis. The obtained data is written into a machine readable text file and processed by the Labview program. The data management, storage and visualisation process will be described in more detail in the following section.

3.4 Data management and visualisation

3.4.1 Data storage

The storage and post-processing of the obtained data sets was designed to be as flexible as possible. As stated before, first the data obtained from the FTIR is stored into a machine readable text file. This text file is being read and analyzed by the Labview program. The Labview program converts the intensity values from the FTIR to corresponding concentrations using previously measured calibration curves and calculates the mean and the standard deviation for each data point. The data is then directly stored into a MySQL database, which can be installed on any computer, which can be located in the in local intranet or even in the Internet. This is achieved by sending the data enclosed into a HTTP-GET request to a webserver. In appendix A in figure 3.3 the Labview source code is shown. This connection is also possible through a HTTP proxy to bypass possible blocking firewalls. The HTTP-GET request is then processed by a PHP script running on the webserver. The PHP script decodes the data points, sorts them according to the corresponding catalysts and experiments and afterwards stores the data into the database. In such a way, the acquired data can be directly visualized online on a website during the experiment. It is possible to monitor the reactor from an arbitrary remote computer, which is connected to the Internet. Also the final analysis is being reduced drastically, which is done in this version of the data management concept by a Matlab script. This final analysis could even be completely omitted, by incorporation of all calculations and fittings into the PHP script. In this version of the automatization concept, it was chosen to do this final analysis of the data using Matlab, mainly due to the limited time resources available for this project. In the next section the database design to store the data into will be emphasised a bit more.

3.4.2 Database design

The database designed for this project is a very simple relational database consisting of three main tables to store the experimental data. In figure 3.5 a representation of the database structure is shown.

During the data storage into the database by the Labview over HTTP to MySQL wrapper as described in the previous section, each measurement (table: 'Analysis') is stored and linked to the corresponding catalyst (table: 'Individual') through the fields 'IID', 'ValvePos' and 'EID'. The catalysts are then linked to the experiments (table: 'Experiment') by the field 'EID'. This makes it easily possible to search and to sort for catalysts and for measurements. Before each experiment, the new population of catalysts is generated automatically by the genetic algorithm and stored into the table 'Individual'. Only the table 'Experiment' has to be filled up manually using the HTML based interface to the MySQL database.

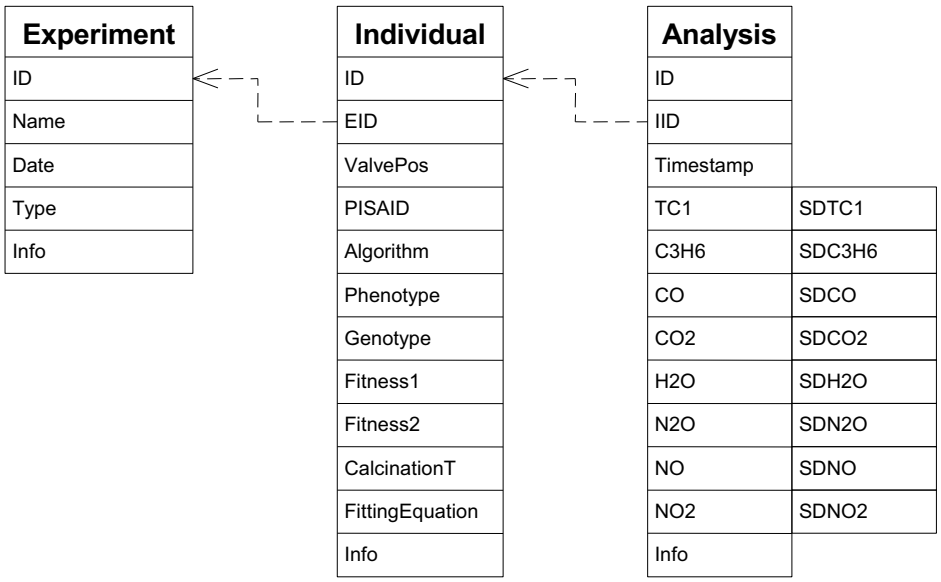

Figure 3.5: Database structure of the deNOx SQL database.

3.4.3 Final post-processing and visualisation

As stated before, the final analysis is done by a Matlab script. The other option, to directly analyze and visualize the data online on a website, was not implemented, mainly due to the limited time resources. In further studies, the online analysis could reduce the post-processing time significantly.

In brief, the post-processing essentially tries to reduce the error of the available data, by rejecting outlier data points and by calculation of the standard deviation δ of each measurement. It also corrects the temperature of each reactor channel by using the temperature correction matrix obtained during the measurements of the temperature distribution as will be described in section 3.5.1.

For NO, C_3H_6 and $NO_x = NO + NO_2$, the conversion is calculated according to the following equation:

$$X_i(t) = \frac{c_i(0) - c_i(t)}{c_i(0)} \pm \frac{\delta c_i(t)}{c_i(0)} \tag{3.1}$$

The conversion of NO to NO_2 and N_2O is obtained as follows:

$$Y_i(t) = \frac{\nu_i c_i(t)}{c_{\mathrm{NO}}(0)} \pm \frac{\delta \nu_i c_i(t)}{c_{\mathrm{NO}}(0)} \tag{3.2}$$

thereby ν_i is 2 in the case N_2O and 1 in the case of NO_2. In the case of N_2, the NO conversion to N_2 can not be directly calculated using this equation, because N_2 is not detectable by FTIR. From the measured concentration values for NO, NO_2 and N_2O in the effluent gas stream the following equation can be used to calculate the conversion to N_2:

$$Y_{N_2}(t) = \frac{c_{\mathrm{NO}}(t) - c_{\mathrm{NO_2}}(t) - 2c_{\mathrm{N_2O}}(t)}{c_{\mathrm{NO}}(0)} \pm \frac{\delta c_{\mathrm{NO}}(t) + \delta c_{\mathrm{NO_2}}(t) + 2\delta c_{\mathrm{N_2O}}(t)}{c_{\mathrm{NO}}(0)} \tag{3.3}$$

A smoothed spline is used to fit the data. Generally the NO to N_2 conversion was fitted. The weighted least square regression method is used to minimize the sum of square residuals. Outlier data points are identified during this process automatically and afterwards the fit is recomputed. From this fit, the objective functions, the maximal conversion to N_2 and the temperature at which the maximal conversion $T_{\mathrm{max,Y}}$ occurs are obtained. The genetic algorithms used in this work try to minimize the objective functions. Therefore the obtained values are normalized and converted to the final objective functions, using the following equations:

$$f_1 = 1 - Y_{N_2} \tag{3.4}$$

$$f_2 = 1 - \frac{T_{\mathrm{max,Y}} - 800\mathrm{K}}{150\mathrm{K} - 800\mathrm{K}} \tag{3.5}$$

Figures of all catalyst for all calculations are automatically generated and saved as images files for visualisation and manual analysis. In appendix C the pseudocode of the final post-processing is listed in algorithm C.1.

3.5 Measurements and results

3.5.1 Temperature characteristics

The temperature characteristics of the reactor with an external insulation was measured using up to 16 type N thermocouples. The thermocouples are connected to the Mini8 controller and thus, it is possible to use the Labview program to obtain and to record the temperature for each thermocouple at the same time. The insulation of the reactor consists of ceramic fiber wool plates of 5 to 10 cm depth.

Heating and cooling behaviour

As already mentioned in the previous section, the heating system of the reactor consists of 48 heating elements, which are controlled by a PID controller. All the 48 elements are treated together as one heating device. The controller was trained previously at an intermediate temperature of 573 K using iTools.

In figure 3.6 the heating behaviour with and without a temperature ramp is shown. In the case of the heating-up of the reactor without a temperature ramp the set-point was set to a constant temperature of 473 K. In the second case, a linear temperature ramp of 200 Kelvin per hour was used to reach the new set-point. The set-point value was calculated by the Labview program. In both cases the starting temperature was 313 K. After reaching the set-point the heater was automatically switched off by the Labview program.

In both cases no overshooting could be observed, which is very important, because the cooling of the reactor takes much more time than the heating. In the second case,

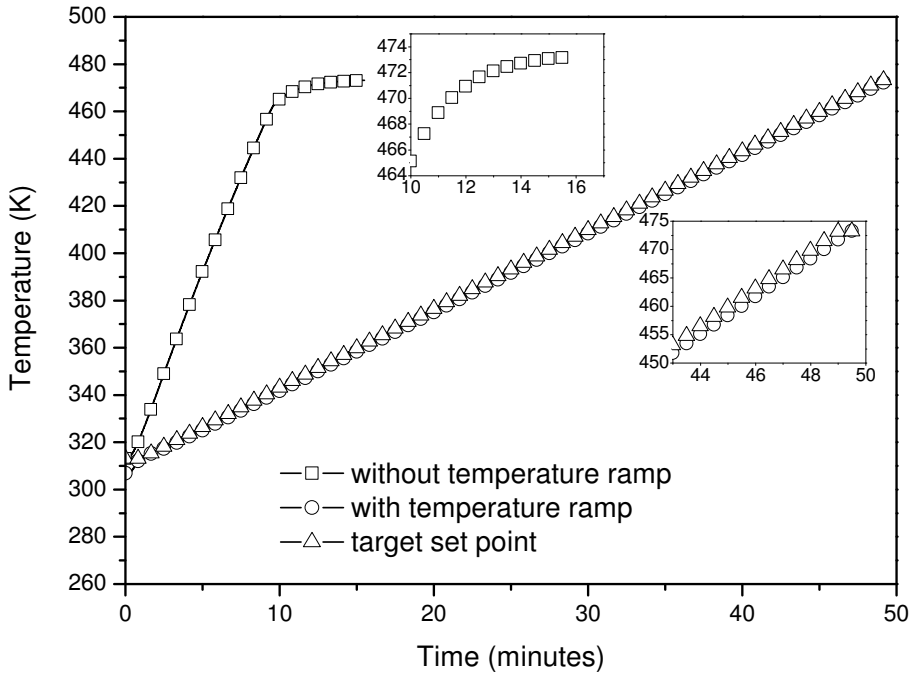

Figure 3.6: Heating-up behaviour of the reactor in the case of a controlled heating with and without temperature ramp.

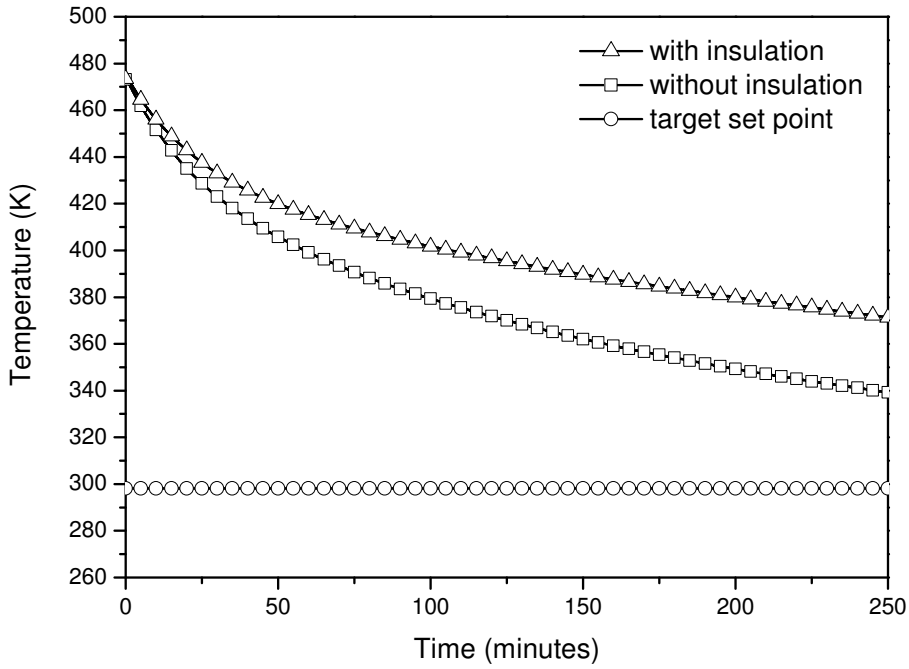

Figure 3.7: Cooling-down behaviour of the reactor, with and without insulation.

where a temperature ramp was used to reach the new set-point, it can be seen, that the actual temperature of the reactor is following the linear ramp with a high accuracy and also linearly.

The cooling behaviour of the reactor is shown in figure 3.7. As expected, the cooling-down follows an exponential trend and takes much more time than the heating-up of the reactor. As can be seen in figure 3.7, the cooling rate can be increased by removing the top insulation of the reactor. The cooling time with insulation from a stating temperature of 773 K is about 12 h, whereas the cooling time without insulation at the top is about half of it.

Temperature distribution

The horizontal temperature distribution of the open reactor was measured with 16 type N thermocouples at 373 K, 573 K and 773 K for all 49 channels independently in a depth of 77 mm. The thermocouples were connected to the Mini8 controller and read out by the Labview program developed to control the reactor. In figure 3.8 the results are shown for the three temperatures in relative units. For the inner channels the temperature is about 1.5 % above the temperature measured at the edge of the reactor. For instance at a reactor set-point temperature of 700 K, the inner channels would be approximately 10.5 K hotter than the channel located at the edge. As can be seen the relative deviations are essentially constant for all three temperatures. Thus it is reasonable to calculate the average relative deviation for each reactor channel and to use these values as correction factors.

The vertical temperature distribution of the open reactor measured for 8 different channels at 573 K (not shown here) reveal that the temperature variates much stronger vertically than horizontally. This is certainly also due to the open reactor, but measurements of the vertical temperature distribution of the closed reactor carried out by the hte company (hte), also indicated an important temperature variation. It is therefore very important to always place the catalyst bed at the same height into the cartridges.

3.5.2 Flow distribution

A uniform and homogeneous flow distribution is very important for good and reproducible results. Several aspects have to be considered and influence the flow distribution. Most important is the pressure drop of the system. The pressure drop in the exhaust and analysis line should be significantly (more than 10 times) higher than the pressure drop of the packed bed in the cartridges. The pressure drop in the exhaust and analysis line for an unpressurized system is mainly due to the pressure drop in the capillaries. An estimation of both pressure drops is possible using the Hagen-Poiseuille equation in the case of the pressure drop of the capillaries and the Ergun equation for the pressure loss

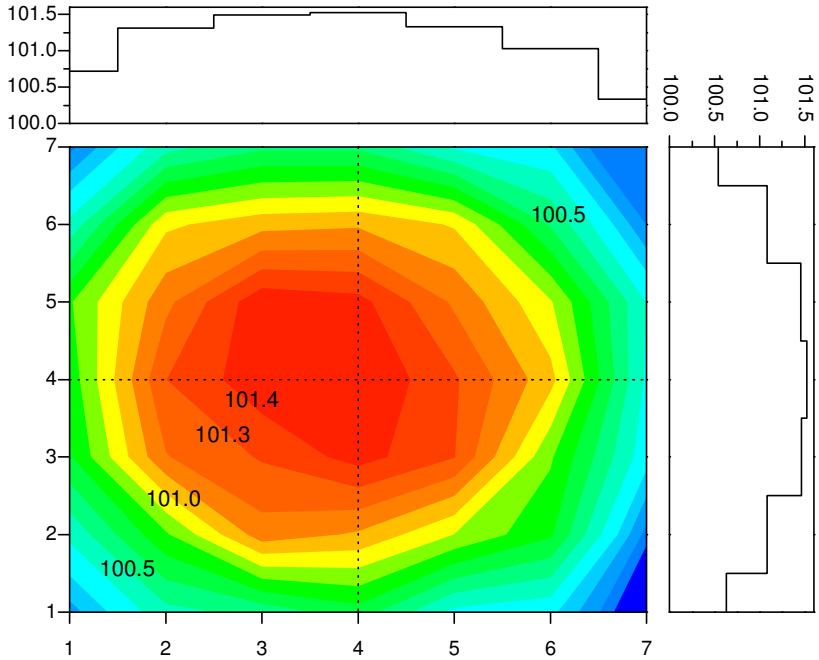

Figure 3.8: Average relative temperature distribution of the open reactor in percent measured at three different temperature. 100% represents the set-point temperature and only the deviations are plotted. The dotted lines show the location of the profiles, shown in the top and right inset figure.

of the packed bed:

$$\Delta p_{\text{capillaries}} = \frac{8\eta l \dot{V}}{\pi r^4} \tag{3.6}$$

$$\Delta p_{\text{bed}} = \lambda \cdot \frac{H_{\text{bed}}}{d_{\text{p}}} \cdot \frac{\rho \dot{V}^2}{2} \tag{3.7}$$

$$\text{with } \lambda = \frac{1-\epsilon}{\epsilon^3}\left(3.5 + (1-\epsilon)\frac{300}{\text{Re}}\right) \tag{3.8}$$

where Δp_i is the corresponding pressure drop, l the length of the capillaries, $\dot{V}$ the fluid velocity of the gas stream, r the radius of the capillary, H_{bed} the height of the packed bed, d_{p} the particle diameter, ϵ the void fraction of the packed bed and $\text{Re} = v\rho d_{\text{p}}/\eta$ the Reynolds number.

The length of the capillaries is about 35 cm, with a diameter of 1.59 mm. For a N_2 flow of 50 ml/min and a particle diameter of 500 μm, the Reynolds number is roughly one. The generally accepted value for the porosity of a randomly packed bed of uniform spheres is 0.36 (Reyes and Iglesia, 1991). According to equation (3.7) the pressure drop due to the packed bed for a space velocity of 20000 GSHV h^{-1} can be calculated to 13 Pa. The resulting pressure drop in the capillaries is about three times higher than the one due to the packed bed. This estimate shows, that the higher pressure drop is as desired

located behind the packed bed, but not as significant as it should be. By additionally controlling the pressure drop of the exhaust and of the analysis line by using mass flow controllers or valves, the pressure drop behind the packed bed can be increased. It should be set to a value such that the flow rate in the analysis line is the 49st part of the total flow rate.

In this work, the pressure of the exhaust line was set to $1.15 \cdot 10^5$ Pa (15000 Pa overpressure) using the valve for the exhaust line. The flow rate in the analysis line was then set to the correct value, by changing the pressure drop of the analysis line using a low flow valve. The resulting pressure in the analysis line was roughly the same as in the exhaust line, which is an indication for a good flow distribution. The flow rates were measured using a soap bubble meter.

The next part of the reactor which influences the flow distribution is the diffusor plate, which is placed between the top of the reactor and the reactor channels. The diffusor plate consists of 2 mm bores opening into conical holes on top of each cartridge. The main task of this plate is the prevention of backmixing, due to the high linear flow through the small bores. Another task is to provide a homogeneous flow distribution. However, more important for the flow distribution is the control of the pressure drop after the packed bed.

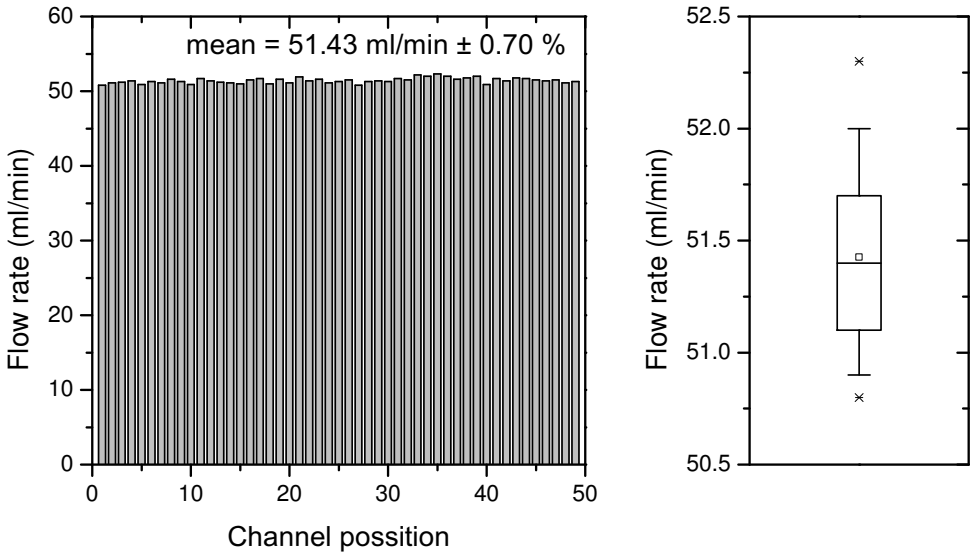

Figure 3.9: Flow distribution of the 49 parallel channel reactor measured at 20000 h^{-1}. The theoretical average flow rate in each channel should be 52 ml/min.

The flow distribution was measured at 20000 h^{-1} corresponding to a total flow rate of 2566 ml/min and a theoretical flow rate of each reactor channel of about 52 ml/min.

The distribution was measured with catalyst loadings just like under reaction conditions with a soap bubble meter connected to the analysis line. In figure 3.9 the measured flow distribution is shown. An average flow rate in the reactor channels of 51.43 ml/min is reached during the experiment. As can be seen in the right of figure 3.9 the distribution is very narrow with a standard deviation of 0.36 ml/min. This indicates a very good flow distribution with an error of less than 1%.

3.5.3 Empty conversion

The activity of the empty reactor was first checked for the new reactor in a preliminary test. During all experiments, one channel was always left empty to check, if the blank activity is increasing over time. In figure 3.11 the maximal conversion of NO to N_2 is shown for 25 reactor channels. The reactor only has a slight activity for the combustion of propene; the reduction of NO under oxygen rich conditions seems to be a too difficult reaction and nearly no activity was observed for all experiments carried out during this work.

3.5.4 Catalytic activity and conversion distribution

Throughout this work the industrial 5%-Pt/Al_2O_3 noble metal catalyst will serve as reference. In figure 3.10 the catalytic activity is shown. As can be seen, the selectivity towards N_2 is most of the times less than 0.5 and a number of byproducts is formed. At maximal NO conversion also the yield to N_2O is maximal. At higher temperatures propene is easily oxidized by oxygen and most of the NO is converted to NO_2 but not any more to N_2. The very narrow temperature window of the NO to N_2 conversion arises from this competitive system of reactions. The Pt/Al_2O_3 system has been extensively studied by several scientists in the last decades (Burch et al., 1998, Captain and Amiridis, 1999).

The conversion distribution of the reactor was obtained by placing the same amount of the reference Pt/Al_2O_3 catalyst from the same batch into 24 channels of the reactor. The other 24 channels were left empty to see if the reactor channels are influencing each other. This should not be the case if the flow rate and the dead time are high enough to guarantee stable conditions. The typical settings for the reactor and the FTIR used throughout this work for the catalytic measurements are listed in the appendix B.

Figure 3.11 and 3.12 show the distribution of the maximal conversion of NO to N_2 and the temperature at which the conversion is maximal (the so called peak temperature). The calculation of these two objective functions was done just as described in section 3.4.3 using equation 3.3 to calculate the conversion of NO to N_2 from the measured concentrations.

The conversion distribution shown in figure 3.11 is very narrow with a standard deviation of 0.0167 corresponding to an error of about 3.4 %. The maximal deviation from the average value is about 0.03 (6 %). This error can be interpreted as the error of

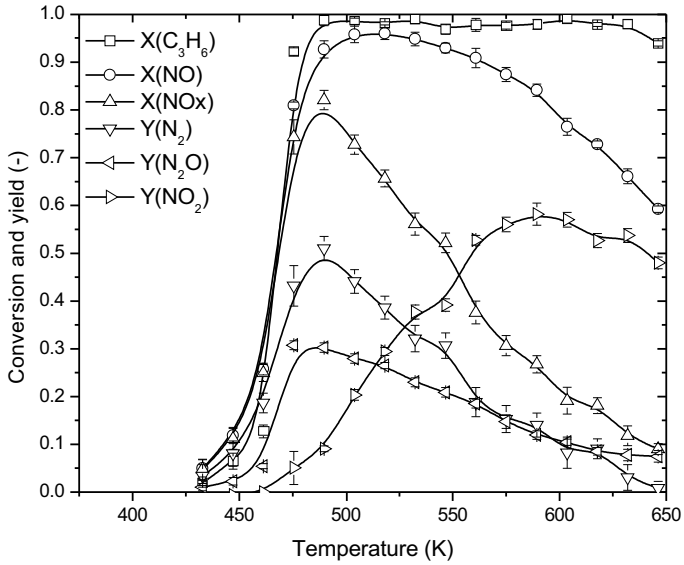

Figure 3.10: Catalytic activity of Pt/Al_2O_3 under lean burn conditions.

the reactor system and is sufficient for a stage II screening. In the case of the distribution of the peak temperature of the NO to N_2 conversion the error is even smaller as visualised in figure 3.12. The standard derivation is about 2 K. Also it can be easily seen, that the channels are not influencing each other. The maximal conversion of the empty channels is in no case higher than 0.03.

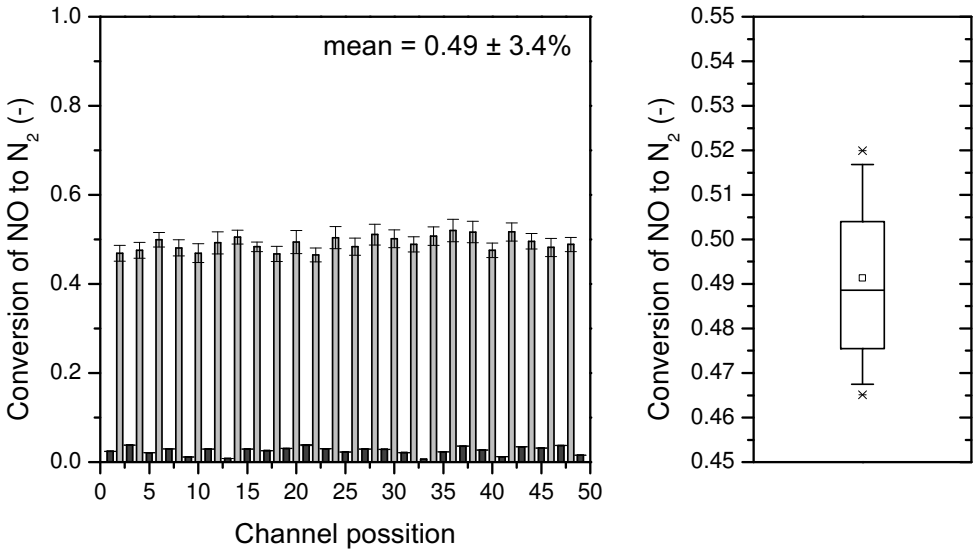

Figure 3.11: NO to N_2 conversion distribution measured with Pt/Al_2O_3.

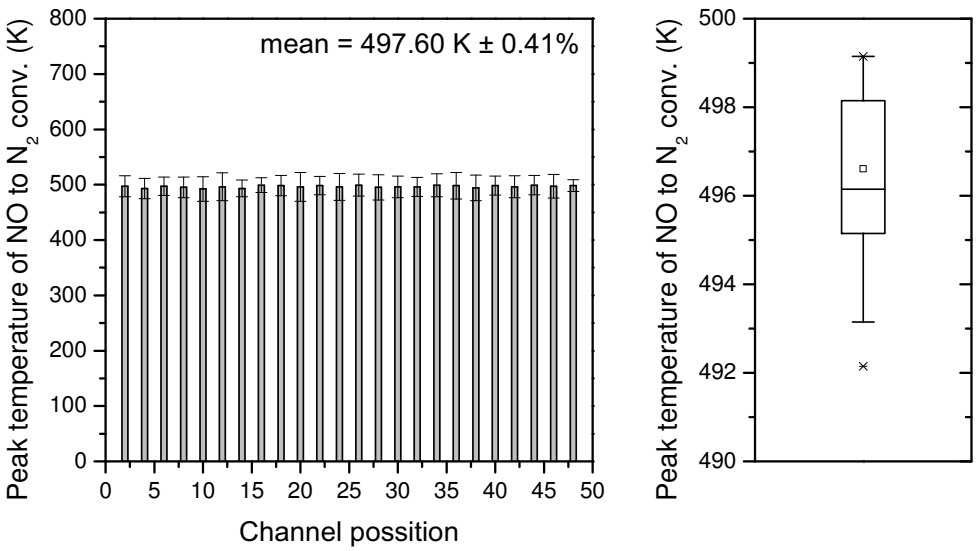

Figure 3.12: Peak temperature distribution of the NO to N_2 conversion.

4 High-throughput synthesis

4.1 Introduction

Solid catalysts are highly complex materials. A material with a very high surface area but without an active phase will show no activity. Even a material with a highly active phase, but which is not accessible to the molecules due to a low surface area, a too small pore system or other hindrances, will show no or only a very low activity. Hence, one general requirement necessary to obtain a highly active catalyst is to provide a surface area high enough, such that the active phase is accessible for the reacting molecules. This is due to the fact that heterogeneous catalyzed chemical reactions basically occur on surfaces or at phase boundaries, thus a higher surface area would, theoretically, directly result in an improved reactivity.

In high-throughput experimentation not only a fast set-up for catalyst testing but also a fast and reproducible synthesis of solid catalyst is required. The synthesis of mixed oxides with multiple components, providing a high surface area, is often very difficult. Schwickardi et al. (2002a) developed in 2002 a synthesis route for high surface area mixed oxides, which is easily parallelizable. The method is based on the hard templating route (Schuth, 2003, Schwickardi et al., 2002a,b), which made it possible to obtain multi component oxides with a high BET surface area in the range of 50 m^2/g to 200 m^2/g, using a very easy synthesis, based on inexpensive components.

In the following section first the synthesis route will be described and afterwards some of the properties of these materials will be shown.

4.2 Synthesis of mixed metal oxides

In brief, the synthesis was carried out using an activated carbon as exotemplate, which was impregnated with highly concentrated metal nitrate solutions. The carbon and the nitrate precursor were afterwards calcined at high temperature, leading to a combustion of the carbon exotemplate and the formation of a metal oxide framework. This complete process was carried out in a high-throughput fashion by using a synthesis robot for the mixture of the nitrate precursors and for impregnation of the active carbon. Up to 80 catalysts can be prepared in such a way in parallel per day. The different steps of this synthesis procedure will be depicted in detail in the following sections.

4.2.1 Activated carbon as exotemplate

The basic idea of templating is shown in figure 4.1A. A porous material with an interconnecting pore system is generally used, in order to form a high surface oxidic material as a replica of the original pore structure. A high loading and an interconnecting pore structure is necessary to obtain a material that is negative to the structure of the template. In contrast, if the exotemplate does not have a continuous pore system or if the loading of the metal precursor is not high enough, small particles are obtained as shown in figure 4.1B.

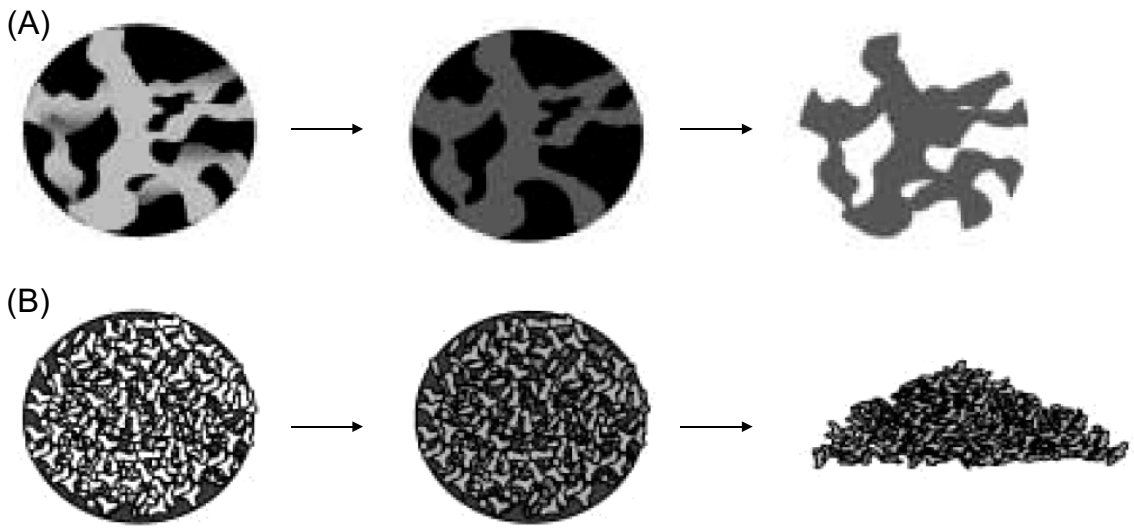

Figure 4.1: Schematic representation of the exotemplating pathway to produce porous and high surface area mixed oxides. In figure (A) the pore system of the exotemplate is continuous and the resulting material corresponds to a negative copy of the template. In figure (B) the resulting material is not 3D connected any more due to a bad impregnation, only a partial filling of the pore system of the exotemplate or a non-continuous pore system, leading to the formation of small particles. Adapted from (Schuth, 2003).

In this work, the activated carbon R1424 from Carbotec / Rütgers was chosen as exotemplate, because of its exceptional properties: the purity is high and the BET surface area (1800 m^2/g) and the pore volume (0.9 cm^3/g) are very high. The particles are almost uniform spheres of 200 to 400 μm diameter as can be seen in figure 4.2B and 4.2C by scanning electron microscopy (SEM) imaging (see appendix A). The adsorption isotherm in figure 4.2A indicates, that the pore structure consists of a very high fraction of micropores with a diameter less than 1 nm. All these properties make this activated carbon an ideal exotemplate for catalyst preparation. Additionally, to make sure that the quality of the activated carbon is the same for all samples, only activated carbon from the same activation batch was used. The synthesis is reproducible as will be shown later in this chapter, the resulting metal oxides have a high surface area, are in parts crystalline or amorphous depending on the metal concentration, and are most of the

times uniform shaped spheres, just like the activated carbon precursor particles. For some metal compositions, the spherical structure collapses and the resulting structure is not spherical any more, but in most of the cases, a regular shape can be assumed, which is very important to compare the results obtained by testing the catalytic activity in the reactor.

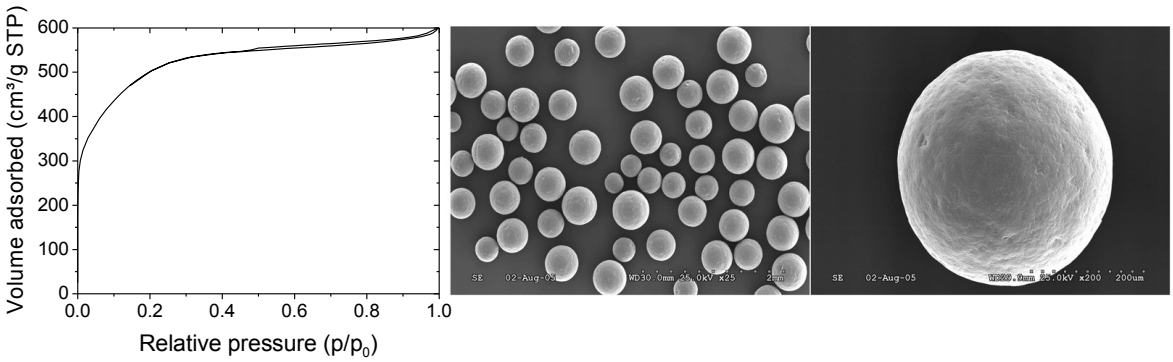

Figure 4.2: Figure (A) shows the adsorption isotherm of activated carbon R1424 containing a large fraction of micropores and nearly no meso- or macropores. In figure (B) and (C) SEM images of activated carbon R1424 particles with a diameter of 200 to 400 μm are shown.

4.2.2 Impregnation and calcination

The impregnation was carried out using an automated liquid handling robot from ABIMED as can be seen in figure 4.3. This is not the most advantageous way to impregnate the activated carbon, but a manual synthesis would not be efficient enough for this project. Schwickardi et al. (2002a) studied different types of impregnation under various conditions and it was observed, that the best results are obtained by vigorous stirring of the active carbon, while adding highly concentrated metal salt precursors. As metal precursors all kind of different metal salts, as for instance nitrates, sulfates, chlorides, alkoxides, acetates or acetylacetonates are possible. The best results with respect to surface area were obtained by impregnation using nitrates. In this work all the metal precursors were 2 M solutions of the corresponding nitrates. Martinez Joaristi found out, that a small amount of isopropanol reduces significantly the surface tension of the nitrate solutions and thus improves the penetration of the precursor molecules into the pore system. A small amount of isopropanol was therefore added to all solutions.

One of the most important parameters influencing the impregnation is the amount of solution added per amount of active carbon. The ratio of added volume of the precursor solution and the available pore volume of the active carbon is denoted as spv-ratio:

$$\text{spv-ratio} = \frac{V_{\text{solution}}}{m_{\text{AC}} \cdot v_{\text{pore}}} \tag{4.1}$$

Figure 4.3: ABIMED liquid handling robot robot for automated precursor mixing and impregnation of activated carbon (Martinez Joaristi, 2007).

where V_{solution} is the volume of the precursor solution in milliliter, m_{AC} the mass of the activated carbon in gram and v_{pore} the specific pore volume in milliliter per gram of activated carbon.

A spv-ratio of 1.0 would mean an impregnation with an amount of precursor solution corresponding exactly to the volume of the pores, hence the pores would be completely filled without solution remaining outside. A spv-ratio less than 1.0 would therefore mean that the pores are not completely filled with solution, a ratio higher than 1.0 means there is still some solution outside the pores. In this work a spv-ratio of 1.1 was used for the automatic impregnation with the robot. A small excess of solution is important for this kind of impregnation in order to be sure, that the metal salts solutions are wetting all the activated carbon, also at the bottom of the quartz glasses (see figure 4.3). This is important, as the metal nitrates catalyse the combustion of the activated carbon and regions of dry carbon would not be combusted completely during the calcination.

The calcination was afterwards performed without additional drying process always in the same oven at a temperature of 973 K for three hours for all samples in this work, if not otherwise specified. This calcination temperature is rather high, but a full combustion of the carbon is guaranteed under these conditions. Such a high temperature improves also the ability to form crystalline phases, which could be active in deNOx. However, it is important to note, that especially for samples with a low amount of aluminium oxide, the metal particles tend to sinter leading to catalysts with low BET surface area. This is due to the fact, that aluminium is able to form oxides with a high surface area and is thus good for providing the support framework for the remaining metal oxides.

4.3 Results and reproducibility of the synthesis

The reproducibility of the synthesis was checked by performing several test on a series of ten equal catalysts composed of a ternary metal oxide supported on aluminium oxide. The synthesis was performed exactly as previously described with the help of the liquid handling robot (see figure 4.3) and a spv-ratio of 1.1. The catalysts were impregnated with a nitrate mixture consisting of 70 % Al, 12 % Cu, 6 % Fe and 12 % Ce (denoted as: Al-0.70-Cu-0.12-Fe-0.06-Ce-0.12). To check the reproducibility and to quantify the error of the synthesis, physisorption, XRD and catalytic measurements were performed. The results are visualized in figure 4.4 and 4.5. The catalytic tests were performed under the same reaction conditions just like all other catalytic measurements in this thesis (the exact conditions are listed in appendix B). The experimental conditions for physisorption and XRD measurements are described in appendix A.

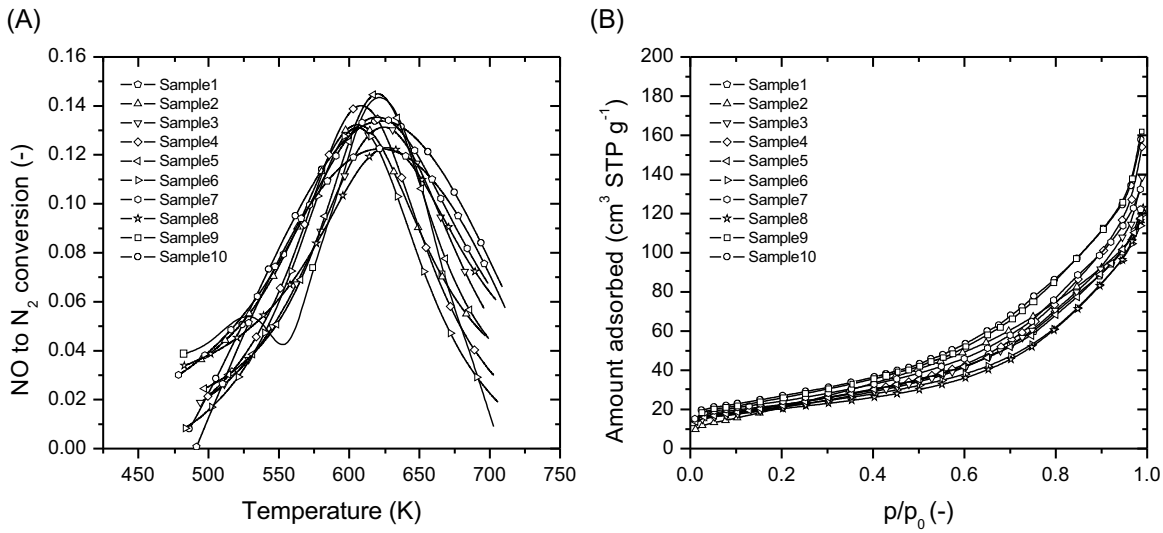

Figure 4.4: Catalytic activity (A) and N_2 physisorption (B) measurements of ten Al-0.70-Cu-0.12-Fe-0.06-Ce-0.12 mixed oxide samples synthesized by automated synthesis with the help of the ABIMED robot.

The results indicate that the reproducibility is high enough for a stage II screening approach. The maximal NO to N_2 conversion of the metal oxide catalyst Al-0.70-Cu-0.12-Fe-0.06-Ce-0.12 is 0.133 ± 0.007 and the peak temperature of the maximal conversion 618.6 ± 7.1 K. This corresponds to an error of about 5 % (standard deviation) in the case of the peak conversion and of less than 1.5 % in the case of the peak temperature. The maximal error in the case of the peak conversion is roughly 9 % as can be seen in figure 4.5 and corresponds to the maximal possible error of the catalytic test together with the synthesis procedure. The error of the physisorption results is about 9 % (standard deviation) for the BET surface area and for the measured total pore volume at $p/p_0 = 0.98$. However, this error is composed of the error of the synthesis, the error of the sorptometer, and the error of the analytical balance used to measure the weight of the

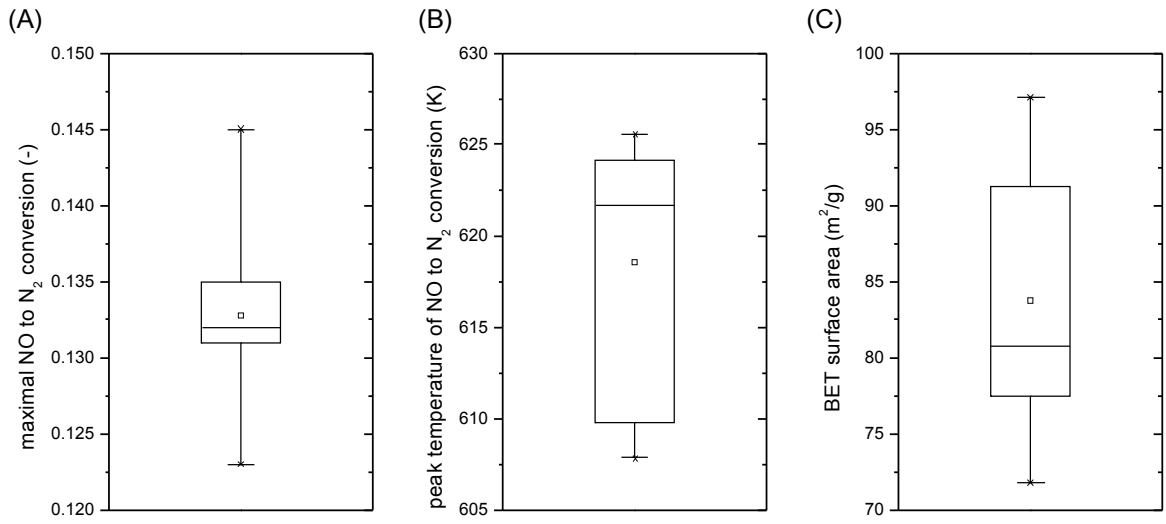

Figure 4.5: Boxplots of ten Al-0.70-Cu-0.12-Fe-0.06-Ce-0.12 mixed oxide samples synthesised by automated synthesis showing the distribution of the maximal NO to N_2 conversion (A), the peak temperature of the NO to N_2 conversion (B) and the BET surface area obtained by N_2 physisorption.

sample. The error obtained by this catalytic test is therefore the relevant error for the interpretation of the optimization results.

Additionally to the reproducibility check of ten identical samples, the morphology of the calcined metal oxide catalysts was studied by scanning electron microscopy. Results of selected samples are shown in figure 4.6. Nearly in all of the cases a very good negative replication of the activated carbon exotemplate was obtained. During the calcination, generally the particle diameter diminished slightly to 100 to 300 μm. In very few cases the structure collapsed completely as can be seen for the case of Al-0.667-Ni-0.333 in figure 4.6. This result is reproducible for single component oxide only containing Ni. As can be seen in the case of Al-0.5-Cu-0.20-Ni-0.20-Co-0.08-Fe-0.02, as an example of a multi component oxide, the resulting particles are not spherical any more, due to an anisotropic shrinkage during the calcination process. The particles are mechanically stable, but in all cases broken particles could be observed. During the loading of the reactor the sample glasses were always shaked slightly, in order to settle the smaller particles to the bottom of the sample glasses, so that the reactor is only loaded with intact particles.

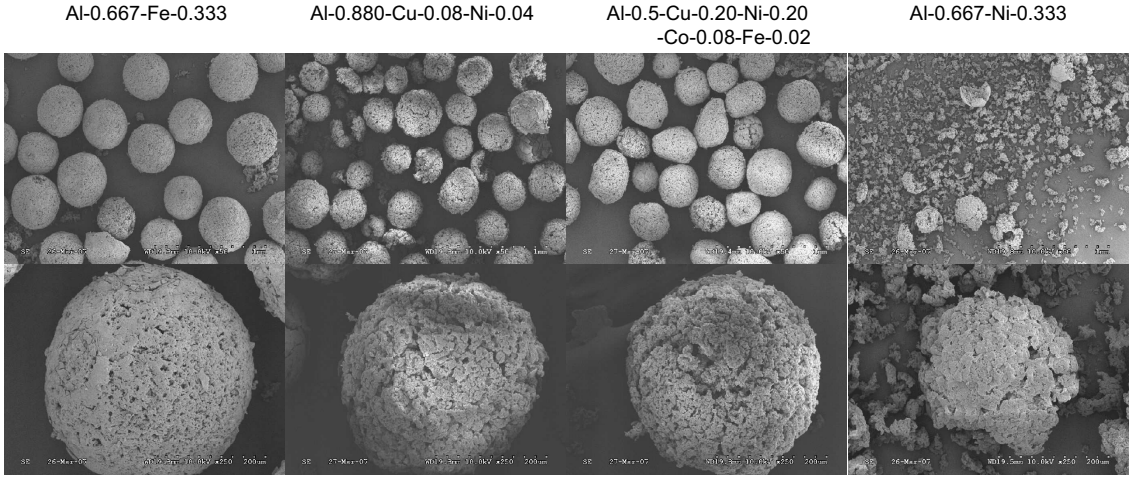

Figure 4.6: SEM images of several mixed oxide samples synthesized by exotemplating and automated impregnation.

5 Evolutionary multi-objective optimization

5.1 Introduction

Optimization can be defined as the search for solutions, which solve a problem in an improved or even optimal way. Optimal means, that the solution to the problem is the best solution in the feasible region. Two different types of optimal solutions exist: the one which are optimal in the complete feasible region, the global optimal solutions, and the one, which are only optimal in a subspace of the feasible region, the local optimal solutions.

A set of known or unknown variables generally span the so called search space, which can be constrained. Optimization problems, which do not require the definition of an objective function are called feasibility problems, but in general single or multiple objective functions are to be minimized or to be maximized.

Especially real world problems often involve the simultaneous optimization of several and often competing objectives. In the case of only one objective the solution is clearly defined and only one possible solution exists. In contrast, in the case of multi-objective optimization, where we try to optimize all the objectives at the same time, the situation is completely different, as two optimal solutions may be different to each other. The optimal solution is thus a composition of all optimal solutions with respect to multiple objectives and usually form a set of optimal trade-off surfaces, which also include the single objective optimum. Generally, the goal in multi-objective optimization, is to approximate this set of optimal solutions. Several techniques were developed to solve this kind of problems ranging from classical techniques (Loganathan and Sherali, 1987, Rosenthal, 1985), which are trying to reduce the search field by weighting the objectives with respect to their importance, to modern and rather sophisticated algorithms (Li, 2003, Shelokar et al., 2002, Zitzler and Thiele, 1999). The concept of a weight based approach to combine several objective functions into one overall objective function f is illustrated by equation 5.1:

$$f(x) = \sum_i w_i f_i(x) \tag{5.1}$$

where f_i are the objective functions and w_i the corresponding weights ($0 \leq w_i \leq 1$). A problem that arises in the case of weight based techniques, is how to normalise, prioritise and weight the contribution of the various objectives.

In the following chapter the algorithms used in this work will be described in detail and tested on several theoretical test cases, with similar properties as the deNOx problem. Also one focus will be the design and encoding of the deNOx problem and the experimental results obtained during the optimization. Preliminarily to this, a brief overview of some

techniques and definitions with a focus on experimental multi-objective evolutionary optimization will be given.

5.1.1 Evolutionary computing

In the last three decades there has been a growing interest in problem solving systems based on evolutionary techniques found in nature (King et al., 2005). Genetic algorithms are one type of evolutionary optimization methods, others are, for instance, swarm-based optimization algorithms (Li, 2003, 2004, Reddy and Kumar, 2007, Santana-Quintero et al., 2006). Such kind of systems are heuristic global search methods, as they include heuristic strategies to search the search space in an intelligent way. Non-heuristic, but stochastic global search methods are, for instance, Monte-Carlo based methods like simulated annealing (Suman, 2004, Suppapitnarm et al., 2000) or parallel tempering (Liu, 1999). Genetic algorithms involve techniques which are inspired by evolutionary biology: they maintain a population of potential solutions and the solutions undergo recombination, mutation and selection steps during each iteration. One iteration loop is called a generation. After a certain number of generations the algorithm converges and it hopefully finds the globally optimal solution. The basic structure of an evolutionary algorithm is shown in algorithm 5.1.

```
1 t := 0
2 initialize P(t)
3 evaluate P(t)
4 while not termination-condition do
5 |   t := t + 1
6 |   select P(t) from P(t − 1)
7 |   alter P(t)
8 |   evaluate P(t)
9 end
```

Algorithm 5.1: Structure of an evolution algorithm.

As can be seen in figure 5.1 three different metric spaces can be defined: the decision space, where the solutions to the actual problem are defined, the individual or search space, which is the representation of the individuals of the decision space, and the objective space, which maps the individuals of the decision space according to their fitness as will be shown in the next section. A decoder function is generally used to map the search space to the decision space. The representation of a solution in the search space is denoted as a chromosome.

Global search methods are typically stochastic and only very few deterministic methods exist. One deterministic global optimization method is, for instance, the terminal repeller unconstrained subenergy tunneling algorithm (TRUST), which was developed by Barhen et al. (1997). In contrast, most of the local search methods are deterministic as for instance the gradient descent method (Battiti, 1992) or the simplex algorithm Lagarias et al. (1998), Watson and Carr (1979). It is important to note, that due to the stochastic

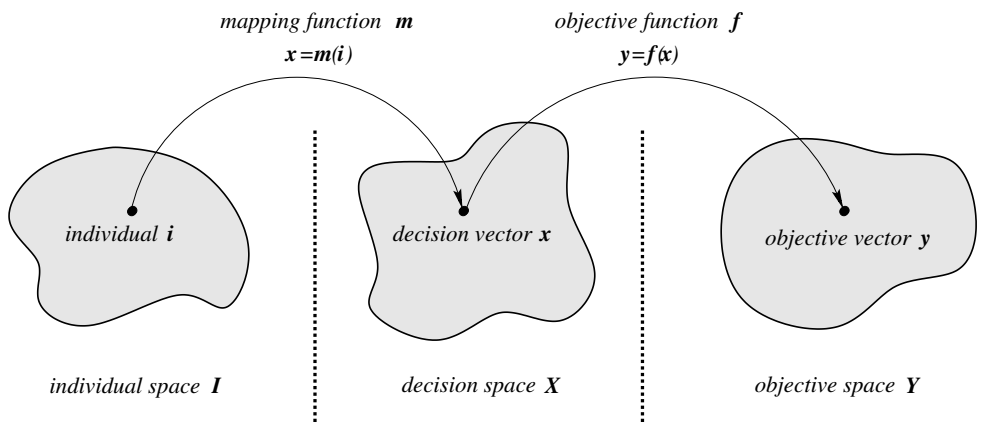

Figure 5.1: Three common metric spaces in evolutionary computation: the search or individual space, the descision space and the objective space (Zitzler, 1999).

nature of the algorithm only a certain probability of converging towards the global optimal solution can be given. One can never be sure, that the algorithm was able to find the optimal solution. Also the performance of a global search method for local optimization is often inferior to the one for a deterministic local search method. However, it is simple to hybridize a global search method with a local search method to combine the strength of both.

5.1.2 The multi-objective optimization problem (MOOP)

An important difference between single- and multi-objective optimization was already given in the introduction. To be more precise, the fact that a trade-off front must exist during multi-objective optimization is, that there is no natural sort order of points of the n-dimensional Euclidean space, if $n \geq 2$. Hence, a solution can not be directly compared to another and a subspace of optimal solutions with respect to the multi-objective problem exists, which is generally denoted as the Pareto-optimal set. The concept of Pareto-optimality will be described in more detail in section 5.1.3. Some examples of multi-objective optimization problems (MOOP) are:

- The design of microwave absorbing structures, with simultaneous optimization of performance and cost (Cui et al., 2005).
- The minimization of the pulsation of the burner and of the emissions during a combustion process (Buche et al., 2002).
- The maximization of the yield of cyanobacteria and of the cell growth or the optical density of the cells at 730 nm (OD_{730}) during media optimization in biotechnology (Havel et al., 2006).

A MOOP can be defined as finding a vector of decision variables $\mathbf{x}$ in the decision space $\mathbf{X}$, which optimizes a vector function

$$\mathbf{f} : \mathbf{X} \rightarrow \mathbf{Y} \tag{5.2}$$

by assigning the quality of a specific solution $\mathbf{x}$ to a vector of objective variables $\mathbf{y}$ in the multi-dimensinal objective space $\mathbf{Y}$.

5.1.3 Pareto-optimality and concept of domination

To compare solutions to each other in the objective space, most of the popular multi-objective optimization algorithms use the concept of Pareto dominance. An objective vector $\mathbf{y}^{(1)}$ is said to dominate another objective vector $\mathbf{y}^{(2)}$ in the objective space $\mathbf{Y}$ if no component of $\mathbf{y}^{(1)}$ is less good than the corresponding component of $\mathbf{y}^{(2)}$ and at least one component evaluates better:

$$\mathbf{y}^{(1)} \succ \mathbf{y}^{(2)} \wedge \mathbf{y}^{(1)} \neq \mathbf{y}^{(2)} \tag{5.3}$$

The same concept can also be applied to the decision space $\mathbf{X}$. One should note that optimal, so called non-dominated solution vectors may be mapped to different objective vectors. This means, that there may be several non-dominated objective vectors.

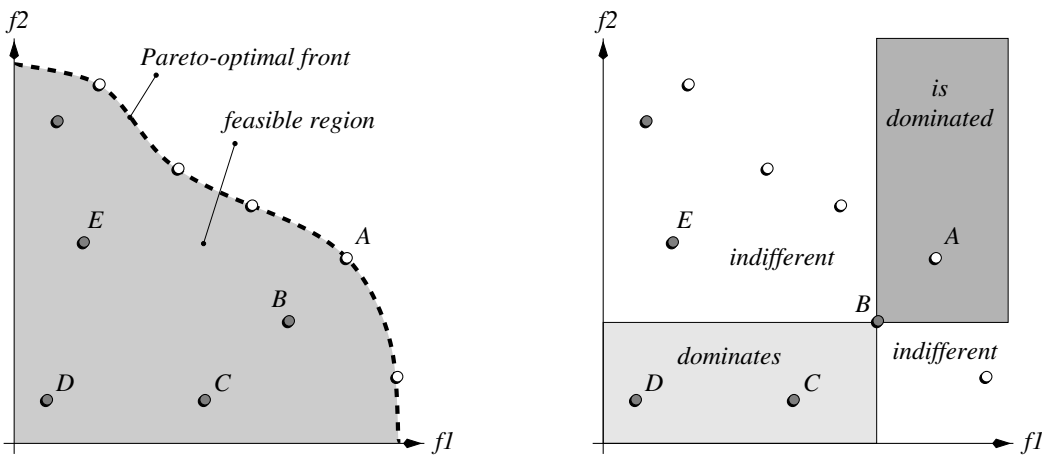

Figure 5.2: Schematic example of Pareto optimality (left) and the possible relations of solutions (right) in the objective space (Zitzler, 1999).

The set of optimal solutions in the decision space $\mathbf{X}$ is generally denoted as the non-dominated set or the Pareto-optimal set $\mathbf{X}^* \subseteq \mathbf{X}$, and its image in the objective space is denoted as the Pareto-optimal front $\mathbf{Y}^* \subseteq \mathbf{Y}$. A globally Pareto-optimal set is the non-dominated set in the entire search space $\mathbf{X}$, whereas a locally Pareto-optimal set can be defined as: if $\forall\, \mathbf{x} \in \mathbf{X}^*$ no $\mathbf{y}$ in the neighbourhood of $\mathbf{x}$ dominates any member of the set $\mathbf{X}^*$, then the solutions constitute a locally Pareto-optimal front.

The concept of domination and of Pareto-optimality is shown in figure 5.2. Both objective functions f_1 and f_2 are to be maximized. Solution A is a member of the Pareto-optimal front and is not dominated by any other solution (solution A is a non-dominated solution). Solution B is not a member of the Pareto-optimal front and is dominated by solution A but dominates the solutions C and D. Solution E is indifferent relative to solution B but dominates solution D.

5.1.4 Experimental optimization

A certain class of optimization problems often arise in experimental sciences. These problems are denoted in this work as experimental optimization problems. Generally, the fitness evaluation is difficult or costly and limits the total number of possible evaluations or generations strongly. In experimental optimization the maximum possible number is in the range of 5 to 10 generations, or 200 to 500 evaluations, which is very low in comparison to a normal genetic optimization process, where several hundred generations or thousands of fitness evaluations can be performed. The limiting factors in experimental optimization are generally time, cost or other resources.

An other characteristic of experimental optimization is the fact, that often the fitness evaluation is not highly accurate, which leads to a noisy objective space. Also often it is not possible to parallelize the fitness evaluations and thus each individual in a population has to be evaluated consecutively. Knowles (2006) developed a hybrid genetic algorithm which incorporates a local search learning heuristic, which is updated after each function evaluation. The results seem promising, but this heuristic is hard to adapt to the deNOx problem in this work, because the evaluation is done in parallel for the complete generation.

As already mentioned, typical for experimental optimization is an inaccurate fitness evaluation, leading to a noisy objective space. The optimization algorithm has to be able to deal with such a noisy landscape. Genetic algorithms already incorporate the feature to deal with noise, which is due to the fact that these algorithms are stochastic and not deterministic and always keep several solutions (a population) in parallel: A high selection pressure or even a deterministic selection would not be able to deal with noise and would therefore be a bad choice for noisy environments. However, much more important to be robust against noise is to keep a set of solutions in parallel. This is due to the simple fact, that the signal to noise ratio of a population improves and the role of outlier solutions is minimized. Therefore a genetic algorithm with a large number of individuals in a population would be more robust with respect to noise than an algorithm with only small populations (Hammel and Baeck, 1994, Miller and Shaw, 1996). The choice of the population size is a critical factor, as a too big population leads to a slower convergence and a too small population is more likely to converge towards a local optimum. For experimental optimization this choice is very difficult, as the number of maximal evaluations is strongly limited. Therefore a large population, which is very robust against noise, may not be the best choice, as the convergence is very low and a lot of evaluations have to be performed. The theoretical minimal number of individuals in a population in order to reach each point in the search space by a binary crossover from a

randomly created start population was investigated by Reeves (1993). This condition is fulfilled with a certain probability p, which is a function of the chromosome length l and the population size M:

$$p(M, l) = (1 - 0.5^{M-1})^l \tag{5.4}$$

For a binary chromosome with 27 genes, a minimum population size of 19 individuals would be required to reach each point in the search space by crossover with a probability of 99.99%. Also it is important to note, that algorithms which keep parents along the evolution process are likely to suffer in the case of a noisy environment, because solutions receiving a fortuitously good evaluation will be kept. It is very important to keep the necessary turnover for a good evolution. It was shown by Hancock (1994) that a way to implement this, is to remove old solutions during the evolution process. The removal of old individuals from the gene pool performs only slightly worse than a model, which does not keep parent solutions (a so called generational model) in the presence of noise. In figure 5.3 the effect of noise for different systems is shown. A Gaussian random variable with a standard deviation of 0.2 was therefore added to the true values to achieve a significant performance reduction.

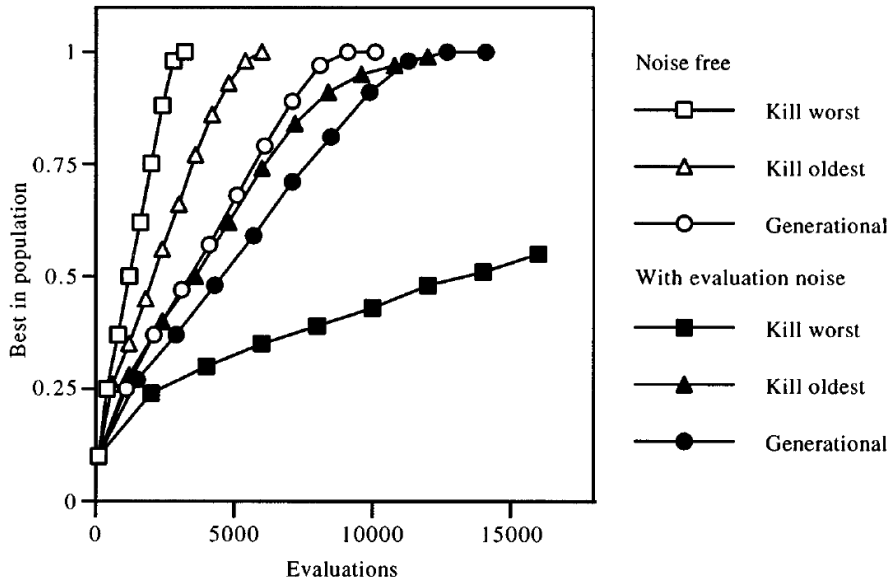

Figure 5.3: Evolution with and without evaluation noise, for a model that does not keep parent individuals (a generational model) and a model that keeps parent individuals (an incremental model). The removal of the oldest individual from the population is denoted as kill oldest and the removal of the individual with the lowest performance as kill worst. A linear ranking selection was used in both cases as mating selection algorithm (Hancock, 1994, 1997).

In this work, the number of parallel fitness evaluations is limited by the size of the reactor and the complete evaluation process (synthesis and catalytic test) takes one week. In the following sections the implementation of the multi-objective optimization framework will be described with a focus on features regarding experimental optimization.

5.2 Optimization framework

The platform and programming language independent interface for search algorithms (PISA) (Bleuler et al., 2003) was chosen to build up the optimization framework used in this work. PISA was recently developed by Beuler et al. in order to reduce the programming and implementation overhead for the application engineer and to facilitate the use of different optimization methods on different test problems. The idea behind PISA was to divide the implementation of an optimization method into an application-specific part, as for instance the deNOx problem in this work, and in an algorithm-specific part. Figure 5.4 shows this concept. This concept is highly flexible, as it makes it possible to use an arbitrary programming language for the implementation of the application-specific part and the algorithm-specific part can be used without any implementation effort. This reduces potential implementation errors significantly. Also due to this concept it is possible to separate physically the application-specific from the algorithm-specific part (for instance by running them on different operating systems), which is sometimes very useful.

In this work the application-specific part was written in Octave and runs under FreeBSD. Octave is a free programming language, which is mostly compatible to Matlab. The application-specific part is denoted as variator, as it includes all the variation operators of an evolutionary algorithm. The algorithm-specific part is denoted as selector, as it performs the ranking and selection of individuals. Several selector algorithms can be found on the PISA website and can be used without any change. In order to run under FreeBSD, only the source code had to be compiled. In figure 5.5 a general model of a search algorithm according to the PISA concept is shown. As can easily be seen, most of the evolutionary operations are performed by the variator, the selector is completely independent from the variator and has its own memory to remember former populations. The variator and selector modules interact through text files. A detailed description of the communication process between both modules can be found in (Bleuler et al., 2003). In the following sections, the variator and selector algorithm and their implementation will be described in detail. The pseudocode of the Matlab variator module is listed in appendix C (algorithm C.2).

5.2.1 Variators

As already mentioned, the complete implementation of the variator module was done in Octave. The module is able to deal with binary or real coded chromosomes and with different initial (α), offspring (λ) and parent (μ) populations sizes. A list of random numbers is included in the package, in order to have reproducible optimization runs if the random seed is kept constant. This, for instance, is required especially in experimental optimization, where sometimes the optimization process has to be restarted from the beginning.

The following variation operators were implemented for binary encoded chromosomes: a classic bit-flip (one gene) mutation, with different probabilities for individuals or

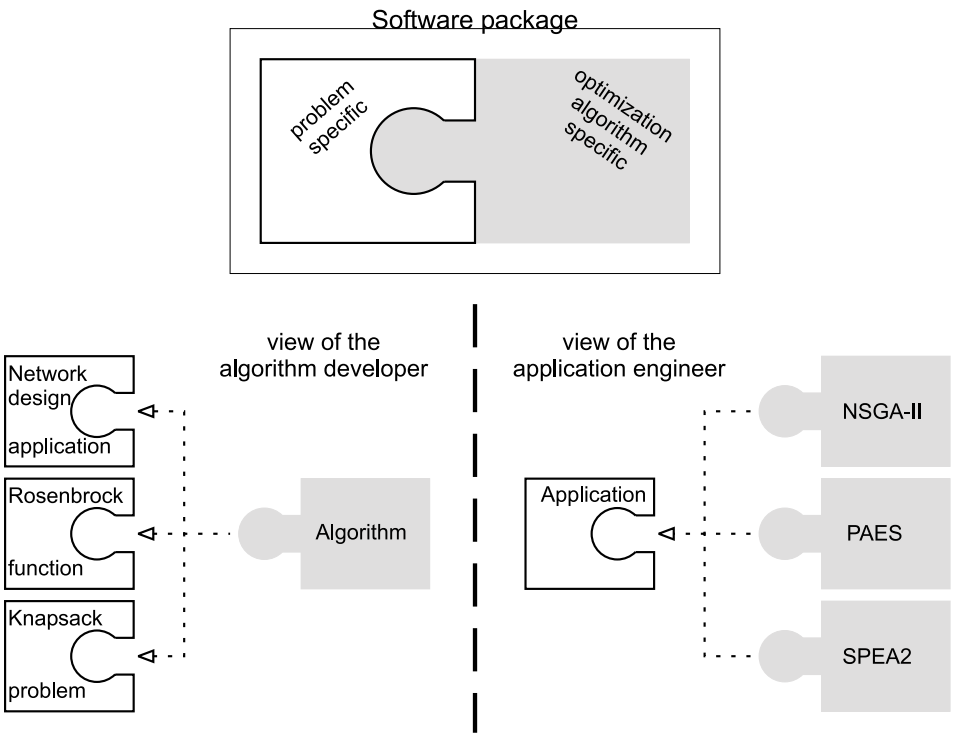

Figure 5.4: Illustration of the concept underlying PISA. The applications on the left hand side and the multiobjective optimizers on the right hand side are examples only and can be replaced arbitrarily (Bleuler et al., 2003).

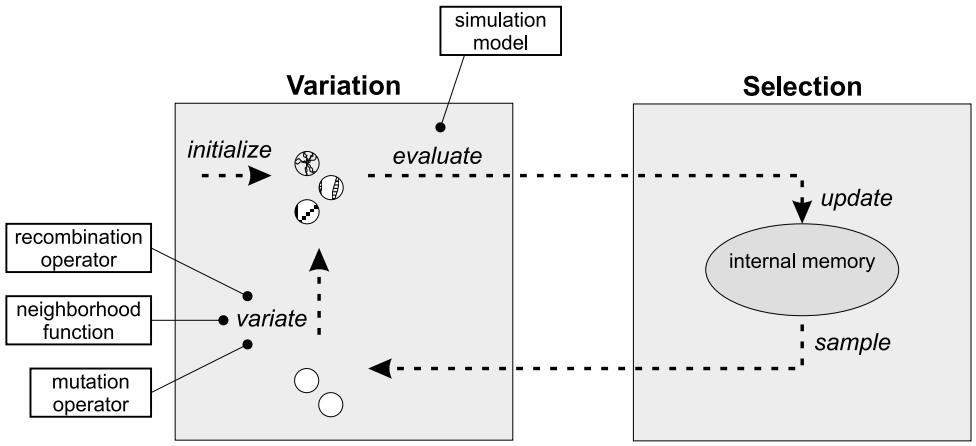

Figure 5.5: Model of a general search algorithm. Circles stand for individuals and the external boxes give examples of operators which could perform the respective basic operation (Bleuler et al., 2003).

genes to undergo a mutation. Also it is possible only to select chromosomes which didn't pass a recombination to mutate. For recombination, one-point, two-point and uniform crossover operators are possible. If the chromosome consists of real numbers, the simulated binary crossover (SBX) operator (Deb and Beyer, 2001) was implemented in the case of chromosome recombination and a polynomial mutation operator (Deb and Goyal, 1996) for mutation. A detailed review of theses variation operators can be found in (Back et al., 1997).

The fitness evaluation is done experimentally. The results of the experiments are written into text files, which are than read by the variator module. The new populations generated by the variation process are also written into text files and into the same MySQL database, which is also used to store the results from the reactor, as described in chapter 3.

Nojima et al. (2005) studied the effects of removing overlapping solutions. These are solutions which have the same positions in the search or in the objective space. They found out, that in the case of a binary tournament selection the diversity increased significantly if overlapping solutions are removed. For a higher order tournament selection the effect was not pronounced any more. This is due to the fact, that both removal of solutions and the binary tournament selection increase the diversity of solutions. In this work, overlapping solutions in the search space were replaced by new solutions created by the variation operators in order to increase the diversity of the population.

A decoder for the encoding of the deNOx problem, in order to satisfy the constraints during variation, was also included into the variator module. Encoding and handling of resulting constraints will be discussed later in chapter 5.3 and 5.4.

5.2.2 Selectors

In a simple genetic algorithm, selection schemes are basically used to select individuals for the later variation or mating process depending on their fitness. This kind of selection is also called mating selection. The main parameter influencing the mating selection is the selection pressure. It is the degree to which the better individuals are favored. The convergence rate of the evolution process is predominantly determined by the magnitude of the selection pressure. However, if a too high selection pressure is applied, the chance to find the global optimum decreases and the loss of diversity of the population is high. On the other hand, a too low selection pressure leads to a slow convergence, which is especially in experimental optimization not desired. The most common mating selection schemes are tournament selection, (μ, λ)-selection, linear ranking selection and stochastic universal selection. In this work a tournament selection, with a tournament size of 2 with a selection intensity of $1/\sqrt{\pi}$ (Blickle and Thiele, 1995) was used. The loss of diversity in the case of a binary tournament selection is significantly less than for instance in the case of a linear ranking selection (Blickle and Thiele, 1995). A complete comparison and review of mating selection schemes was done by Blickle and Thiele (1995) and can also be found in the handbook of evolutionary computation (Back et al., 1997).

In more sophisticated evolutionary algorithms, additionally to providing selection pressure, the selection schemes also try to preserve the population diversity by using special, so called environmental selection operators. The goal of these operators is not only to find the optimal solution to the problem, but for instance in the case of single-objective optimization also to find local optimal solutions. In the case of multi-objective optimization the preservation of the diversity, in order to have a good distribution of solutions along the Pareto-optimal front, is highly desired. In both cases, the environmental selection generally helps to keep a diverse population and to avoid premature convergence.

The third important feature of the selection process is to be able not to loose good solutions during the evolution process. This concept is called elitism and several studies agreed, that elitism is very important to improve the performance of a genetic algorithm. In multi-objective optimization elitism is generally implemented by using a second population, which is called the archive population. The archive population keeps track of the best individuals.

The exact implementation of mating and environmental selection in combination with fitness assignment and the handling of the archive population depend on the specific selection algorithm. In this work, three multi-objective selection algorithms, namely NSGA2 (Deb et al., 2002), SPEA2 Zitzler et al. (2002) and IBEA (Zitzler and Kunzli, 2004), were tested on theoretical optimization problems and two of them (SPEA2 and IBEA) were applied to the experimental deNOx optimization problem. These three algorithms will be described more in detail, because the understanding is fundamental for the analysis of the results. Common to all of these three algorithms is the fact, that they use an internal memory, also called archive population, to keep track of the best individuals found so far. The selection of the individuals to keep in the archive is the environmental selection, whereas the selection of the individuals from the archive is the mating selection, which is as previously mentioned done in this work by tournament selection. In this approach new individuals in the archive are preferred over old individuals. The major difference between NSGA2, SPEA2 and IBEA is the implementation of the environmental selection and of the diversity preservation algorithm.

Non-dominated sorting algorithm version 2 (NSGA2)

The non-dominated sorting genetic algorithm version 2 (NSGA2) was developed by Deb et al. (2002). It is based on NSGA developed by Srinivas and Deb (1994). NSGA incorporates the idea to use a non-dominated sorting procedure in conjunction with a sharing technique, as suggested by Deb and Goldberg (1989). The non-dominated sorting groups the individuals of a population to several fronts according to their level of non-domination and assigns fitness values to each of these fronts. The same fitness value is assigned to all members of a front in order to give an equal reproductive potential. The first front is constituted by the non-dominated individuals. The diversity is maintained by applying sharing methods (Deb and Goldberg, 1989, Goldberg and Richardson, 1987) to each front separately. This causes multiple optimal solutions to co-exist in the population. NSGA2 a non-dominated sorting algorithm with a reduced computational complexity was

developed, which is denoted as fast non-dominated sorting. The diversity preservation was improved by replacing the sharing function approach of NSGA with a so called crowded comparison approach (Deb et al., 2002). The crowded comparison does not require any additional user defined sharing parameter and has a better computational complexity. A special density estimation technique is incorporated in NSGA2. It is based on the so called crowding distance, which is obtained by calculating the average distance of two solutions ($i-1$ and $i+1$) on either side of a solution i and gives an estimate of the size of the largest cuboid enclosing of solution i. The solutions in a population are afterwards sorted according to their crowding distance and their density is obtained by assigning relative distance values to each solution. Using the crowded comparison operator, the overall fitness is calculated with respect to the non-domination rank and the crowding distance. The NSGA2 procedure is also visualised in figure 5.6.

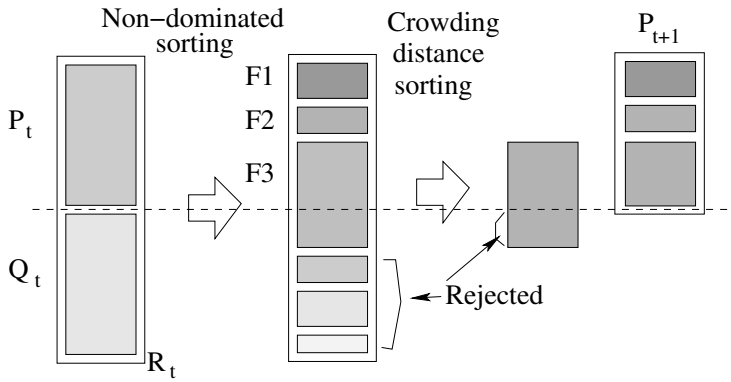

Figure 5.6: A representation of the NSGA2 algorithm. R_t denotes a combined population of the parent population P_t and the offspring population Q_t. F_n are non-dominated fronts of different order, which are ordered according to their order of non-domination.

Strength Pareto evolutionary algorithm version 2 (SPEA2)

The strength Pareto evolutionary algorithm (SPEA) (Zitzler and Thiele, 1999) was a new approach to multiobjective optimization in 1999. It was mixture of established and at that time new techniques in order to approximate the Pareto-optimal set. The concept of Pareto dominance (see section 5.1.3) is used in order to assign scalar fitness values to the solutions. Solutions that represent a non-dominated front among all solutions considered so far are stored externally. The average linkage clustering method (Morse, 1980) is used as parameter-less niching method to reduce the number of stored non-dominated solutions and to preserve the diversity in the population. In 2002, Zitzler et al. (2002) presented an improved version of SPEA which tried to incorporate new ideas and to eliminate potential weaknesses. The main differences of SPEA2 in comparison to SPEA are: an improved fitness assignment scheme, which takes for each solutions into account how many other solutions it dominates and it is dominated by, a new clustering and

truncation technique, namely the nearest neighbor density estimation technique, which is also able to preserve boundary solutions in the archive. Furthermore, the archive size in SPEA2 is fixed, i.e. if the number of non-dominated solutions is less than the archive size, the archive is filled up by dominated solution. In contrast, in SPEA the archive size is variable. Finally, in SPEA2 only members of the archive population participate in the mating selection process.

It was found, that SPEA2 performs better on all tested problems than its predecessor SPEA and performs better that NSGA2 for some problems. The best overall performance at the time of the development of SPEA2 was achieved by NSGA2 and SPEA2 (Zitzler et al., 2002).

Indicator-based evolutionary algorithm (IBEA)

Recently Zitzler and Kunzli (2004) proposed a new method to direct the search of an evolutionary algorithm towards the Pareto-optimal front. The indicator-based algorithm (IBEA) is based on performance measures (indicators), which are integrated into the multiobjective search. It uses an archive population just like in the case of SPEA2, however, this approach is different from the dominance based approaches (as for instance NSGA2 and SPEA2) as it does not require any special diversity preservation mechanism. The idea behind IBEA was to design a flexible algorithm, which is able to deal with different preference information. Most of the multiobjective evolutionary algorithm implement in some way preference information, as for instance to minimize the distance to the Pareto-optimal set and to maximize the diversity of the solution set, but the preferences are not clearly defined and only emerge as a result of the implementation of the algorithm. The idea of preference information was first investigated by Fonseca and Fleming (1998) and Knowles (2002). With IBEA, Zitzler and Kunzli (2004) proposed a general implementation for multi-objective optimization, which does not need any diversity preservation techniques. It uses binary quality indicators to compare solutions of a population pairwise. Several indicators, as for instance the hypervolume indicator I_{HD} or the ϵ-indicator can be used to assign fitness values to the population members. The easiest way to assign the fitness is simply to sum up the indicator values for each population member with respect to the rest of the population. The resulting fitness value is a measure for the loss in quality if the corresponding member is removed from the population. The concept of the ϵ and the hypervolume binary quality indicators is shown in figure 5.7. The hypervolume indicator measures the volume of the space that is dominated by B but not by A with respect to a predefined point. The ϵ-indicator works similary, but does not compare the hypervolume. The indicators return a pair of numbers, which indicates that A is strictly better than B ($I_A \leq 0 \wedge I_B > 0$), or neither A or B is stricly better than the other ($I_A > 0 \wedge I_B > 0$). However, if I_A is less than I_B, then in a weaker sense, A is better than B. A detailed comparison of IBEA, SPEA2 and NSGA2 and of both quality indicators can be found in (Zitzler and Kunzli, 2004). For most problems IBEA was found to perform significantly better than SPEA2 or NSGA2.

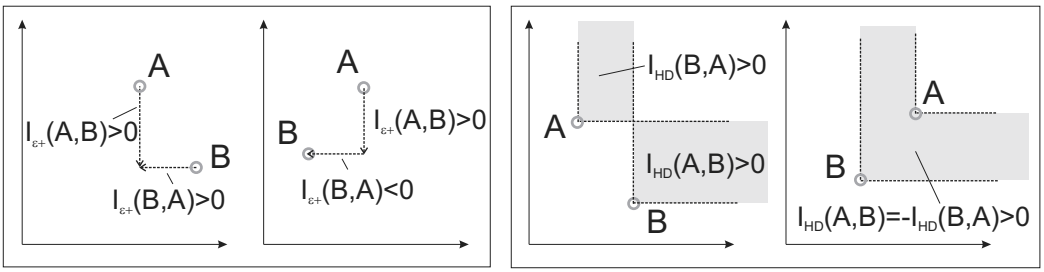

Figure 5.7: Illustration of the two binary quality indicators implemented in the PISA version of IBEA (on the left hand side the ϵ-indicator and on the right hand side the hypervolume indicator) (Zitzler and Kunzli, 2004).

5.3 Encoding

During the development of a genetic algorithm to solve an optimization problem, the encoding, that is the representation of the decision space of a given problem by a data structure, is one if the most important parts. An inconvenient encoding of the decision space, which is in principle equal to inconvenient variation operators, can be as much or even more disastrous than a bad choice of the parameters for the optimization or of the algorithm for the selection process.

The classical way to encode a problem are data structures such as binary vectors. The so called binary encoding is typical for genetic algorithms. When using more complex data structures, such as vectors of floating point numbers, binary or floating point matrices or even trees or networks, the algorithm is generally called evolution strategy in the case of floating point vectors or evolution program in the case of more complex data structures like trees. The crucial part when using complex data structures is to adapt the genetic operators to produce meaningful offsprings.

The encoding of the individuals should be natural, but at the same time it should preferably be able to represent the decision space without encoding not allowed individuals. This is in real world problems generally a very difficult task, especially if the problem is highly constrained or in parts combinatorial.

Natural means, that no complex transformations on the decision space are necessary to encode the problem and that the genetic operators are able to produce desired effects during recombination or mutation of the individuals.

For instance, for the traveling salesman problem (Bellmore and Nehause.Gl, 1968, Held and Karp, 1970), the binary representation of a tour is not well suited, since a change of a single bit may result in an illegal tour. A more natural encoding is the use of binary matrix chromosomes, since it encapsulates all the information about the sequence, including topologies of city to city connections. It is therefore possible to develop operators that can produce desired effects while preserving the properties of the tour (Michalewicz, 1999).

In this work binary vectors are chosen to encode the catalyst. This decision will be further explained in the next sections.

Encoding of the deNOx problem

A total of 11 elements in different combinations and varying concentrations compose the search space of the deNOx problem. The elements can be classified into three groups: elements acting as support with a high mole fraction in the catalyst, the main elements with a probably major contribution to the catalytic reactivity of the catalyst, and elements acting as promotor, with only a small mole fraction in the catalyst. As stated before, aluminum was chosen as element for the support, copper, nickel, cobalt, iron, manganese, lanthanum, cerium and samarium as main elements and potassium and strontium as promotors.

Some boundary conditions were introduced to reduce the search space and to incorporate chemical knowledge into the encoding. Systems with and without support are treated separately:

C.1 The maximal number of main elements in a catalyst is less or equal than four.

C.2 For systems with support, the aluminium concentration has to be higher than 33.3 mole-% and less than 95.0 mole-%. The individual concentration of the main elements is limited to 35 mole-%.

C.3 For systems without support, the maximum allowed aluminium concentration in a catalyst is 33.3 mole-% and the individual concentration of the main elements is unrestricted.

C.4 Only a maximum of two elements from the lanthanoid series are allowed to be at the same time in a catalyst.

C.5 The sum of the concentrations of the promotor elements is limited to 5.0 mole-%; it is possible that a catalyst contains both promotor elements.

Superimposed to these self-introduced boundary conditions is the fact, that the total sum of all concentrations equals 100 mole-%. For both systems aluminium constitutes the remainder, but the total sum of mole fractions of main and promotor elements is not allowed to be higher than the minimal support mole fraction (constraint C.6).

Encoding of the element combinations

A variety of encodings can be thought of to encode the combinations of the elements. For such combinatorial problems the binary representation is generally used for encoding (Back et al., 1997, Michalewicz, 1999). Vectors of integer numbers could also be used, but special genetic operators would be required. The most direct way of binary encoding

is to use for each element one bit. Wolf et al. (2000) used this encoding for a very similar problem, but without any additional constraint. Limiting the number of elements for each catalyst (constraint C.1) leads to a combinatorial problem, where all valid combinations can fit into less than eight bits. For instance the unique number of combinations of four elements out of eight is $8!/(4!(8-4)!)$ or 70. Under consideration of constraint C.4 all the combinations fit into six bits, which is significantly less than eights bits if one bit is used for each element. In section 5.5 these two encodings will be tested using reasonable test functions.

Encoding of the element concentrations

In contrast to the combinatorial and discrete problem of encoding of the element combinations, the encoding of the element concentrations is a continuous problem. For such problems the use of an evolution strategy with floating point vectors as data type seems to be the natural way to represent the search space properly. However, the use of binary vectors has some important advantages, especially when dealing with experimental optimization problems.

Wolf et al. (2000) used an evolution strategy for the encoding of the concentrations. Using on the one hand binary vectors for the element combinations and on the other hand floating point vectors for the concentrations, it is not straightforward to develop a recombination operator for the whole vector. Baerns and Wolf treated both parts of the chromosome separately. Only a mutation operator was applied to the floating point vector, thus the advantages of a properly chosen recombination operator could not be played off. Also the schema theorem (Rudolph, 1994, Schmitt, 2001) is only valid for the binary part of the vector.

The use of continuous data structures in experimental optimization only makes sense if the experimental error of the design variables tends towards zero. Typically the experimental procedures are not as accurate and an unintentional discretization of the search space occurs. Therefore a binary encoding seems to be more reasonable. The step size should be significantly higher than the expected experimental error. Another advantage of the discretization of a continuous problem, is to reduce the accuracy and thus the dimension of the search space to promote a faster convergence (Hannes and Weuster-Botz, 2006).

In this thesis the concentrations are discretisized into 16 steps and a binary representation of four bits for each concentration is chosen. Due to the maximal number of 4 main elements in a catalyst, 16 bits are required for the encoding of the concentrations. A linear distribution of these 16 steps would lead to a step size of about two or six for the systems with and without support respectively. Using the ABIMED robot for synthesis of the catalyst, the minimal volume which can be handled is about 1-3 μl, hence a minimal step size of 5 μl (0.5 mole-%) is reasonable.

The discretization of the problem, also allows the use of different step sizes and thus to incorporate some problem specific knowledge to the encoding of the problem. Most of the metal oxides form spinel phases at 33 mole-%, thus these concentrations should

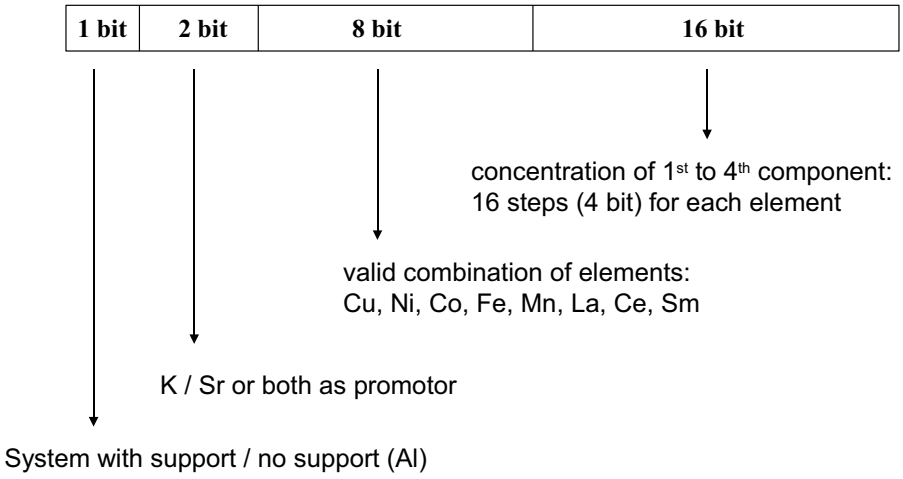

Figure 5.8: Final encoding of the deNOx problem using 11 bit for the combinatorial part of the problem.

be encoded regardless of the step size. Also it could make sense to use a smaller step size for the region below 15 mole-% and around the spinel concentrations, in contrast, the step size at high loading can be more coarse. In table 5.1 the discrete concentration encodings (genotypes) with the corresponding decoded values (phenotypes) are listed. In figure 5.8 the final encoding of the deNOx problem is shown.

5.4 Handling constraints

Michalewicz (1995) investigated several techniques to deal with constrained problems. In brief these are: (a) the design of two evaluation functions for the feasible and infeasible domains, (b) the rejection of infeasible individuals (death penalty), (c) the penalizing of infeasible individuals by penalty functions, (d) the use of so called repair functions to repair infeasible individuals and (e) the adaptation of genetic operators and the use of special representations to maintain a feasible population. This list is surely not complete, but summarizes some of the most popular techniques. The application of these methods may also vary, for instance after repairing an infeasible individual, it can be used for evaluation purpose only, or it can replace the original and infeasible individual in the population (Lamarckian evolution (Whitley et al., 1994)).

In experimental optimization, the evaluation of the fitness is typically the limiting step, also the population size is given on the basis of the experimental evaluation procedure. In high-throughput experimentation, a good choice of the population size is a multiple of the number of simultaneous parallel experiments that can be analyzed in one go. For the parallel reactor system of 49 capillaries used in this work, a reasonable population size is thus a multiple of 49 individuals. To keep the experimental evaluation time short with respect to maximal capacity, also all these capillaries should preferably be used

genotype	phenotype (mole-%) with support	phenotype (mole-%) without support
0000	0.5	2.0
0001	1.0	4.0
0010	2.0	8.0
0011	4.0	12.0
0100	6.0	16.0
0101	8.0	20.0
0110	10.0	25.0
0111	12.0	30.0
1000	16.0	33.3
1001	20.0	35.0
1010	24.0	40.0
1011	28.0	50.0
1100	32.0	63.3
1101	33.3	75.0
1110	34.1	88.0
1111	35.0	100.0

Table 5.1: Discrete encodings of the element concentrations.

for evaluation. Therefore option (b), the rejection of infeasible individuals, which is, due to its simple implementation, a popular option in many evolutionary techniques, seems not to be good for experimental optimization. Also it is known (Michalewicz, 1999, page 320), that this option only works reasonably well, when the search space is convex and constitutes a large fraction of the whole search space. Also the option (a) and (c), apart from being difficult to implement, do not seem to be reasonable options in experimental optimization, because the experimental evaluation system is used below maximal capacity.

In contrast options (d) and (e), the maintaining of a feasible population by special representations, genetic operators or repair functions, seem to be a good choice in the case of experimental optimization, as the evaluation system is used at maximal capacity. The possibilities to maintain a feasible population using different representations have already been discussed in section 5.3. Since it is relatively easy to repair infeasible individuals in the case of the deNOx problem, repair functions will be used to repair both invalid

combinations of elements and invalid concentration ranges.

```
Input: chromosome with invalid combination of elements
Output: chromosome with valid combination of elements
if number of valid elements = 0 then
    select a random gene from the element combination and apply the bit-flip
    mutation operator on it.
else
    while number of valid elements > 4 do
        select a random gene from the element combination.
        if gene = 1 then
            apply the bit-flip mutation operator on the selected gene.
        end
    end
end
```

Algorithm 5.2: Repair algorithm of the combinatorial part of the chromosome

```
Input: chromosome with invalid concentration ranges
Output: chromosome with valid concentration ranges
valid := false
while not valid do
    if ∑(PromotorConc + ElementConc) > 1 - MinSupportConc then
        decrease the element concentration by one step for a randomly chosen
        element
    else if ∑(PromotorConc + ElementConc) < 1 - MaxSupportConc then
        increase the element concentration by one step for a randomly chosen
        element
    else
        valid := true
    end
end
```

Algorithm 5.3: Repair algorithm of the continuous part of the chromosome

5.5 Evaluation of parameters and encoding scheme

Deb et al. (2001) described a method to develop test functions for multi-objective optimization. These functions are easy to construct, scalable to any number of objectives and decision variables and the Pareto-optimal front is exactly known. Also it is easy to control the hindrance to converge to the true Pareto-optimal front.

In order to use the best possible encoding, genetic operators and parameter sets for the deNOx problem, several test problems from (Deb et al., 2001) were used to create a

new test problem, with some properties very close to the actual deNOx problem. Before developing the new problem, some of the original test problems will be discussed and evaluated using the optimization framework developed in this work. For this the number of objective functions in all the cases is set to two and the number of decision variables to four, just like for the experimental deNOx problem.

5.5.1 Theoretical test problems

Test Problem DTLZ1

The DTLZ1 problem is a simple test problem with a linear Pareto-optimal front. Two different versions will be used for testing, the original DTLZ1 problem with many local Pareto-optimal fronts and the DTLZ1-easy version with only one Pareto-optimal front. The problem is defined as:

$$\begin{aligned} \text{Minimize} \quad & f_1(\mathbf{x}) = x_P\,(1 + g(\mathbf{x}))\,x_1 \\ \text{Minimize} \quad & f_2(\mathbf{x}) = x_P\,(1 + g(\mathbf{x}))\,(1 - x_1) \\ \text{subject to} \quad & 0 \leq x_i \leq 1, \quad \text{for} \quad i = 1, 2, 3, 4 \end{aligned} \tag{5.5}$$

where

$$g(\mathbf{x})_{\text{DTLZ1}} = 100\left(4 + \sum_{i=1}^{4}\left(\left(x_i - x_S\right)^2 - \cos\left(20\pi\left(x_i - x_S\right)\right)\right)\right) \tag{5.6}$$

$$g(\mathbf{x})^{\text{easy}}_{\text{DTLZ1}} = \sum_{i=1}^{4}\left(x_i - x_S\right)^2 \tag{5.7}$$

for the original and easy DTLZ1 problem.

Test Problem DTLZ2 and DTLZ3

The next two problems have a spherical Pareto-optimal front:

$$\begin{aligned} \text{Minimize} \quad & f_2(\mathbf{x}) = x_P\,(1 + g(\mathbf{x}))\,\cos\left(x_1\pi/2\right) \\ \text{Minimize} \quad & f_2(\mathbf{x}) = x_P\,(1 + g(\mathbf{x}))\,\sin\left(x_1\pi/2\right) \\ \text{subject to} \quad & 0 \leq x_i \leq 1, \quad \text{for} \quad i = 1, 2, 3, 4 \end{aligned} \tag{5.8}$$

where $g(\mathbf{x})$ is in the case of problem DTLZ2 the g function given in equation (5.7) and in the case of problem DTLZ3 the function given in equation (5.6). Hence DTLZ3 can also be named as the hard version of DTLZ2.

For all these test problems, the Pareto-optimal solution corresponds to $\mathbf{x}^* = (x_S \ldots x_S)^T$. The objective function values lie on a linear hyperplane of order 2 in the case of DTLZ1 and DTLZ1-easy:

$$\sum_{m=1}^{2} f_m^* = x_P \tag{5.9}$$

or on a spherical hyper-surface of order 2 in the case of DTLZ2 and DTLZ3:

$$\sum_{m=1}^{2}(f_m^*)^2 = x_P \tag{5.10}$$

Test problems DTLZ1 and DTLZ3 are good to test the ability of a MOEA to converge to the global Pareto-optimal front. The easy versions of both problems are good to construct new kinds of problems as will be shown in the next section. All these problems can be modified, in order to test the ability to maintain a good distribution of solution by using a variable mapping: $x_i \rightarrow x_i^\alpha$. Deb et al. (2001) suggested a parameter of $\alpha = 100$.

Design of a new combinatorial problem

In order to simulate some properties of the deNOx problem, a new combinatorial problem, build up using the test problems DTLZ1 and DTLZ2, will be designed in the following.

The deNOx problem consists of two parts: first, the combinatorial problem to find the best combination of elements in a catalyst and second, the continuous part, where for a certain combination the best concentration values have to be found. If only one combination of elements would exist, the problem would only be a function of the element concentration, and this problem would reduce to a continuous only problem, just like in the case of the continuous test problem DTLZx described in the last section.

The combinatorial part of the deNOx problem, can for instance be modeled as different combinations of the theoretical test problems (DTLZ1, DTLZ2, ...), of the absolute location of the global Pareto-optimal front x_P and of the x-values (the concentrations) corresponding to the Pareto-optimal solution $(x_S \dots x_S)^T$.

The x_P-values, the values, which influence the location of the global Pareto-optimal front as described by equations (5.9) and (5.10) for the linear and spherical front respectively, can be used to describe the optimal activity of a main element. A small x_P-value for a certain element would describe its single activity without other elements. Interactions could be simulated by adding a certain value Δx_P to the other x_P-values in order to influence its activity. This can also be done to influence interactions due to the support or the promotor elements. The true location of the global Pareto-optimal front x_P^* of a combination of n elements and the x-values corresponding to the Pareto-optimal solution x_S can then be calculated using the following equations, if a linear relationship is assumed:

$$x_P^* = \frac{1}{n}\sum^{n} x_P + \sum \Delta x_P \tag{5.11}$$

$$x_S^* = x_P^* \tag{5.12}$$

The x_P-values of the elements can be chosen arbitrary in the range from zero to one. The Δx_P should not be too high, because the sum and not the mean value is added to x_P^*. For the deNOx simulation problem, table (5.2) gives an overview of the chosen

Type	Element	x_P	Δx_P	Problem
main component	Cu	0.50	-0.10	DTLZ1-easy
main component	Ni	0.60	0.10	DTLZ1-easy
main component	Co	0.60	-0.05	DTLZ2
main component	Fe	0.50	0.10	DTLZ1-easy
main component	Mn	0.55	0.10	DTLZ1-easy
main component	La	0.60	-0.05	DTLZ2
main component	Ce	0.70	0	DTLZ2
main component	Sm	0.65	-0.05	DTLZ2
promotor	K		-0.025	
promotor	Sr		-0.025	
with support	Al		0	
without support	Al		0.1	

Table 5.2: Parameters for the simulated deNOx test problem.

values. The problem with the highest number of incidences is chosen for the resulting system. If the incidences of DTLZ1-easy and DTLZ2 are equal, DTLZ1-easy is chosen.

Using this test problem, the constraints C.1 to C.5 can be implemented just like for the real deNOx problem. It is also possible to test the different encoding schemes and the parameters of the MOEA with respect to the deNOx application. To also incorporate constraint C.6 to the test problem, the lower and upper boundary of the decision variables x_i can be adjusted:

$$0 \leq x_i \leq 2, \quad \text{for} \quad i = 1, 2, 3, 4 \tag{5.13}$$

and a modified boundary condition C.6 can then be used:

$$\sum_{i=1}^{n} x_i \leq 4 \tag{5.14}$$

The global Pareto-optimal front of this problem is a combination of a Pareto-optimal front from the DTLZ1-easy and DTLZ2 problem. More precisely the best combinations are Al-Cu-K-Sr (DTLZ1-easy, with support) with $x_P^* = 0.35$ and Al-Cu-Co-La-Sm-K-Sr $x_P^* = 0.2875$ (DTLZ2, with support). One should note that due to the different shapes of the Pareto fronts from the two DTLZ problems a linear Pareto front from the DTLZ1 problem with a higher x_P-value can still be better than a Pareto front with a lower x_P-value from the DTLZ2 problem. In figure 5.9 the Pareto-optimal fronts of DTLZ1 and DTLZ2 with $x_P = 0.5$ and of the theoretical deNOx test problem are shown. The combined DTLZ1 and DTLZ2 front clearly show, that this approach of constructing new problems is indeed possible.

5.5.2 Performance metrics

To measure the quality of the solution found by an evolution algorithm, several performance metrics need to be defined. The metrics used in this work are specifically defined

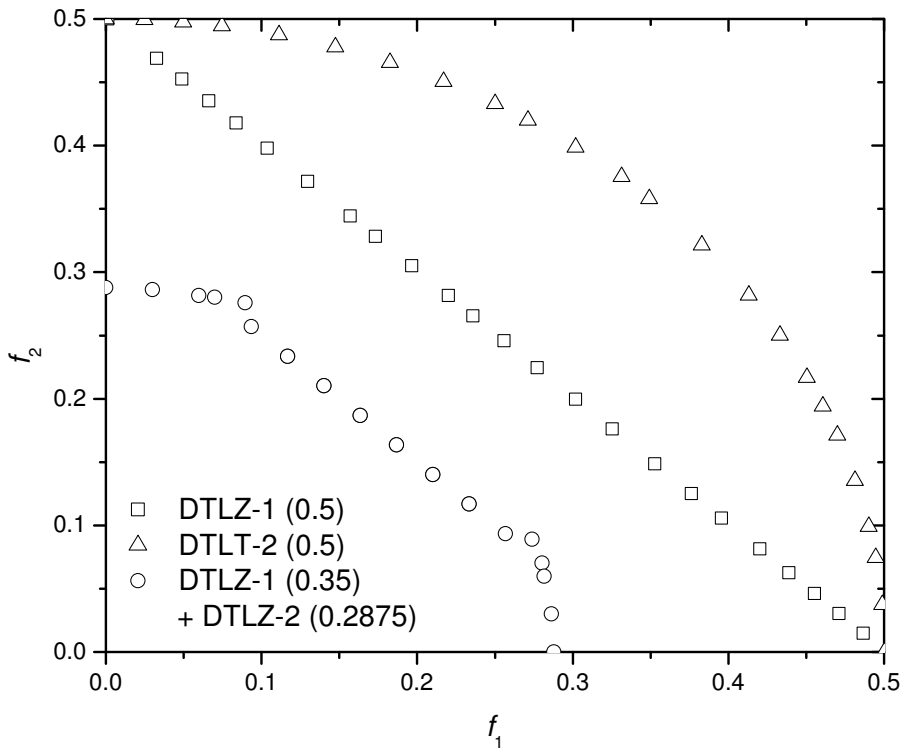

Figure 5.9: Pareto-optimal fronts of the multiobjective DTLZ1 and DTLZ2 problems and the here developped combinatorial and continuous theoretical deNOx problem, which is a combination of DTLZ1 and DTLZ2. The number in brackets correspond to the x_P^* value. The results were obtained after 100 generations using SPEA2 and binary strings of 27 bit for each chromosome. The population size was set to 24.

with respect to the test functions described in the previous section.

The first metric is the average of the x_P-values of the solutions of the Pareto-optimal front:

$$M_1 = \frac{1}{N^*} \sum x_P \tag{5.15}$$

For the deNOx problem it was shown in the previous section that the Pareto-optimal front is a combination of optimal fronts with two different x_P-values. For a uniform distribution of solutions on the Pareto-optimal front, more solutions will be found for the linear region corresponding to the DTLZ1-easy problem with $x_P^* = 0.35$. Hence the minimal convergence metric M_1 is not the average of 0.35 and 0.2875, but nearer to 0.35. The best value found so far for M_1 after 50 generations is about 0.33.

The second metric is defined as the average of the objective values for the solutions of the Pareto-optimal front as defined by the equations (5.9) and (5.10). The difference of both metric 1 and 2 is therefore a strong indication for the convergence rate of the algorithm to a global or local Pareto-optimal front. Equation (5.9) can also be used to

measure the performance of an arbitrary problem, where the real Pareto-optimal front is unknown.

Additionally to these two metrics which are applied to the continuous part of the deNOx problem, some information can also be gained about the quality to solve the combinatorial part of the deNOx problem. As will be described in the next section, to obtain statistically relevant data, each optimization run was repeated 50 times. Thus it is possible to calculate the probability to find one or both of the best element combinations. For instance if in 25 runs the algorithm was able to find both combinations, the probability would be 50%.

5.5.3 Test cases

Several test cases have to be defined, to compare and to evaluate some parameters of the variator module. For all test cases the initial, the parent and the offspring population size was set to 24 individuals, which are binary encoded. The variation is done using a binary bit-flip mutation and a one-point binary crossover operator. Tournament selection, where one individual competes with two other individuals is used as environmental selection algorithm. The test cases can be summarized as follows:

TC1: Encoding of the combinatorial part of the deNOx problem using 9 bit (6 bit for the element combinations and 3 bit for the support and promotor combination). The concentrations are encoded using for each concentration 4 bit, thus a chromosome size of 25 bit is obtained. Only combinations of four out of 8 elements are encoded in this version. The repair algorithm 5.3 is used to repair invalid concentration ranges. A detailed description of this encoding can be found in section 5.3. The probability of mutation was set to $p_m = 0.1$ and the probability of crossover to $p_c = 1$.

TC2: Encoding of the combinatorial part of the deNOx problem using 11 bit. For each element one bit, where a '1' denotes an active element and a '0' an inactive. The concentrations are encoded just like in TC1. The total chromosome size is 27 bit. Invalid combinations and concentrations are repaired using the algorithms 5.2 and 5.3. The probability of mutation was set to $p_m = 0.1$ and the probability of crossover to $p_c = 1$.

TC3: The same encoding as for TC2.
The probability of mutation was set to $p_m = 1/(\text{chromosome size}) = 0.037$ and the probability of crossover to $p_c = 1$.

TC4: The same encoding as for TC2.
The probability of mutation was set to $p_m = 2/(\text{chromosome size}) = 0.074$ and the probability of crossover to $p_c = 1$.

TC5: The same encoding as for TC2.
The probability of mutation was set to $p_m = 1/(\text{chromosome size}) = 0.037$ and

the probability of crossover to $p_c = 0$. This encoding is denoted as multiobjective random search.

TC6: The same encoding as for TC2.
The probability of mutation was set to $p_m = 0$ and the probability of crossover to $p_c = 1$.

5.5.4 Theoretical results

In this section, first the results obtained for the different encoding schemes (TC1 and TC2) will be discussed in order to choose the right encoding for the experimental optimization. Afterwards different effects observed when varying the probabilities of the variation operators will be investigated (TC2 to TC4). The two extreme cases (TC5 and TC6) will show how an evolutionary algorithm without mutation competes against a multi-objective random search in the case of a partially combinatorial and continuous problem, as for instance the deNOx problem in this work.

All the tests were done using the three selector algorithms, SPEA2, NSGA2 and IBEA, as described in section 5.2.2. Due to the fact that evolutionary algorithms are nondeterministic each test was repeated 50 times using different random seeds for both variator and selector modules to obtain statistically meaningful results.

Comparison of the encoding schemes

In figure 5.10 the two convergence metrics as specified in section 5.5.2 are visualized for the test cases TC1 and TC2 after 5, 10, 20 and 50 generations for different selector algorithms. The error bars are obtained from the standard deviation of multiple test runs.

As can be easily seen, for all selector algorithms the second test case performs significantly better than the first test case even after only few generations. Thereby the difference between the first and the second convergence metric, which is an indication of the convergence of the algorithm, decreases in the case of TC2 clearly, in the case of TC1 nearly not. Nevertheless after 50 generations, both encoding schemes are able to produce solutions lying on or near the Pareto-optimal front. This can be seen in figure 5.10, due to the fact, that the first metric nearly approaches the optimal value of 0.33 for both test cases.

One should keep in mind, that TC2 is encoded with 2 bits more, therefore one would expect it to perform worse than TC1. To understand the reason why the results for TC2 are much better, the probabilities of finding the two optimal combinations Al-Cu-K-Sr with $x_P^* = 0.35$ and Al-Cu-Co-La-Sm-K-Sr with $x_P^* = 0.2875$ are shown in figure 5.11. After only 5 generations, for both encodings, the probabilities of finding the optimal solutions are relatively low. In this case the probability to find the optimal combination with one main component (Al-Cu-K-Sr) is relatively high for TC2, while it is very low for TC1. In contrast the probability to find the combination with four main components

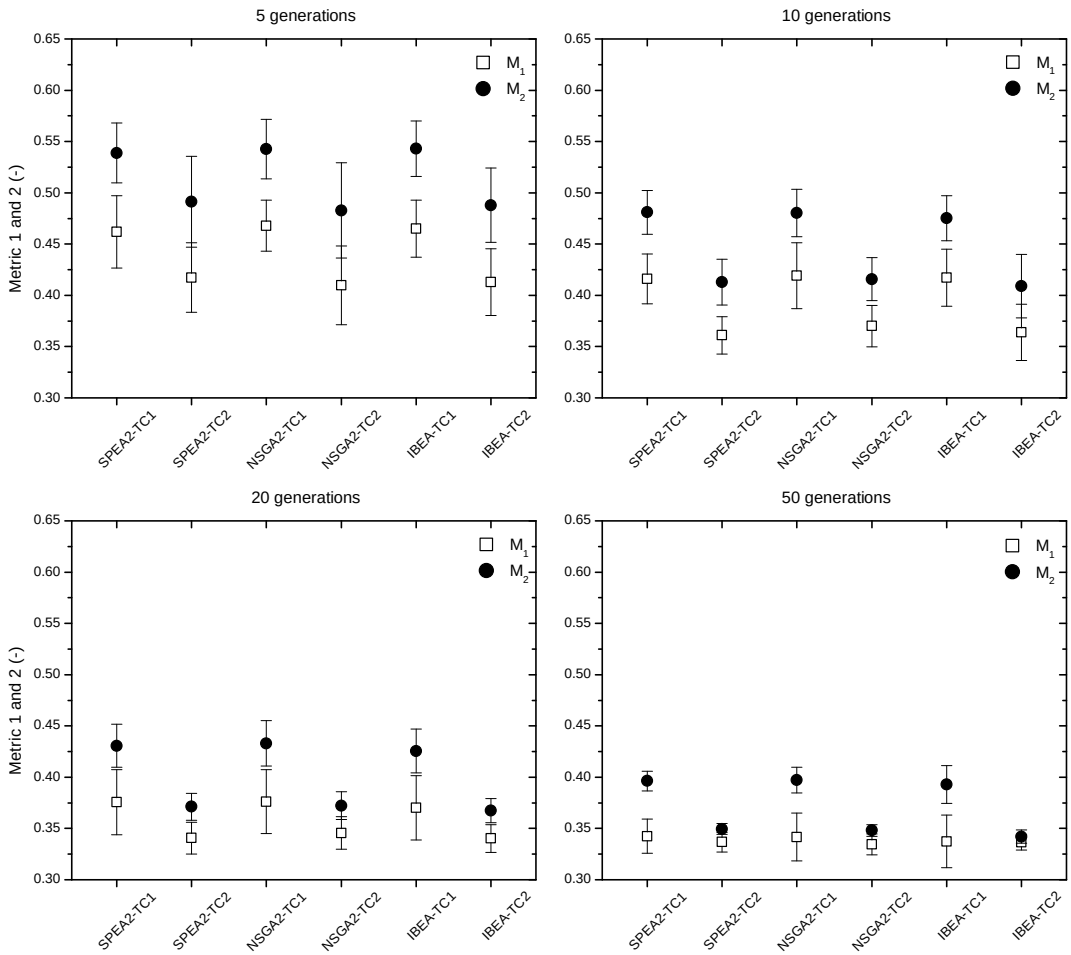

Figure 5.10: Convergence metrics M_1 and M_2 for TC1 and TC2.

(Al-Cu-Co-La-Sm-K-Sr) is comparable for both test cases. After 10 generations TC1 is still nearly not able to find the combination with only one main component, while in the case of TC2 the solution is found in more than 75% of the test runs. Here again, the probability to find the combination with four main components is nearly the same for both test cases. After 20 and 50 generations TC1 still performs poorly with respect to find the combination with only one main component. In contrast, for most algorithms the probability to find the combination with four main components is a bit higher for TC1 than for TC2.

There are different aspects which have to be considered to explain the observed phenomena. First it obvious, that for TC1, where only combinations of four main components out of eight are encoded in the combinatorial part (6 bit), combinations with less than four main components are much more difficult to find, because the only possibility to obtain such a combination, is by setting the continuous part to zero. Thus, some combinations are in this encoding only accessible through evolution of the continuous part of the chromosome. This is much more difficult and leads to a low performance with respect to these combinations. The incorporation of all possible combinations into the

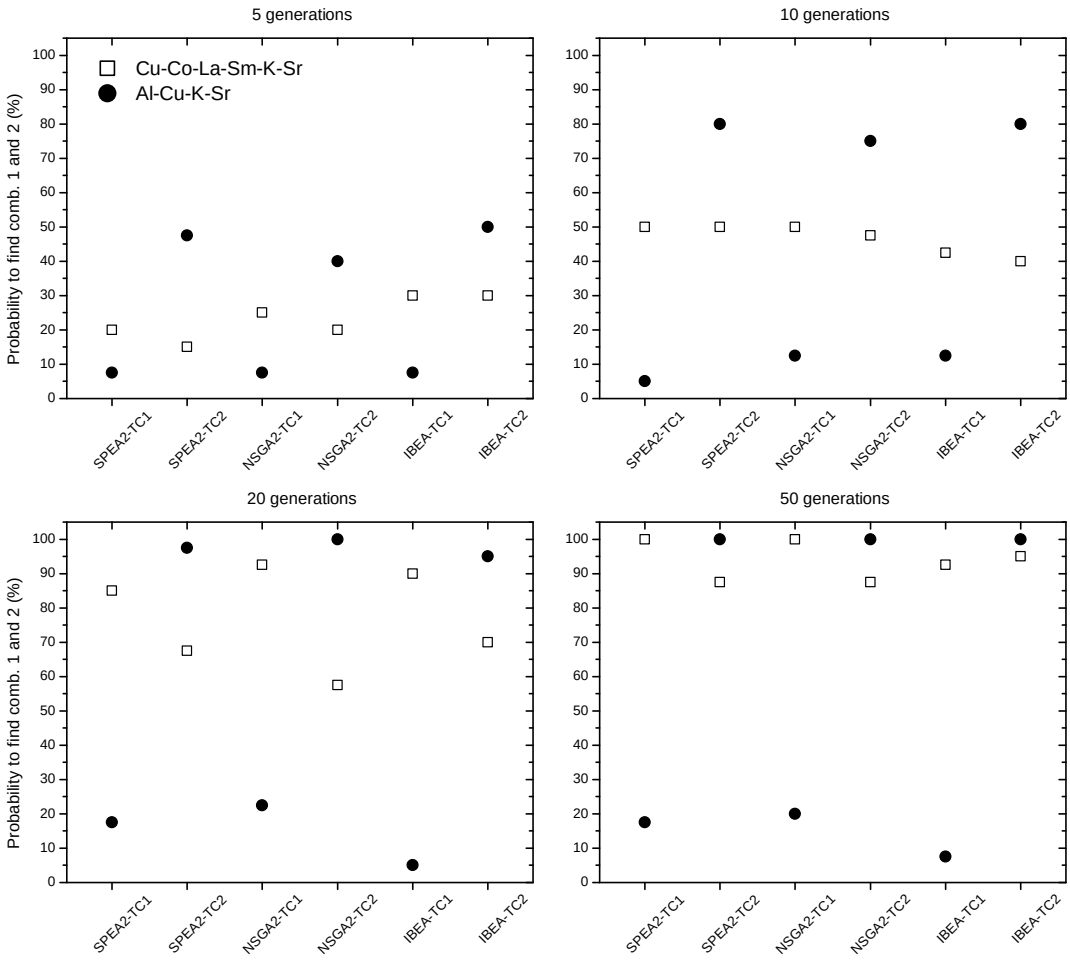

Figure 5.11: Probabilities of finding the optimal combinations for TC1 and TC2.

combinatorial part would solve this problem and leads to a better performance, but just like for TC2 8 bit would be necessary the encode the combinations and some kind of boundary conditions would also be necessary. Hence the more natural encoding with 8 bits and repair functions to satisfy the constraints was found to perform best, when using the traditional one-point binary crossover operator. This is due to the fact, that the traditional crossover operator is able to mate properties of the combinatorial part, because each bit encodes a property. In contrast, the encoding of only valid combinations leads to an un-natural mating, which is like a random crossover or another kind of mutation operator. This problem could be solved, by using a specialized crossover operator, which is able to mate the properties of two individuals just like in the case of TC2. In this work the use of the classical crossover operator in combination with intelligent repair algorithms to satisfy the constraints was chosen as preferred option.

The reason for the slightly better performance of TC1 with respect to the probability of finding the composition with four main components after 20 and more generations is due to the fact, that the algorithm in most of the cases only tries to reach a single Pareto-optimal front and not the combination of both. The algorithm just finds one

possible solution and converges with a slightly better performance than TC2 towards it. Anyhow, the ability to converge towards both Pareto-optimal fronts without neglecting one of them is a much harder problem to solve. After 50 generations it can be seen that all the three selector algorithms are able in nearly 90% of the cases to converge towards both solutions.

Influence of the crossover and mutation probabilities

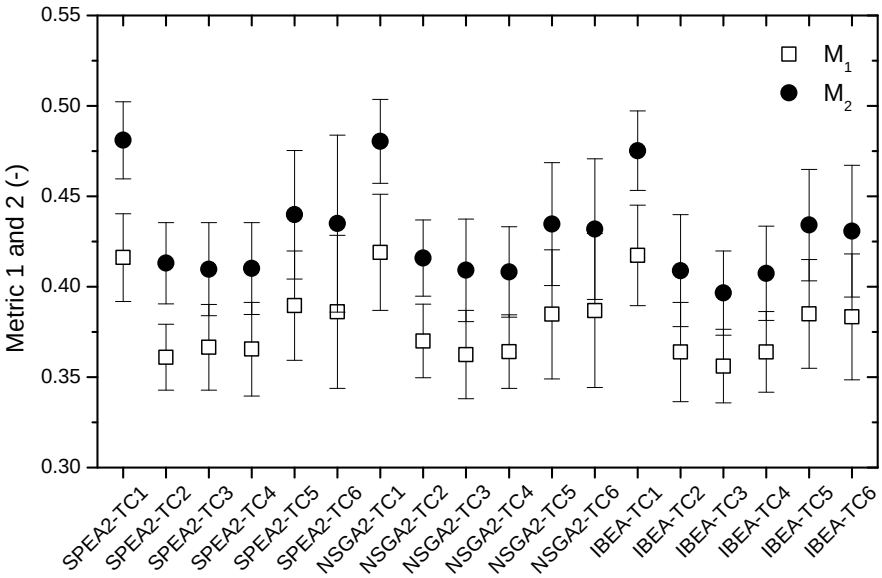

Figure 5.12: Results after 10 generations for all test cases.

To choose reasonable settings for the variator module, the probabilities of crossover and mutation ware varied on the basis of the second encoding scheme. Previous works on multiobjective optimization showed that a high rate of crossover is a good choice for most problems (Grefenstette, 1986). This is due to the fact, that the evolutionary knowledge gained during the optimization is mainly achieved by the mating in combination with the selection process, as described for binary encodings by the schema theorem (Rudolph, 1994, Schmitt, 2001). In contrast the mutation operator serves as an option to avoid the search of being trapped in a local Pareto-optimal front and to find new solutions to the problem. The knowledge gained by the algorithm on the basis of the mating and selection process may be disturbed by the mutation process. This distribution can be favorable or not, depending strongly on the roughness of the search space, but in most of the cases it will lead to individuals with poorer performance. Therefore, the mutation rate is generally kept very small. A good choice for the mutation probability is equal or greater than the inverse of the number of genes used for encoding the problem in the case of binary encoding, because this would lead to at least one mutation per individual in the population (Bremermann et al., 1966).

In figure 5.12 the results of the two performance metrics are shown after 10 generations for all test cases. The results for TC2, TC3 and TC4, where only the mutation probability

was varied from 0.037 to 0.1, are nearly the same. Only TC3 performs slightly better for NSGA2 and IBEA than the two other test cases. For the experimental optimization the mutation rate was set to 0.037 (TC3), which correspond to the inverse of the number of genes used for the encoding (1/27). In the work from Wolf et al. (2000) the probabilities for both crossover and mutation operator were not constant during the hole optimization process, but were defined as a function of the diversity of the population. The diversity was measured by calculation of the fraction of the average fitness of the population and of the fitness of the best individual. In multiobjective optimization with more than only one possible objective, the direct application of this diversity calculation is not possible. A more sophisticated diversity calculation can be developed, but the effects of such adaptation are uncertain. Also, for the selection algorithms used in this work, a diversity preservation mechanism in the objective space is already implemented, thus the effects caused by an additional adaptation of the variator rates are even more uncertain and could lead to a significantly lower performance of the optimization process. Hence, in this work constant probabilities were chosen to be adequate for the optimization. However, the investigation of the influence of variable probabilities could be interesting and should be considered for further studies.

The test cases TC5 and TC6 in figure 5.12 clearly show that an algorithm, where only crossover or mutation is generating new solutions, is performing significantly worse than an algorithm, which includes both variation operators (test cases TC2-4). Only the combination of a recombination with a high probability and a mutation with a low probability is able to find in a reasonable number of generations very good solutions to the problem. However, the performance of TC5 and TC6 is similar, which is an indication that the actual knowledge gained during the optimization process is mainly conserved due to the selection step.

5.6 Experimental optimization of the deNOx problem

In this section all the previously described methods and results will be brought together in order to optimize experimentally the complex deNOx problem. The methods needed to evaluate the fitness of the catalysts were described in chapter 3. A 49-parallel channel reactor set-up for stage II screening was build up an tested and showed a good accuracy and a fast analysis, which is needed for a reasonable optimization procedure. The synthesis of the deNOx catalysts was described and checked for reproducibility in chapter 4. The error of the synthesis and of the catalytic evaluation by the reactor was found to be in the order of 5%. A description of the optimization framework and of the theoretical aspects of evolutionary multi-objective optimization was given in the first part of chapter 5. In the second part the application of these methods to a real world problem, the deNOx problem, will be demonstrated. It is very important to point out, that the optimization of the deNOx problem, that is the problem of finding the best combination and composition of elements in the catalyst, requires to keep all other parameters constant. For instance the BET surface area is highly depending on the synthesis method and on the metal loading and the catalytic activity of a catalyst is likely to suffer as a result of a low BET surface area. Thus, not the ideal deNOx problem will be optimized. Only a boundary problem, in which the systematic features of the synthesis and of the catalytic test act as constaints to the ideal deNOx problem, will be processed.

In addition to the mere optimization of the deNOx system, it was chosen to compare SPEA2 and IBEA. The reactor was therefore subdivided into two parts consisting of 24 reactor channels for each of the optimization algorithms. The population size for each algorithm was chosen to be identical to the number of reactor channels used for the evaluation (24). In a premilary test, 48 randomly chosen catalysts were tested and the 19 best catalysts were selected to build up the initial population. Additionally to these 19 randomly created catalysts, five selected single oxide catalysts (Cu,Mn,Ni on Al_2O_3) were included into the initial population, which was the same for both algorithms, in order to have the same starting point for the optimization process. Also all the parameters and settings of the variation module were the same for both algorithms and are summarized in appendix B.

5.6.1 Optimization results after seven generations

In figure 5.13 the evolution of the archive population is visualised by boxplots for both objective functions and for both selection algorithms. As can be clearly seen, the average fitness is improving with each generation. The population of the first generation, which is represented by a black boxplot is identical for both algorithms. The second generation already shows, that SPEA2 and IBEA are evolving in a slightly different way. SPEA2 was able to find a better solution for the NO conversion after seven generations than IBEA. In contrast IBEA found a better solution with respect to the peak temperature of the NO conversion. The best solution of each generation is represented by the lower outlier of the boxplot. It can be seen, that the best solutions are not steadily improving just like the average fitness of the archive population, but step-wise. For instance after six

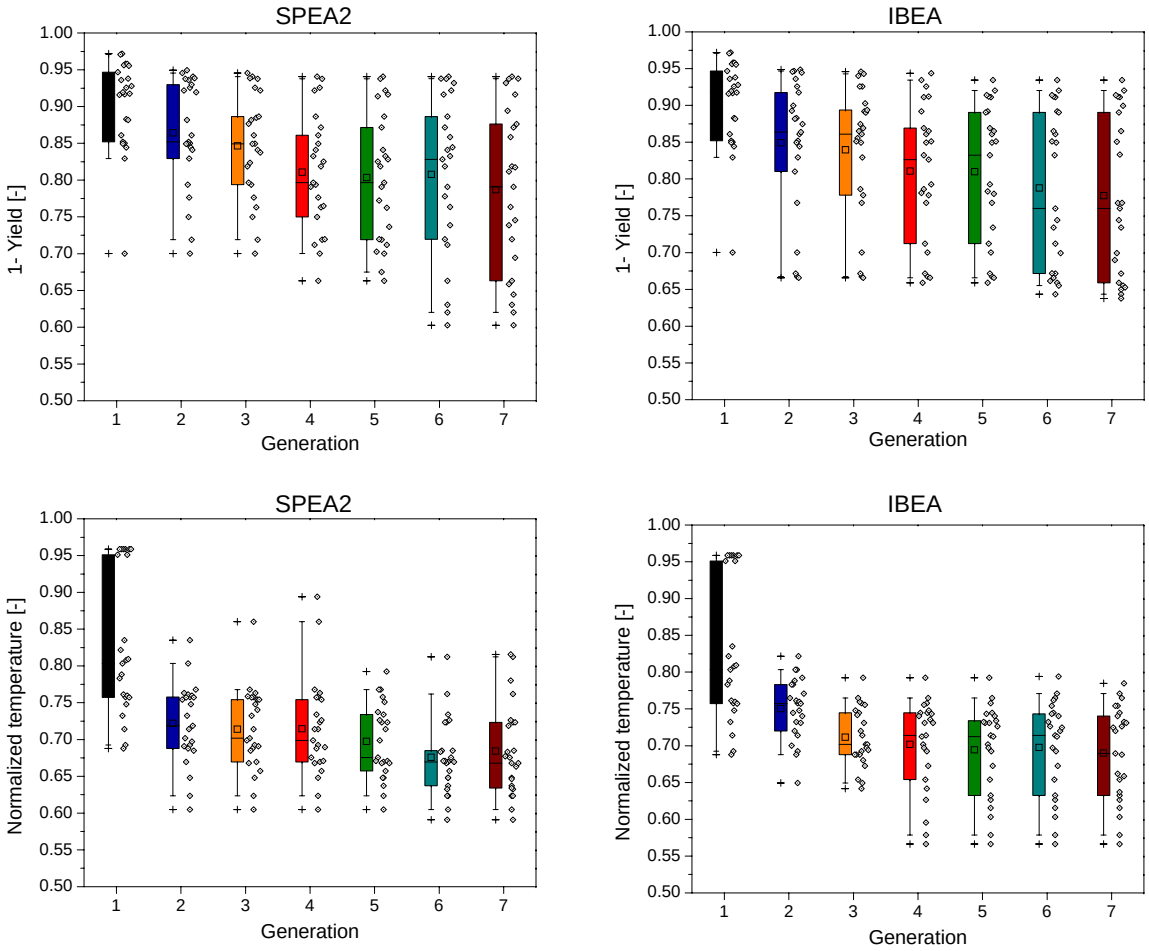

Figure 5.13: Evolution of the objective functions for the solutions of the archive population.

generations SPEA2 was able to find the catalyst with the highest NO to N_2 conversion, which is a catalysts containing a small fraction of copper and nickel supported on a high amount of Al_2O_3 as will be later shown. The best low temperature catalysts are catalysts containing a high amount of cobalt or manganese and a smaller fraction of nickel or copper on a small fraction of Al_2O_3. Another interesting result is the fact, that the boxes representing 50% of the data are increasing in most of the cases and the length of the upper and lower whiskers tend to decrease during the evolution.

Figure 5.14 shows the evolution of the occurrences of the archive population up to the seventh generation. The maximal number of occurrences is 24 (the size of the population). As stated before the initial population was created randomly, but the constraints C.1 to C.6 (see section 5.3) have nevertheless to be satisfied. This lead to the elemental distribution of the first generation as can be seen in figure 5.14. The evolution shows a clear trend for most of the elements. Systems with support (constraint C.2) are preferred to systems without support (C.3), both algorithms are converging towards copper and nickel containing catalysts. The convergence rate is, however, different for SPEA2 and

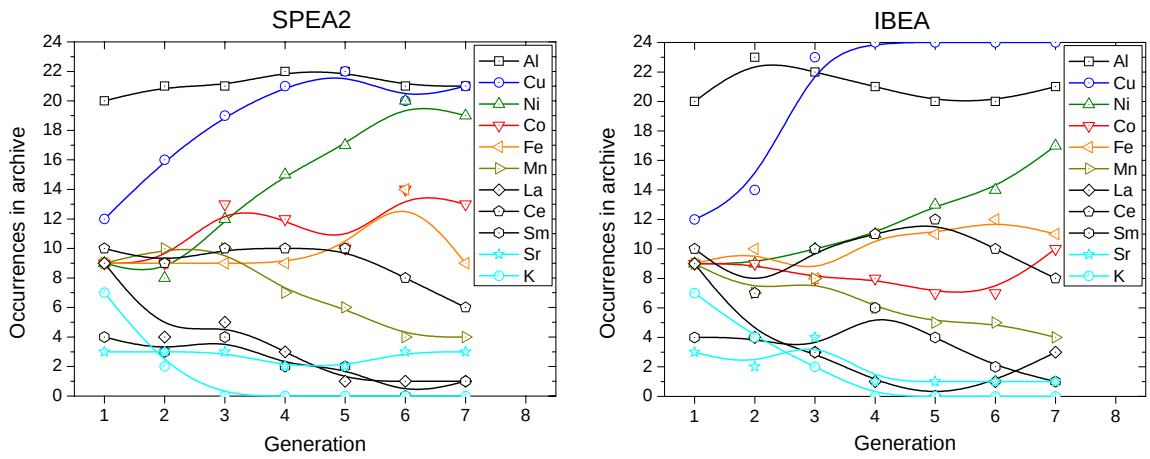

Figure 5.14: Evolution of the occurrences of elements in the archive population for SPEA2 and IBEA.

IBEA. The trend of the promotor elements strontium and potassium is slightly different, potassium shows a clear negative trend and disappears completely after three or four generations in the case of SPEA2 and IBEA. In contrast strontium does not disappear during the evolution but is neither increasing. The occurrences are constantly in the range of two to three catalysts in the archive. The trend of manganese, samarium, lanthanum and also cerium at higher generation number is negative. However, the elements do not disappear completely, but in the case of manganese, samarium and lanthanum a clear decrease is observed. The trend for cobalt and iron containing catalysts is not clear. The occurrences of both elements seem to be fluctuating, and only a slightly positive trend can be distinguished.

In figure 5.15A and 5.16A the archive populations of SPEA2 and IBEA for all generations are visualised by Pareto-plots in the objective space. Since both objective functions are to be minimized, the non-dominated individuals form a trade-off front from the upper left to the lower right part of the plot. The evolution of the archive solutions is visualised by using for each generation a different color. Both algorithms are approaching the Pareto-optimal front with each generation. In figure 5.17 the archive population is shown separately for both algorithms at different evolution stages. The convergence process can be clearly distinguished and it can also be seen, that both algorithms are approaching the Pareto-optimal front in a different way. As already shown in figure 5.14 IBEA tends to converge strongly towards copper containing catalysts. In figure 5.17 this effect can be seen by cluster formation in the region with a high yield to N_2. For SPEA2 as well some clustering can be observed, but less pronounced. After the seventh generation for both algorithms the solutions are well distributed along the Pareto-optimal front. However, SPEA2 was able to approach the Pareto-optimal front better than IBEA and also the distribution is slightly better. A guess of the Pareto-optimal front of this system is visualized in figure 5.15A and 5.16A by a gray line.

In figure 5.15B and 5.16B different regions of the Pareto plots are magnified in order to

visualise the best solutions. The NO to N_2 yield of selected solutions is furthermore shown in the figure 5.18. It can be seen, that the Pareto-optimal trade-off front is composed predominantly of copper and nickel containing catalysts with varying concentrations. Interestingly these binary oxides are more active than the corresponding single element oxide catalysts (see figure 5.18A). The incorporation of a third element as for instance cobalt or iron generally yields in an activity loss as can be seen in figure 5.15B or 5.18B. However, at temperatures below 600 K copper and nickel catalysts in combination with cobalt, iron and sometimes also manganese are optimal solutions as shown in figure 5.16B and 5.18C.

5.6.2 Discussion and comparison of SPEA2 and IBEA

In the following section explanations for the observed results will be given. Also the results of SPEA2 and IBEA will be compared. It is important to note, that both evolutionary processes are stochastic and a real comparison of the actual algorithms is not possible. Only the results observed here, which may be influenced by random effects, can be compared. For a proper comparison of IBEA and SPEA at least 50 runs, always with the same settings, but with different random seeds, have to be performed, just like the theoretical experiments in section 5.5.4.

In figure 5.13 the enlargement of the boxes (the 50% quantiles) during the evolution was observed. This is due to the fact, that the distribution along the (1-yield) axis and along the peak temperature axis is improving. The same phenomena can be nicely distinguished in figure 5.17. In the first generation the archive population shows no clear orientation in the objective space. Already after the first few generations for both algorithms the distribution along the (1-yield) axis improves significantly and leads to an enlargement of the 50% quantiles in the boxplots in figure 5.13. This is furthermore an indication for a successful convergence towards the true Pareto-optimal front and for a good diversity preservation for both algorithms.

The next interesting phenomenum is the fact, that IBEA was not able to approach the Pareto-optimal front as good as SPEA2. It is very likely, that the fast convergence of IBEA towards copper containing catalysts, as can be seen in figure 5.14, had a negative effect on the performance of the algorithm. Of course this may not be due to the algorithm itself, but only a random effect, as stated before. However, also in the theoretical part in section 5.5.4 of this work, it was observed, that a strong convergence towards a certain solution led to a reduced performance to find the globally optimal set. In the case of the theoretical problem a strong convergence towards only one of the two Pareto-optimal fronts reduced the performance of finding simultaneously both Pareto-optimal fronts. In figure 5.14 it can also be seen, that the strong favorization of copper containing catalysts decreased the speed of convergence towards nickel containing catalysts and also inhibited the other elements to be be maintained in the population. Nevertheless in the last two generations also IBEA was able to find promising copper and nickel catalysts and showed a strong convergence towards nickel additionally to copper. In conclusion, it seems to be important for a genetic algorithm not to favor a single solution strongly. However,

a properly working algorithm should still be able to find optimal solutions after a few more generations.

5.6.3 Discussion of the chemical properties of the system

In this section a closer look at the chemical properties of the system will be presented and the influence of the elements on the catalytic activity will be discussed on the basis of the results observed during the evolution of the system.

Copper and nickel

Both copper and nickel the are the only elements in this system, which show a high SCR activity. These two elements predominantly form the Pareto-optimal trade-off front. Copper is especially active at low metal loadings around 8 to 12 mole-%, higher copper loadings lead to a distinct activity drop. This is somewhat different for nickel containing catalysts, which are highly active at metal loadings up to 30-35 mole-% depending on the catalyst composition. Catalysts with a peak activity at low temperatures, generally have a relatively high nickel loading (15 to 30 mole-%), whereas catalysts with low metal loading (5 to 15 mole-%) are located in the upper right region (the high activity region) of the Pareto front. XRD measurements (not shown here) of a highly active Al-84-Cu-0.08-Ni-0.08 catalyst show, that nickel is forming in parts a crystalline spinel phase. No clear reflex for copper spinel or copper oxide can be distinguished, it is therefore likely, that amorphous copper(II) oxide is embedded into the amorphous aluminium oxide support matrix. The active phase in this catalyst would therefore be a crystalline nickel oxide spinel phase in combination with an amorphous copper(II) oxide phase. Catalysts containing a high amount of copper spinel, as for instance in the case of a copper catalyst synthesised with 67 mole-% aluminium and 33 mole-% copper, are still active, but only about one third as active as catalysts containing amorphous copper oxide. Hence the active phase in the case of copper seems to be amorphous copper(II) oxide and not crystalline spinel, and in contrast the active phase in the case of nickel is crystalline spinel and probably also in parts amorphous nickel oxide. For a better investigation of the active sites, more XRD measurements would have to be performed.

Cobalt, iron and manganese

As already described in the previous section, the addition of cobalt and iron to a catalyst does not result in a clear trend. Sometimes the addition results in an improved activity and sometimes there is no clear change in activity. However, in most of the cases the activity of a catalyst is decreasing. In the case of manganese, which by itself has a SCR activity of about 15%, in all of the cases an addition results in a significant decrease of the activity. There are several possible general explanations for this behaviour. The addition of an element to an active composition can lead to the inhibition of the formation of the active phase. For instance, if copper(II) oxide is highly active, the addition of manganese

may lead to a disturbance of this phase and of the active sites. Another explanation is the formation of a new phase, which is not active for the SCR of NO, but for the selective oxidation of propene. It was, for instance, observed during the experiments, that most of the manganese containing catalysts were highly active at low temperature for the oxidation of propene. The third possible explanation, which is somehow related to the first explanation is the possibility, that the addition of an element prevents the formation of an ordered crystalline phase. This, for instance, may be the case for lanthanum containing catalysts. As already said, only an elaborated investigation of the crystalline structure by XRD would be able to clarify this effect.

Cobalt and iron are elements, which do not decrease the activity of a catalyst significantly. At higher metal loadings, a cobalt oxide, sometimes in a crystalline spinel structure, is emerging, which is highly active at low temperatures for the NO oxidation to NO_2. NO_2 can be in some cases more reactive than NO as described in the state of the art chapter (chapter 2). In combination with a highly active element for the SCR such as copper or nickel, this leads to catalysts, which are active at low temperatures. Iron is an element, which is known in literature to be highly active for the SCR of NO by NH_3 (Sato et al., 1992, Willey et al., 1991). In this work, no clear increase in activity could be identified.

Lanthanoid

As already mentioned in the previous section, the negative trend of the occurrences of lanthanum and samarium in the archive population as shown in figure 5.14 might be related to the disturbance of the formation of a crystalline phase upon calcination. In contrast, the addition of cerium improves the formation of oxide particles with a high BET surface area and does not seem to disturb the other elements. Also cerium oxide can be considered itself as a catalyst support, if the cerium metal loading is high. This is probably the explanation, why the occurrences of cerium in the archive population are stable during the evolution as can be seen in figure 5.14.

Potassium and strontium

Both potassium and strontium are denoted as promotor elements and the maximal concentration of these elements was limited to 5 mole-%. For strontium no clear conclusion can be given, the element does not seem to have any positive or strongly negative effect on the performance. In contrast, the addition of potassium resulted in all cases in a very pronounced drop in the activity of the corresponding catalyst. It was observed, that the resulting catalysts containing potassium were differently colored and sometimes very inhomogeneous. Thus it is likely to assume, that the activity drop is due to a very poor synthesis. Potassium is known to promote highly the combustion of the activated carbon. A possible explanation for the bad synthesis of potassium containing catalysts could therefore be the formation of hot spots during the calcination process, which destroy or disturb the formation of an active phase.

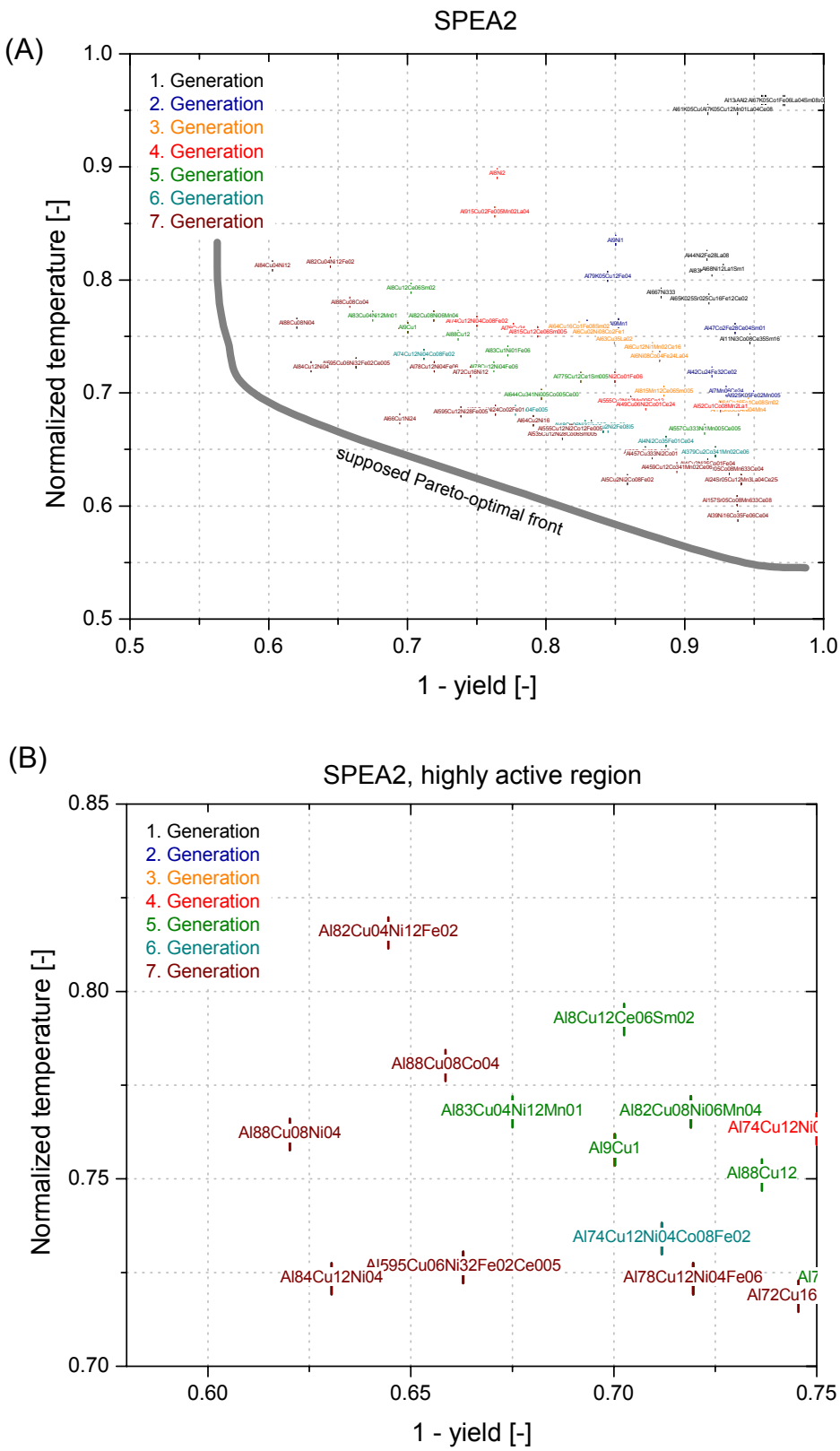

Figure 5.15: Visualisation of the solutions of the archive population in the objective space for SPEA2 (A). Figure (B) shows the solutions located in the highly active region of the objective space.

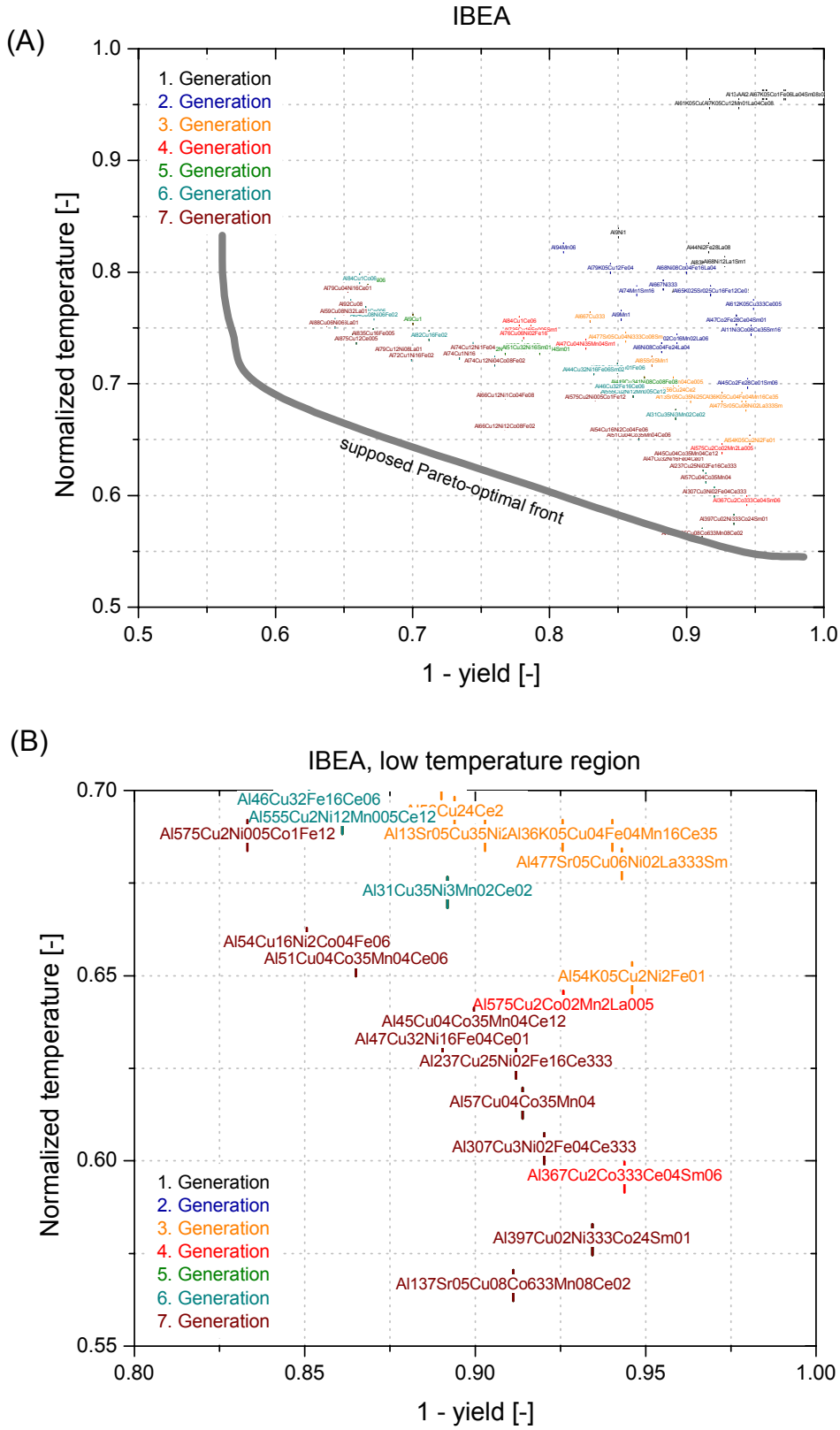

Figure 5.16: Visualisation of the solutions of the archive population in the objective space for IBEA (A). Figure (B) shows the solutions located in the low temperature region of the objective space.

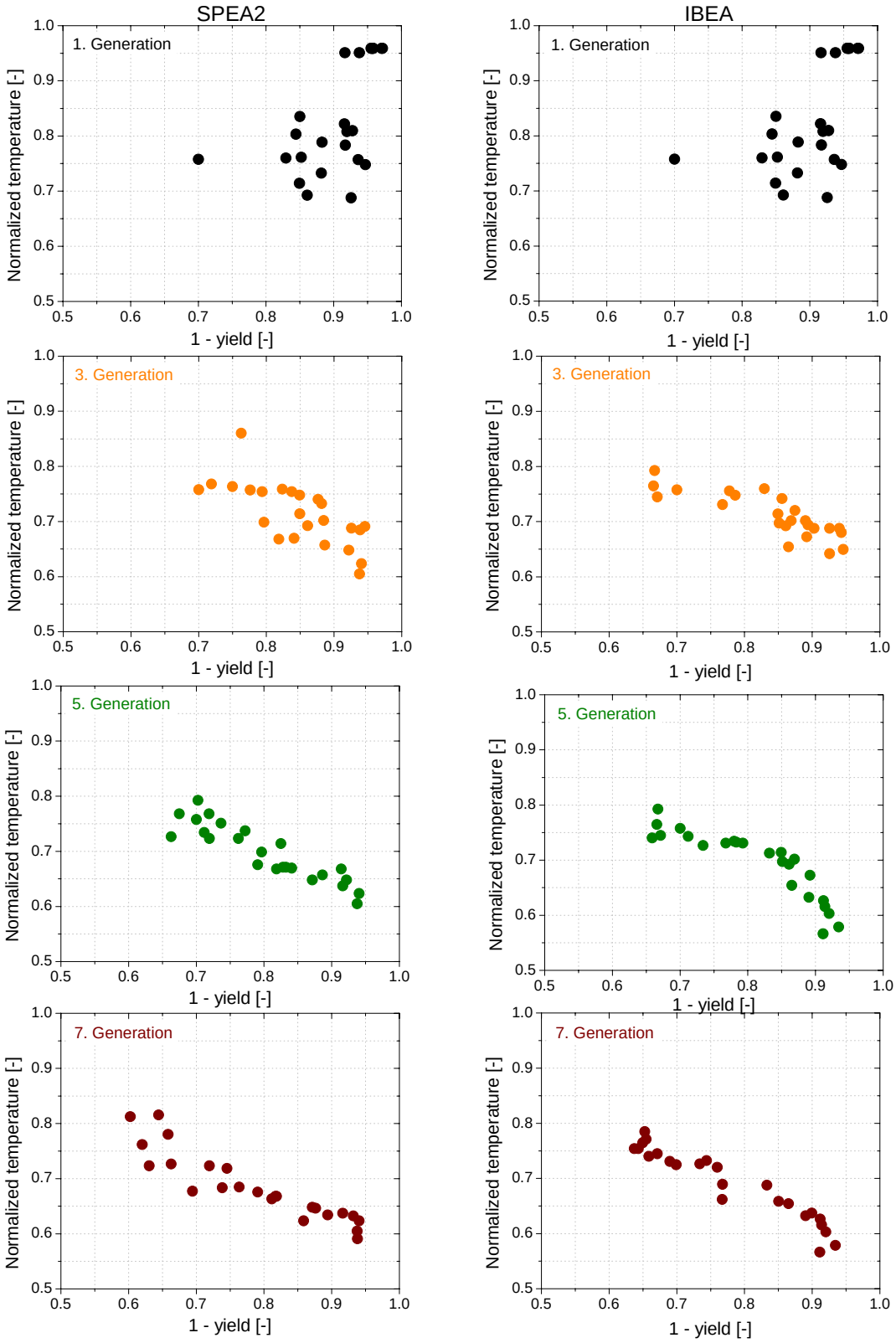

Figure 5.17: Visualisation of the evolution of the archive population of SPEA2 and IBEA for selected generations.

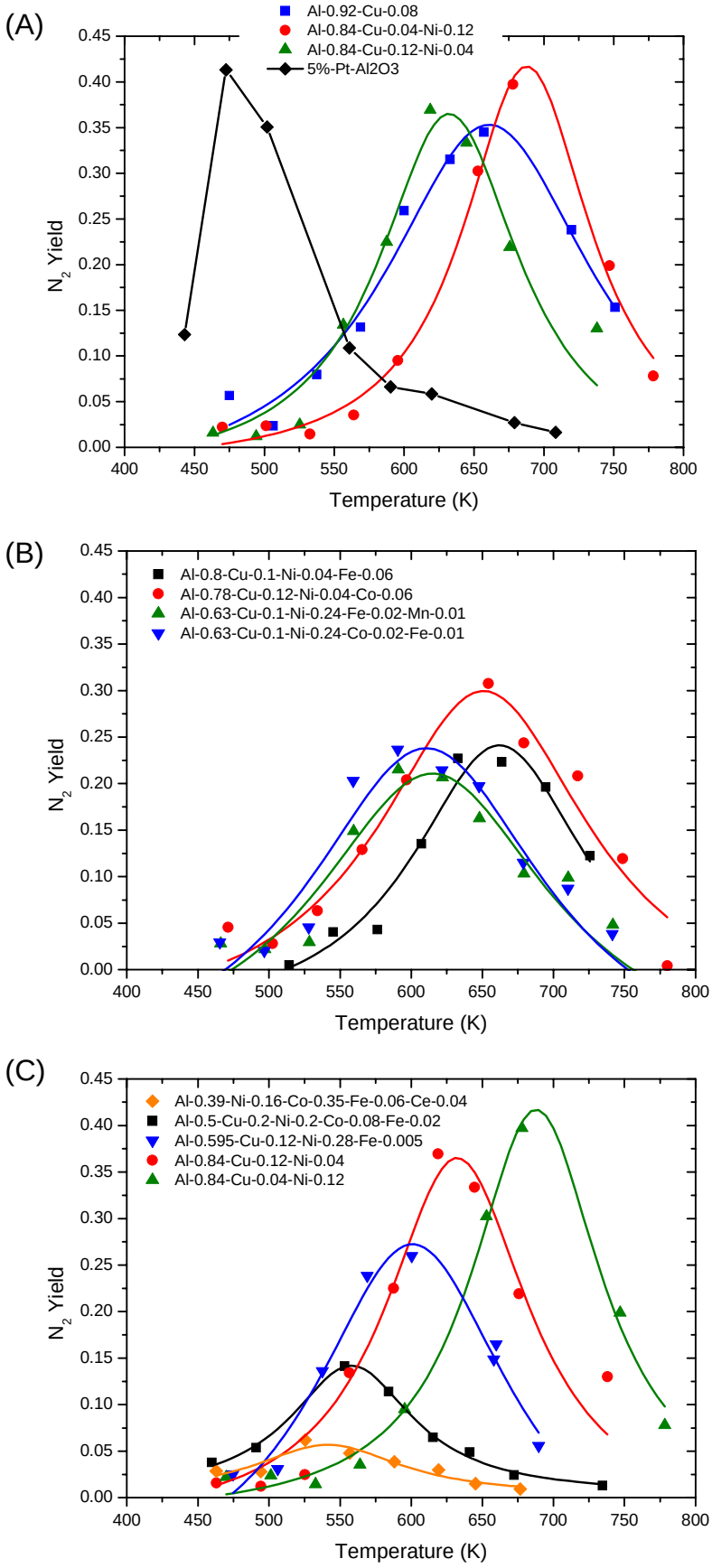

Figure 5.18: NO to N_2 conversion curves as a function of the temperature. Figure (A) shows copper and nickel single and binary oxide catalysts, figure (B) higher order oxide catalysts and figure (C) selected Pareto-optimal solutions.

6 Conclusions and outlook

In order to optimize a complex noble metal free solid catalyst system, several methods have successfully been developed and combined in this thesis. A highly flexible, high-throughput parallel reactor system for catalysts testing was assembled and installed in the first part. Due to a very fast FTIR analysis, it is possible to measure the catalytic activity at 10 different temperatures of 49 catalysts in about 26 hours. In combination with a fast and reproducible synthesis method, based on exotemplating, it is possible to analyse in less than one week 49 catalysts. The optimization of the noble metal free catalyst system was carried out on the basis of a highly flexible framework, the platform and programming language independent interface for search algorithms (PISA). Multiple objectives were chosen to be optimized by using two different multi-objective evolutionary algorithms, namely SPEA2 and IBEA. The application of genetic algorithms to the solid catalyst system was found to be difficult. However, by using a special encoding in combination with repair algorithms, it was possible to successfully optimize the catalyst system. The results show, that evolutionary algorithms are valuable tools for screening and optimization of huge search spaces. Especially if no detailed information of the system is known, the full strength of these methods can be played off. SPEA2 was found to perform better than IBEA. This, however, may not be due to the algorithm itself, but only a result of random effects. During the optimization new chemical knowledge was gained. The best noble free catalyst found by this method, are combinations of copper and nickel. Catalysts, which are active at low temperature, furthermore include cobalt and iron.

A hybridisation of the developed optimization framework with neural networks, acting as local search during the evolution, could improve the optimization process. Also the problem of encoding solid catalysts and the impact of the encoding on the performance of the experimental evolution should be investigated in more detail in further studies. With respect to the reactor set-up, automatization improvements can be achieved by further development of the Labview program in order to have a fully automated system, which is capable to change the flow rate and the temperature according to previously defined programs. Also a fully automated synthesis procedure would significantly reduce the experimental time. From the chemical point of view, the optimization of a catalyst system, where calcination temperature and other synthesis parameters are incorporated, would be interesting. Also the investigation of different supports and mechanical mixtures of catalysts, could lead to interesting results. Furthermore, the active species could be identified by an in depth XRD analysis of the samples.

A Characterisation methods

A.1 Physisorption

A common method for determination of pore volume, pore sizes, areas or volumes is the sorption of probe molecules on a porous solid. Nitrogen or argon physisorption has found to be a generally accepted method for this kind of characterization of porous materials.

The adsorption of a gas on a solid can be quantitatively described by an adsorption isotherm, which represents the amount of condensed molecules (the adsorbates) in a porous solid (the absorbent) as a function of the partial pressure of the gas-phase at a constant temperature. Because of the temperature dependence of sorption in general, it is necessary to measure under isothermic conditions.

Depending on the structure of the solid and on the forces during adsorption, the IUPAC developed in 1985 a standard classification into six general sorption isotherm types. Type I is characteristic for microporous solids like zeolites or monolayer adsorption, type II for nonporous and type III for macroporous solids. Type IV and V possess a hysteresis loop typical for sorption in mesopores proceeding through multilayer adsorption and capillary condensation. Type VI represents the relatively rare stepped multilayer sorption isotherm.

The BET-surface analysis

Brunnauer, Emmett and Teller introduced the concept of multilayer adsorption. Here the first layer of adsorbed molecules acts as new substrate for further adsorption. The classical 2-parameter equation is the well known BET-equation:

$$\theta_{\mathrm{BET}}(x) = \frac{n}{n_m} = \frac{1}{1-x} \cdot \frac{Kx}{1+(K-1)x} \tag{1.1}$$

with the total amount of adsorbates n, the amount of adsorbates in a monolayer n_m, the relative concentration or pressure x and a constant K which is related to the net heat of adsorption of the monolayer. It is important to note that this classical form is only valid for an infinite number of layers on a flat surface taking into account the same heat of adsorption for each layer. To calculate the parameters n_m and K equation (1.1) can be rewritten into the classic BET linear form:

$$\frac{x}{n(1-x)} = \frac{1}{n_m K}\left(1+(K-1)\,x\right) = \frac{1}{n_m K} + \frac{K-1}{n_m K}x \tag{1.2}$$

Now a plot of $x/n(1-x)$ against x should yield in a straight line in a pressure range of about 0.05 to 0.3 p/p_0. From the slope and the intercept it is now possible to determine the above two parameters. The specific surface S_{BET} occupied by the monolayer of the adsorbates can be obtained from n_m and the net heat of adsorption from K. Some restrictions to the parameter K can be used to optimize the BET analysis. For instance K always has to be positive and larger than zero. Also it should not be too high or too low.

The analysis of the adsorption isotherm by the BET method is a common method to determine the surface area of a porous material, but is mostly restricted to mesoporous or macroporous materials. The application of the BET method to materials containing micropores has to be done with care and only an apparent surface area can be obtained.

Measurements

Nitrogen physisorption isotherms were measured on a Nova 3000 sorptometer from Quantachrome at liquid nitrogen temperature (77 K). The samples were first activated under under vacuum at 573 K for at least 2 hours. After the measurements the weight of the samples was determined on an analytical balance at room temperature. Total pore volumes were determined using the adsorbed volume at a relative pressure of 0.97. The BET surface area was estimated from the relative pressure range from 0.05 to 0.30.

A.2 X-ray powder diffraction (XRD)

X-ray diffraction (XRD) is an extensively used technique in material science to determine crystallographic and textural properties and inner stress due to defects.

The powder X-ray diffraction patterns were recorded with a STOE STADI P θ-θ powder X-ray diffractometer in reflection geometry (Bragg-Brentano) using Cu-K$_{\alpha 1+2}$ radiation.

A.3 Scanning electron microscopy (SEM)

Scanning electron microscopy (SEM) is a powerful technique to study the surface morphologies (texture, shape and size) of the bulk samples of solid materials. A beam of electrons is scanned across the surface of the sample. This method can be combined with energy dispersive X-ray microanalysis (EDX) to analyze the backscattered and secondary electrons produced by the primary beam of electrons. In this thesis, SEM images were used to estimate the size and shape of particles of the samples.

For all SEM images, a Hitachi S-3500N scanning electron microscope operated at 10 kV was used. The samples were coated by a thin layer of gold before analysis.

B Parameters and settings

B.1 Catalytic measurements

Feed composition:	
C_3H_6 concentration:	2000 ppm
NO concentration:	1500 ppm
O_2 concentration:	50000 ppm
Reactor settings:	
total flow:	2566 ml/min
analysis flow:	52 ml/min
volume of the catalytic bed:	0.157 ml
GSHV:	20000-25000 h^{-1}
temperature range:	473.15 to 773.15 K
temperature ramp:	11-13 K/h
time to wait:	120 s
FTIR settings:	
Volume of the IR cell:	17 ml
Resolution:	1
Apperture:	100
Gain:	8
Number of scans:	8

B.2 Genetic algorithm

Initial population size (α):	24
Parent population size (μ):	24
Offspring population size (λ):	24
Chromosome encoding:	27 bit
Mutation type:	bit flip mutation
Mutation probability:	$1/27 = 0.037$
Crossover type:	one point binary crossover
Crossover probability:	1
Number of objectives:	2
Mating selection:	binary tournament selection
Enviromental selection:	NSGA2 / SPEA2 / IBEA
IBEA indicator type:	ϵ-indicator
IBEA κ:	0.05
IBEA ρ:	1.1

C Source codes

C.1 Labview

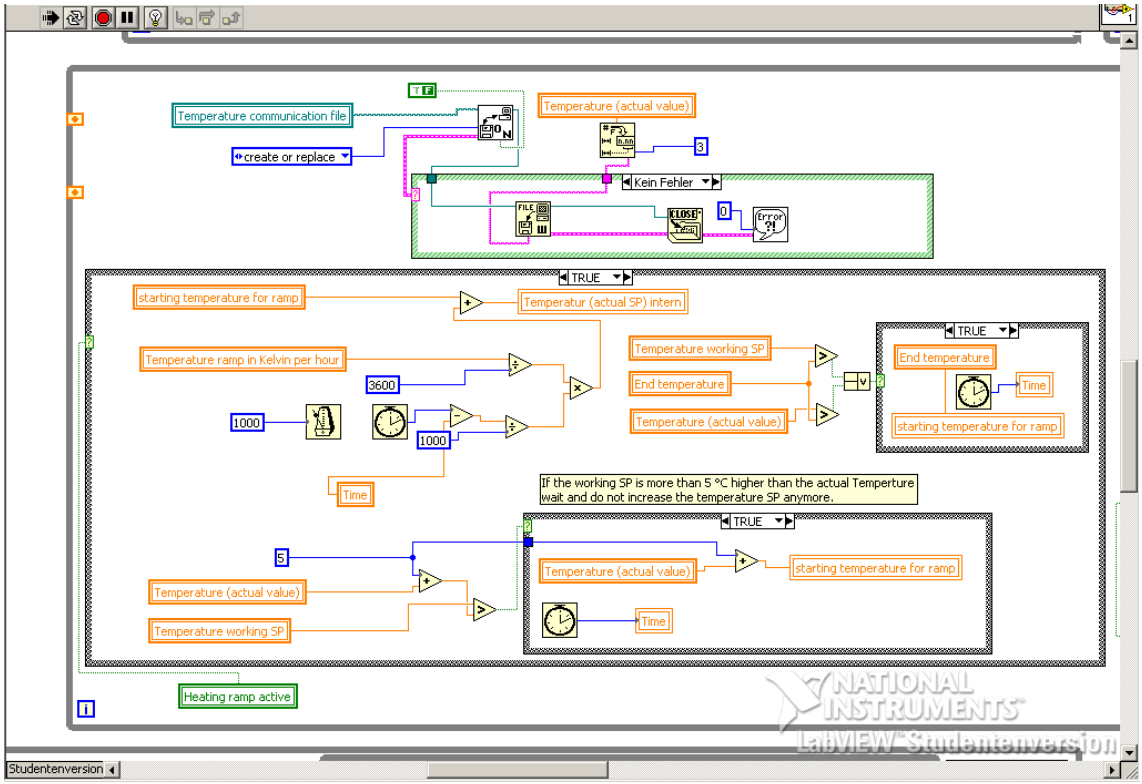

Figure 3.1: Temperature ramp.

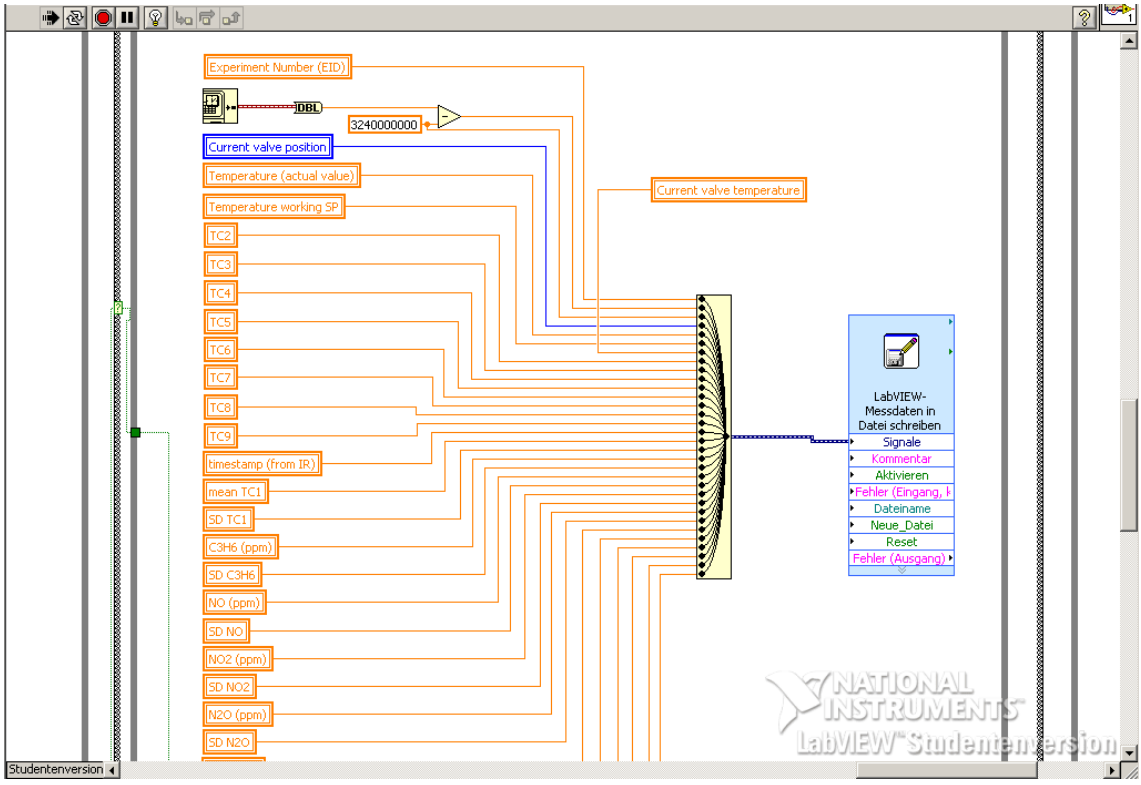

Figure 3.2: Data logging into a text file.

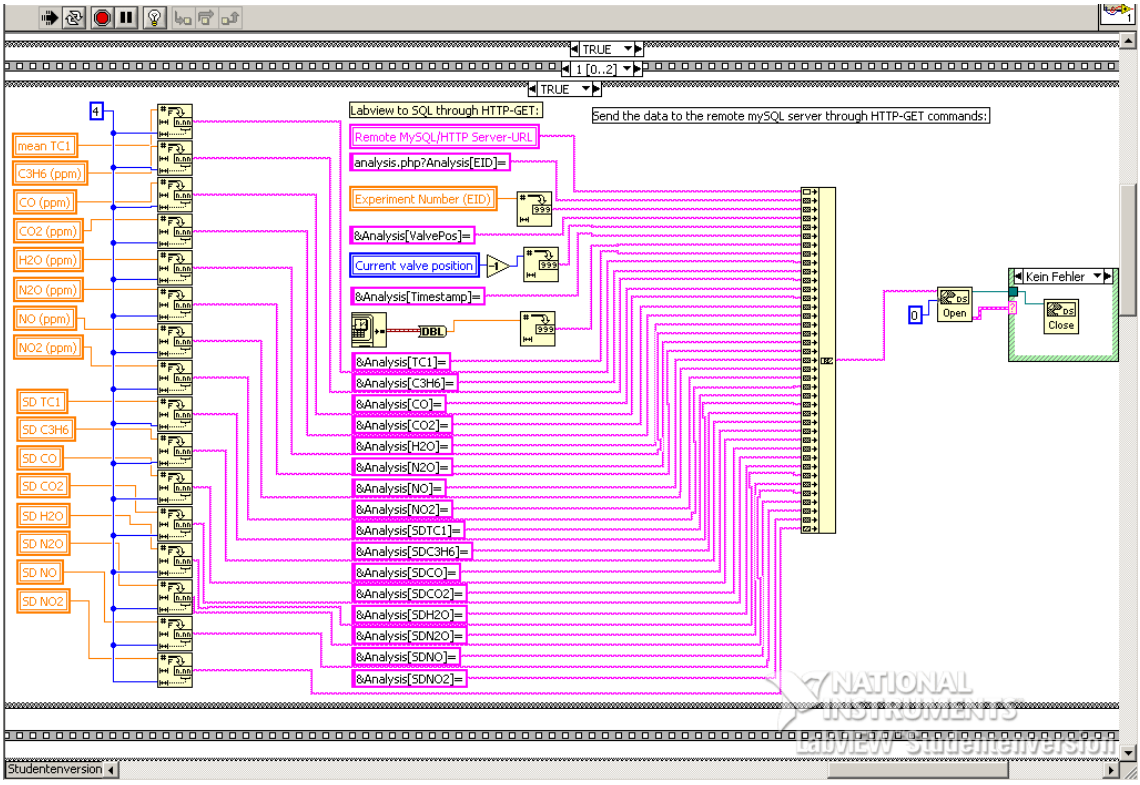

Figure 3.3: Labview to MySQL by a HTTP-GET request.

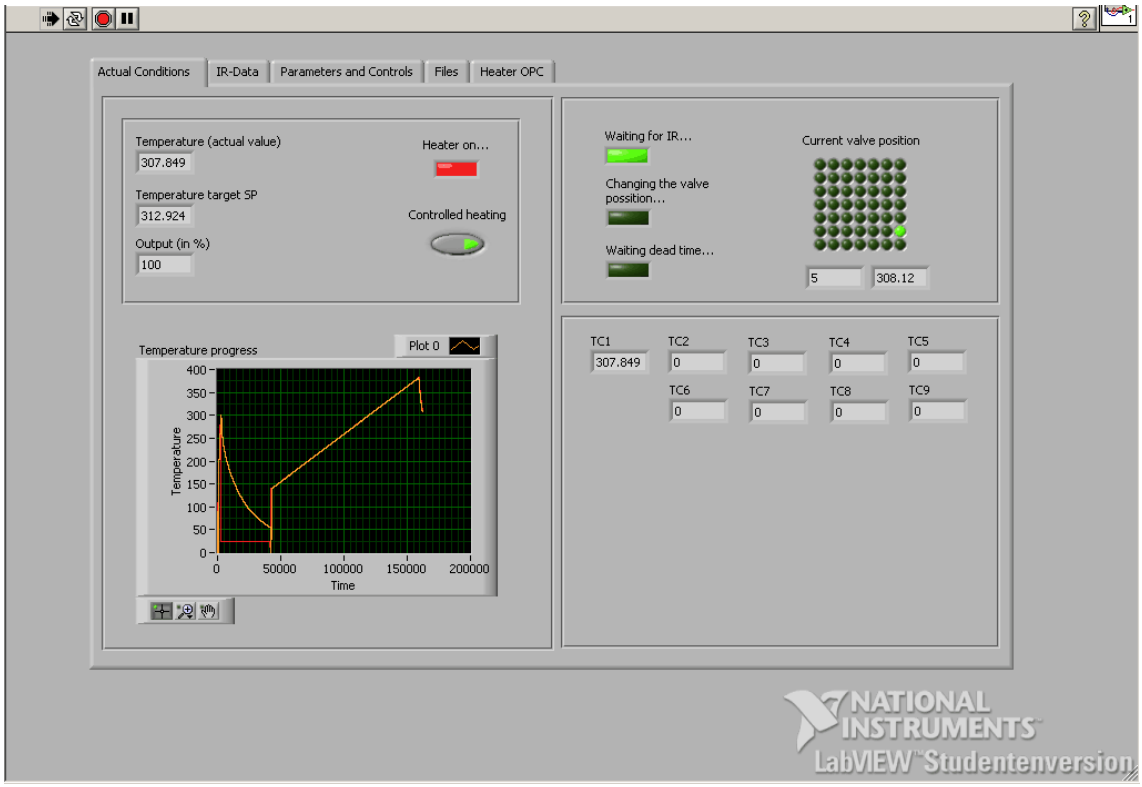

Figure 3.4: First page of the GUI of the Labview program

C.2 Matlab

```
error of the system := 0.05
error outliner := 0.2
while not end of file do
    convert raw data to concentrations
    calculate standard deviation for each datapoint
    sort datapoints by valve position
end
while datapoints do
    calculate conversions and yields of components
    assign weights to each datapoint
end
outliner := true
while outliner do
    outliner := false
    fit a smoothing spline to the datapoints using the weightened nonlinear
    least squares method
    for each datapoint do
        if (datapoint - smoothing spline) > error outliner then
            remove datapoint from dataset
            outliner := true
        end
    end
end
do plots of conversions and yields
```

Algorithm C.1: Pseudocode for parsing the raw data file and calculation of the NO conversion.

```
initialize variables and constants
initialize variation operators
initialize PISA communication files
initialize random seed
write random seed to PISA parameter file
create inital population randomly
evaluate inital population
write objective functions values to PISA population file
while not termination condition do
    while selector not ready do
        if PISA state == 2 then
            read PISA archive list
            read PISA population list
            reset PISA archive list
            reset PISA population list
            if not error then
                create archive from list
                create new population from list
            end
        end
    end
    apply variation operators on population
    decode individuals
    if not individuals valid then
        repair individuals
    end
    write robot synthesis file
    while not valid fitness values do
        evalute fitness experimentally
    end
    remember populations and archives
    write PISA population file
end
```

Algorithm C.2: Pseudocode of the PISA variator module.

C.3 OMNIC

Listing C.1: Main loop to read and write the main data file

```
(...)
send updateReadout "Request", 3
send setRequestVal 90,2,"\\Reaktor\communicate\measurements.txt"
send updateReadout "Start of Loop", 4
(...)
do
        increment _index
        send updateReadout "Loop[]: Report", 5
        send report 3,"\\Reaktor\data\data-gen0#mv50#.txt",0,0,"#mv50# ; #mv5# ; #mv10# ;"
        send updateReadout "Loop[]: Collect Sample", 6
        send enableApp false
        send executeOmnic "[Invoke CollectSample
                        ""#mv50#-#mv1#-#mv5#-#mv10#-#mv101#"" AUTO POLLING]"
        send waitOnInvoke "CollectSample"
        send updateReadout "Loop[]: Save As", 7
        send executeOmnic "[Export " &
                    getRTSFN("\\Reaktor\data\data-gen0#mv50#-#mv1#-#mv5#-#mv10#-#mv101#.spa"
        send updateReadout "Loop[]: Macro mess_NO.mac", 8
        send runUserTask "\\Reaktor\source code\IR\mess_NO.mac","#mv1#, #mv5#, #mv10#, #mv50#","103"
        get peek()
        send updateReadout "Loop[]: Macro mess_C3H6.mac", 9
        send runUserTask "\\Reaktor\source code\IR\mess_C3H6.mac","#mv1#, #mv5#, #mv10#, #mv50#","103
        get peek()
        send updateReadout "Loop[]: Macro mess_CO2.mac", 10
        send runUserTask "\\Reaktor\source code\IR\mess_CO2.mac","#mv1#, #mv5#, #mv10#, #mv50#","103"
        get peek()
        send updateReadout "Loop[]: Macro mess_CO.mac", 11
        send runUserTask "\\Reaktor\source code\IR\mess_CO.mac","#mv1#, #mv5#, #mv10#, #mv50#","103"
        get peek()
        send updateReadout "Loop[]: Macro mess_NO2.mac", 12
        send runUserTask "\\Reaktor\source code\IR\mess_NO2.mac","#mv1#, #mv5#, #mv10#, #mv50#","103"
        get peek()
        send updateReadout "Loop[]: Macro mess_H2O.mac", 13
        send runUserTask "\\Reaktor\source code\IR\mess_H2O.mac","#mv1#, #mv5#, #mv10#, #mv50#","103"
        get peek()
        send updateReadout "Loop[]: Macro mess_N2O.mac", 14
        send runUserTask "\\Reaktor\source code\IR\mess_N2O.mac","#mv1#, #mv5#, #mv10#, #mv50#","103"
        get peek()
        send updateReadout "Loop[]: Math", 15
        send setMathVal 101,"#mv101# + 1","0"
        send updateReadout "Loop[]: End of Loop", 16
until _index = item 1 of _svLTstack
(...)
```

Listing C.2: Main loop to collect and evaluate several spectra

```
(...)
send updateReadout "Request", 6
send setRequestVal 50,2,"\\Reaktor\communicate\generation_number.txt"
send updateReadout "Request", 7
send setRequestVal 90,2,"\\Reaktor\communicate\measurements.txt"
```

```
send updateReadout "Request", 8
send setRequestVal 10,2,"\\Reaktor\communicate\valve_position.txt"
send updateReadout "Start of Loop", 9
(...)
do
        increment _index
        send updateReadout "Loop[]: Request", 10
        send setRequestVal 1,2,"\\Reaktor\communicate\timestamp.txt"
        send updateReadout "Loop[]: Delete File", 11
        send executeOmnic "[DeleteFile ""\\Reaktor\communicate\variables\time#mv101#.txt""]"
        send updateReadout "Loop[]: Report", 12
        send report 3,"\\Reaktor\communicate\variables\time#mv101#.txt",0,0,"#mv1#"
        send updateReadout "Loop[]: Request", 13
        send setRequestVal 5,2,"\\Reaktor\communicate\temperature.txt"
        send updateReadout "Loop[]: Delete File", 14
        send executeOmnic "[DeleteFile ""\\Reaktor\communicate\variables\T#mv101#.txt""]"
        send updateReadout "Loop[]: Report", 15
        send report 3,"\\Reaktor\communicate\variables\T#mv101#.txt",0,0,"#mv5#"
        send updateReadout "Loop[]: Collect Sample", 16
        send enableApp false
        send executeOmnic "[Invoke CollectSample
                        ""#mv50#-#mv1#-#mv5#-#mv10#-#mv101#"" AUTO POLLING]"
        send waitOnInvoke "CollectSample"
        send updateReadout "Loop[]: Save As", 17
        send executeOmnic "[Export " &
                    getRTSFN("\\Reaktor\data\data-gen0#mv50#-#mv1#-#mv10#-#mv5#-#mv101#.spa"
        send updateReadout "Loop[]: Baseline Correct", 18
        send executeOmnic "[AutoBaseline]"
        send updateReadout "Loop[]: Math", 19
        send setMathVal 101,"#mv101# + 1","0"
        send updateReadout "Loop[]: End of Loop", 20
until _index = item 1 of _svLTstack
sysError = "ok"
(...)
```

Listing C.3: NO peak identification and calculation

```
(...)
send updateReadout "Store Arguments", 1
send setStoArgVal "1, 5, 10, 50"
send updateReadout "Find Peaks", 2
(...)
send setOmnic "Display RegionStart", "1898.5"
send setOmnic "Display RegionEnd", "1901.5"
send executeOmnic "[PeakPick 1e-002 50]"
(...)
send updateReadout "Store Result", 3
send setStoResVal 111,1,5,1
send updateReadout "Peak Height", 4
send executeOmnic "[CorrectedPeakHeight 1901.5 1900 1898.5 Shift]"
(...)
send updateReadout "Store Result", 5
send setStoResVal 112,4,1,1
send updateReadout "Find Peaks", 6
(...)
send setOmnic "Display RegionStart", "1878"
```

```
send setOmnic "Display RegionEnd", "1872"
send executeOmnic "[PeakPick 1e−002 50]"
(...)
send updateReadout "Store Result", 7
send setStoResVal 113,1,5,1
send updateReadout "Peak Height", 8
send executeOmnic "[CorrectedPeakHeight 1878 1875 1872 Shift]"
(...)
send updateReadout "Store Result", 9
send setStoResVal 114,4,1,1
send updateReadout "Peak Area", 10
send executeOmnic "[CorrectedPeakArea 1980 1980 1882 1882]"
(...)
send updateReadout "Store Result", 11
send setStoResVal 115,5,1,1
(...)
send report 3,"\\Reaktor\data\data−gen0#mv50#.txt","Excel","#mv1#",
                "NO ; #mv111# ; #mv112# ; #mv113# ; #mv114# ; #mv115# ;"
(...)
```

Bibliography

G. P. Ansell, A. F. Diwell, S. E. Golunski, J. W. Hayes, R. R. Rajaram, T. J. Truex, and A. P. Walker. Mechanism of the lean NOx reaction over Cu/ZSM-5. *Applied Catalysis B: Environmental*, 2(1):81–100, 1993.

J. N. Armor. Environmental catalysis. *Applied Catalysis B-Environmental*, 1(4):221–256, 1992.

J. N. Armor. Catalytic removal of nitrogen oxides: where are the opportunities? *Catalysis Today*, 26(2):99–105, 1995.

T. Back, D. B. Fogel, and Z. Michalewicz. *Handbook of Evolutionary Computation*. IOP Publishing Ltd and Oxford University Press, 7 edition, 1997.

M. Baerns and M. Holena. Catalyst development for alkane dehydrogenation to olefins; a high-throughput-experimentation approach accounting for input of fundamental knowledge and data mining based on neural networks. *Abstracts of Papers of the American Chemical Society*, 224:U269–U269, 2002.

J. Barhen, V. Protopopescu, and D. Reister. Trust: A deterministic algorithm for global optimization. *Science*, 276(5315):1094–1097, 1997.

T. Battiti. First and second-order methods for learning: Between steepest descent and newton's method. *Neural Computation*, 4(2):141–166, 1992.

M. Bellmore and Nehause.Gl. Traveling salesman problem - a survey. *Operations Research*, 16(3):538–&, 1968.

S. Bleuler, M. Laumanns, L. Thiele, and E. Zitzler. Pisa - a platform and programming language independent interface for search algorithms. In *Evolutionary Multi-Criterion Optimization, Proceedings*, volume 2632 of *Lecture Notes In Computer Science*, pages 494–508. 2003.

T. Blickle and L. Thiele. A comparison of selection schemes used in genetic algorithms. Technical report, 1995.

H. Bosch and F. Janssen. Formation and control of nitrogen oxides. *Journal of Catalysis*, 2(4):369–379, 1988.

H.J. Bremermann, J. Rogson, and S. Salaff. Global properties of evolution processes. Natural Automata and Useful Simulations, pages 3–42, 1966.

D. Buche, P. Stoll, R. Dornberger, and P. Koumoutsakos. Multiobjective evolutionary algorithm for the optimization of noisy combustion processes. *IEEE Transactions on Systems Man and Cybernetics Part C-Applications and Reviews*, 32(4):460–473, 2002.

R. Burch, J. A. Sullivan, and T. C. Watling. Mechanistic considerations for the reduction of NOx over Pt/Al_2O_3 and Al_2O_3 catalysts under lean-burn conditions. *Catalysis Today*, 42(1-2):13–23, 1998.

G. Busca, L. Lietti, G. Ramis, and F. Berti. Chemical and mechanistic aspects of the selective catalytic reduction of NOx by ammonia over oxide catalysts: A review. *Applied Catalysis B-Environmental*, 18(1-2):1–36, 1998.

D. K. Captain and M. D. Amiridis. In situ FTIR studies of the selective catalytic reduction of no by C_3H_6 over Pt/Al_2O_3. *Journal of Catalysis*, 184(2):377–389, 1999.

Mario J. Castagnola, Michael K. Neylon, and Christopher L. Marshall. Coated bifunctional catalysts for NOx SCR with C_3H_6: Part II. in situ spectroscopic characterization. *Catalysis Today*, 96(1-2):61–70, 2004.

S. M. Cui, A. Mohan, and D. S. Weile. Pareto optimal design of absorbers using a parallel elitist nondominate sorting genetic algorithm and the finite element-boundary integral method. *IEEE Transactions on Antennas and Propagation*, 53(6):2099–2107, 2005.

H. Dathe. *Nanostructured Sulfur Traps for the protection of high performance NOx storage/reduction catalysts in low emission engine applications*. PhD thesis, Technische Universität München, 2005.

K. Deb and H. G. Beyer. Self-adaptive genetic algorithms with simulated binary crossover. *Evolutionary Computation*, 9(2):197–221, 2001.

K. Deb and D. E. Goldberg. An investigation of niche and species formation in genetic function optimization. In *the third international conference on Genetic algorithms*, pages 42–50, George Mason University, United States, 1989. Morgan Kaufmann Publishers Inc.

K. Deb and M. Goyal. A combined genetic adaptive search geneas for engineering design. *Computer Science and Informatics*, 26(4):30–45, 1996.

K. Deb, A. Pratap, and T. Meyarivan. Constrained test problems for multi-objective evolutionary optimization. In *Evolutionary Multi-Criterion Optimization, Proceedings*, volume 1993 of *Lecture Notes in Computer Science*, pages 284–298. Springer-Verlag Berlin, Berlin, 2001.

K. Deb, A. Pratap, S. Agarwal, and T. Meyarivan. A fast and elitist multiobjective genetic algorithm: NSGA-II. *IEEE Transactions on Evolutionary Computation*, 6(2): 182–197, 2002.

EPA. U.S. Environmental Protection Agency. http://www.epa.gov

References

R. J. Farrauto and R. M. Heck. Catalytic converters: state of the art and perspectives. *Catalysis Today*, 51(3-4):351–360, 1999.

C. M. Fonseca and P. J. Fleming. Multiobjective optimization and multiple constraint handling with evolutionary algorithms - part I: A unified formulation. *IEEE Transactions on Systems Man and Cybernetics Part a-Systems and Humans*, 28(1):26–37, 1998.

A. Fritz and V. Pitchon. The current state of research on automotive lean NOx catalysis. *Applied Catalysis B: Environmental*, 13(1):1–25, 1997.

J. M. Garcia-Cortes, J. Perez-Ramirez, M. J. Illan-Gomez, F. Kapteijn, J. A. Moulijn, and C. S. M. de Lecea. Effect of the support in de-NOx HS-SCR over transition metal catalysts. *Reaction Kinetics And Catalysis Letters*, 70(2):199–206, 2000.

H. S. Glick, J. J. Klein, and W. Squire. Single-pulse shock tube studies of the kinetics of the reaction N_2+O_2 reversible 2NO between 2000-3000-degrees-K. *Journal Of Chemical Physics*, 27(4):850–857, 1957.

D. E. Goldberg and J. Richardson. Genetic algorithms with sharing for multimodal function optimization. In *the Second International Conference on Genetic Algorithms on Genetic algorithms and their application*, pages 41–49. Lawrence Erlbaum Associates, Inc., 1987.

J Grefenstette. Optimization of control parameters for genetic algorithms. *IEEE Transactions on Systems, Man, and Cybernetics*, 16(1):122–128, 1986.

I. Hahndorf, O. Buyevskaya, M. Langpape, G. Grubert, S. Kolf, E. Guillon, and M. Baerns. Experimental equipment for high-throughput synthesis and testing of catalytic materials. *Chemical Engineering Journal*, 89(1-3):119–125, 2002.

U. Hammel and T. Baeck. Evolution strategies on noisy functions: How to improve convergence properties. In *International Conference on Evolutionary Computation, the 3rd Conference on Parallel Problem Solving from Nature*, volume 866, pages 159–168. Springer, 1994.

P. J. B. Hancock. An empirical comparison of selection methods in evolutionary algorithms. In *Evolutionary Computing, AISB Workshop*, pages 80–94, 1994.

P. J. B. Hancock. A comparison of selection mechanisms. In IOP Publishing Ltd Press and Oxford University, editors, *Handbook of Evolutionary Computation*, volume 97/1, pages 80–94. 1997.

L. Hannes and D. Weuster-Botz. Genetic algorithm for multi-objective experimental optimization. *Bioprocess and Biosystems Engineering*, 29(5):385–390, 2006.

J. Havel, H. Link, M. Hofinger, E. Franco-Lara, and D. Weuster-Botz. Comparison of genetic algorithms for experimental multi-objective optimization on the example of medium design for cyanobacteria. *Journal of Biotechnology*, 1:549–555, 2006.

R. M. Heck. Catalytic abatement of nitrogen oxides-stationary applications. *Catalysis Today*, 53(4):519–523, 1999.

M. Held and R. M. Karp. Traveling-salesman problem and minimum spanning trees. *Operations Research*, 18(6):1138–&, 1970.

C. Hoffmann. *Entwicklung von Methoden für die parallelisierte Herstellung und Ausprüfung von Feststoffkatalysatoren*. PhD thesis, Ruhr-Universität Bochum, 2002.

hte. the high throughput experimentation company. http://www.hte-company.de

E. Hums. Is advanced scr technology at a standstill? a provocation for the academic community and catalyst manufacturers. *Catalysis Today*, 42(1-2):25–35, 1998.

M. Iwamoto. Heterogeneous catalysis for removal of NO in excess oxygen - progress in 1994. *Catalysis Today*, 29(1-4):29–35, 1996.

M. Iwamoto, H. Furukawa, Y. Mine, F. Uemura, S. I. Mikuriya, and S. Kagawa. Copper(II) ion-exchanged ZSM-5 zeolites as highly-active catalysts for direct and continuous decomposition of nitrogen monoxide. *Journal Of The Chemical Society-Chemical Communications*, (16):1272–1273, 1986.

C. Kiener. *Verwendung von Hochdurchsatz-Methoden zur Untersuchung starker Metall-Träger-Wechselwirkungen bei Cu/ZnO-Katalysatoren für die Methanolsynthese*. PhD thesis, Ruhr-Universität Bochum, 2004.

C. Kiener, M. Kurtz, H. Wilmer, C. Hoffmann, H. W. Schmidt, J. D. Grunwaldt, M. Muhler, and F. Schuth. High-throughput screening under demanding conditions: Cu/ZnO catalysts in high pressure methanol synthesis as an example. *Journal of Catalysis*, 216(1-2):110–119, 2003.

Rtfa King, H. C. S. Rughooputh, and K. Deb. Evolutionary multi-objective environmental/economic dispatch: Stochastic versus deterministic approaches. In *Evolutionary Multi-Criterion Optimization*, volume 3410 of *Lecture Notes In Computer Science*, pages 677–691. 2005.

Y. Kintaichi, H. Hamada, M. Tabata, M. Sasaki, and T. Ito. Selective reduction of nitrogen-oxides with hydrocarbons over solid acid catalysts in oxygen-rich atmospheres. *Catalysis Letters*, 6(2):239–244, 1990.

J. Knowles. *Local-Search and Hybrid Evolutionary Algorithms for Pareto Optimization*. PhD thesis, University of Reading, 2002.

J. Knowles. Parego: A hybrid algorithm with on-line landscape approximation for expensive multiobjective optimization problems. *IEEE Transactions on Evolutionary Computation*, 10(1):50–66, 2006.

T. Kreuzer, E. S. Lox, D. Lindner, and J. Leyrer. Advanced exhaust gas aftertreatment systems for gasoline and diesel fuelled vehicles. *Catalysis Today*, 29(1-4):17–27, 1996.

J. C. Lagarias, J. A. Reeds, M. H. Wright, and P. E. Wright. Convergence properties of the nelder-mead simplex method in low dimensions. *Siam Journal on Optimization*, 9 (1):112–147, 1998.

X. D. Li. A non-dominated sorting particle swarm optimizer for multiobjective optimization. In *Genetic and Evolutionary Computation - Gecco 2003, Pt I, Proceedings*, volume 2723 of *Lecture Notes in Computer Science*, pages 37–48. Springer-Verlag Berlin, Berlin, 2003.

X. D. Li. Better spread and convergence: Particle swarm multiobjective optimization using the maximin fitness function. In *Genetic and Evolutionary Computation - Gecco 2004, Pt 1, Proceedings*, volume 3102 of *Lecture Notes in Computer Science*, pages 117–128. Springer-Verlag Berlin, Berlin, 2004.

J. S. Liu. Markov chain monte carlo and related topics. Technical report, Stanford University, 1999.

Z. M. Liu and S. I. Woo. Recent advances in catalytic DeNOx science and technology. *Catalysis Reviews-Science and Engineering*, 48(1):43–89, 2006.

Z. M. Liu, K. S. Oh, and S. I. Woo. Overview on the selective lean NOx reduction by hydrocarbons over pt-based catalysts. *Catalysis Surveys from Asia*, 10(1):8–15, 2006.

G. V. Loganathan and H. D. Sherali. A convergent interactive cutting-plane algorithm for multiobjective optimization. *Operations Research*, 35(3):365–377, 1987.

A. Martinez Joaristi. *Stage I High Throughput Techniques for the Development of mixed oxides DeNOx catalysts*. PhD thesis, Ruhr-Universität Bochum, 2007.

Z. Michalewicz. A survey of constraint handling techniques in evolutionary computation methods. In J.R. McDonnell, Reynolds R.G., and Fogel D.B., editors, *Annual Conference on Evolutionary Programming*, pages 135–155. MIT Press, 1995.

Z. Michalewicz. *Genetic Algorithms + Data Structures = Evolution Programs*. Springer-Verlag, 3 edition, 1999.

B. L. Miller and M.J. Shaw. Genetic algorithms with dynamic niche sharing for multimodal function optimization. In *International Conference on Evolutionary Computation*, pages 786–791, 1996.

J. N. Morse. Reducing the size of the non-dominated set - pruning by clustering. *Computers & Operations Research*, 7(1-2):55–66, 1980.

V. Murphy, A. F. Volpe, and W. H. Weinberg. High-throughput approaches to catalyst discovery. *Current Opinion in Chemical Biology*, 7(3):427–433, 2003.

N. Nejar, J. M. Garcia-Cortes, C. S. M. de Lecea, and M. J. Illan-Gomez. Bimetallic catalysts for the simultaneous removal of NOx and soot from diesel engine exhaust: A preliminary study using intrinsic catalysts. *Catalysis Communications*, 6(4):263–267, 2005.

Michael K. Neylon, Mario J. Castagnola, Norma B. Castagnola, and Christopher L. Marshall. Coated bifunctional catalysts for NOx SCR with C_3H_6: Part I: water-enhanced activity. *Catalysis Today*, 96(1-2):53–60, 2004.

Y. Nojima, K. Narukawa, S. Kaige, and H. Ishibuchi. Effects of removing overlapping solutions on the performance of the NSGA-II algorithm. In *Evolutionary Multi-Criterion Optimization*, volume 3410 of *Lecture Notes in Computer Science*, pages 341–354. Springer-Verlag Berlin, Berlin, 2005.

V. I. Parvulescu, P. Grange, and B. Delmon. Catalytic removal of no. *Catalysis Today*, 46(4):233–316, 1998.

M. J. Reddy and D. N. Kumar. An efficient multi-objective optimization algorithm based on swarm intelligence for engineering design. *Engineering Optimization*, 39(1):49–68, 2007.

C. Reeves. Using genetic algorithms with small populations. In Stephanie Forrest, editor, *the Fifth International Conference on Genetic Algorithms*, San Mateo, CA, 1993. Morgan Kaufman.

S. C. Reyes and E. Iglesia. Monte-carlo simulations of structural-properties of packed-beds. *Chemical Engineering Science*, 46(4):1089–1099, 1991.

R. E. Rosenthal. Principles of multiobjective optimization. *Decision Sciences*, 16(2): 133–152, 1985.

G. Rudolph. Convergence analysis of canonical genetic algorithms. *IEEE Transactions on Neural Networks*, 5(1):96–101, 1994.

V. A. Sadykov, T. G. Kuznetsova, V. P. Doronin, E. M. Moroz, D. A. Ziuzin, D. I. Kochubei, B. N. Novgorodov, V. N. Kolomiichuk, G. M. Alikina, R. V. Bunina, E. A. Paukshtis, V. B. Fenelonov, O. B. Lapina, I. V. Yudaev, N. V. Mezentseva, A. M. Volodin, V. A. Matyshak, V. V. Lunin, A. Ya Rozovskii, V. F. Tretyakov, T. N. Burdeynaya, and J. R. H. Ross. Molecular design and characterization of catalysts for NOx selective reduction by hydrocarbons in the oxygen excess based upon ultramicroporous zirconia pillared clays. *Topics in Catalysis*, 32(1 - 2):29–38, 2005.

L. V. Santana-Quintero, N. Ramirez-Santiago, C. A. C. Coello, J. M. Luque, and A. G. Hernandez-Diaz. A new proposal for multiobjective optimization using particle swarm optimization and rough sets theory. In *Parallel Problem Solving from Nature - PPSN Ix, Proceedings*, volume 4193 of *Lecture Notes in Computer Science*, pages 483–492. Springer-Verlag Berlin, Berlin, 2006.

S. Sato, H. Hirabayashi, H. Yahiro, N. Mizuno, and M. Iwamoto. Iron ion-exchanged zeolite - the most active catalyst at 473 K for selective reduction of nitrogen monoxide by ethene in oxidizing atmosphere. *Catalysis Letters*, 12(1-3):193–200, 1992.

L. M. Schmitt. Theory of genetic algorithms. *Theoretical Computer Science*, 259(1-2): 1–61, 2001.

F. Schuth. Endo- and exotemplating to create high-surface-area inorganic materials. *Angewandte Chemie-International Edition*, 42(31):3604–3622, 2003.

F. Schuth and D. Demuth. High-throughput-experimentation in heterogenic catalysis. *Chemie Ingenieur Technik*, 78(7):851–861, 2006.

F. Schuth, O. Busch, C. Hoffmann, T. Johann, C. Kiener, D. Demuth, J. Klein, S. Schunk, W. Strehlau, and T. Zech. High-throughput experimentation in oxidation catalysis. *Topics in Catalysis*, 21(1-3):55–66, 2002.

M. Schwickardi, T. Johann, W. Schmidt, O. Busch, and F. Schuth. High surface area metal oxides from matrix assisted preparation in activated carbons. In *Scientific Bases For The Preparation Of Heterogeneous Catalysts*, volume 143 of *Studies In Surface Science And Catalysis*, pages 93–100. Elsevier Science Bv, Amsterdam, 2002a.

M. Schwickardi, T. Johann, W. Schmidt, and F. Schuth. High-surface-area oxides obtained by an activated carbon route. *Chem. Mater.*, 14(9):3913–3919, 2002b.

M. Shelef and G. W. Graham. Why rhodium in automotive 3-way catalysts. *Catalysis Reviews-Science and Engineering*, 36(3):433–457, 1994.

P. S. Shelokar, V. K. Jayaraman, and B. D. Kulkarni. Ant algorithm for single and multiobjective reliability optimization problems. *Quality and Reliability Engineering International*, 18(6):497–514, 2002.

N. Srinivas and K. Deb. Multiobjective optimization using nondominated sorting in genetic algorithms. 1994.

B. Suman. Study of simulated annealing based algorithms for multiobjective optimization of a constrained problem. *Computers & Chemical Engineering*, 28(9):1849–1871, 2004.

A. Suppapitnarm, K. A. Seffen, G. T. Parks, and P. J. Clarkson. A simulated annealing algorithm for multiobjective optimization. *Engineering Optimization*, 33(1):59–85, 2000.

Y. Traa, B. Burger, and J. Weitkamp. Zeolite-based materials for the selective catalytic reduction of NOx with hydrocarbons. *Microporous and Mesoporous Materials*, 30(1): 3–41, 1999.

M. V. Twigg. Progress and future challenges in controlling automotive exhaust gas emissions. *Applied Catalysis B-Environmental*, 70(1-4):2–15, 2007.

M. W. Watson and P. W. Carr. Simplex algorithm for the optimization of gradient elution high-performance liquid-chromatography. *Analytical Chemistry*, 51(11):1835–1842, 1979.

W. H. Weinberg and E. W. McFarland. Combinatorial approaches to materials discovery. *Trends in Biotechnology*, 17(3):107–115, 1999.

D. Whitley, V. Gordon, and K. Mathias. Lamarckian evolution, the baldwin effect and function optimization. *Lecture Notes in Computer Science*, 866:6–15, 1994.

References

R. J. Willey, H. Lai, and J. B. Peri. Investigation of iron-oxide chromia alumina aerogels for the selective catalytic reduction of nitric-oxide by ammonia. *Journal of Catalysis*, 130(2):319–331, 1991.

D. Wolf, O. V. Buyevskaya, and M. Baerns. An evolutionary approach in the combinatorial selection and optimization of catalytic materials. *Applied Catalysis a-General*, 200 (1-2):63–77, 2000.

E. Zitzler. *Evolutionary Algorithms for Multiobjective Optimization: Methods and Applications*. Phd, Swiss Federal Institute of Technology Zurich, 1999.

E. Zitzler and S. Kunzli. Indicator-based selection in multiobjective search. In *Parallel Problem Solving From Nature - Ppsn Viii*, volume 3242 of *Lecture Notes In Computer Science*, pages 832–842. 2004.

E. Zitzler and L. Thiele. Multiobjective evolutionary algorithms: A comparative case study and the strength pareto approach. *IEEE Transactions on Evolutionary Computation*, 3(4):257–271, 1999.

E. Zitzler, M. Laumanns, and L. Thiele. SPEA2: Improving the strength pareto evolutionary algorithm for multiobjective optimization. In *Evolutionary Methods for Design, Optimisation and Control with Application to Industrial Problems. Proceedings of the EUROGEN2001 Conference*, pages 95–100, Athens, Greece, September 19-21, 2001, 2002.